

# **A New Strategy for Synthesizing Zeolites and Zeolite-like Materials**

Thesis by

Hyunjoo Lee

In Partial Fulfillment of the Requirements

For the Degree of

Doctor of Philosophy

California Institute of Technology

Pasadena, California

2005

(Defended May 27, 2005)

© 2005

Hyunjoo Lee

All Rights Reserved

## ACKNOWLEDGEMENTS

When I decided to pursue my Ph.D. in America five years ago, I felt very afraid of the new life I would have in a totally different environment. It was not easy to adapt in a new environment while learning to communicate in English and surviving in a different social system. But the time I spent at Caltech was the happiest in my life. I met many talented people with good hearts and I was inspired by their brilliant insight in both research and life.

I wish to express my most sincere appreciation to my advisor, Prof. Mark E. Davis. He showed an ideal image of a professor to me. I always admired his creativity and hard work. In addition to academic research, his advice for my various difficulties was incredibly helpful. I would like to thank Dr. Stacey I. Zones for his support and guidance. The discussions with him were always cheerful and enjoyable. I also thank the other members of my committee, Prof. Jay Labinger and Prof. Richard Flagan for their time, interest and encouragement. In addition, I thank Prof. Yushan Yan of University of California, Riverside for valuable collaborations.

All the members of Davis group made the work in the lab interesting and enjoyable. I know how fortunate I was to have such good people as coworkers. Jon Galownia, who joined and will leave the group with me, has been a really good friend. His support and encouragement was indispensable. I will miss the intellectual and profitable conversations, especially about religion, that we had. I thank Patrick Piccione and Andrea Wight for the things they taught me about zeolite synthesis and characterization. I should acknowledge Dr. Sonjong Hwang for his help with solid state NMR measurements. I won't forget the support of all the other members who also enabled me to finish my Ph.D.

I met two of the best friends of my life, Byung-Jun Yoon and Wonjin Jang, at Caltech. I couldn't appreciate their support and care more. I was able to overcome physically and emotionally difficult times due to their help. They showed me an example of Christian life and helped me have true faith in Jesus Christ. I sincerely hope to keep this precious friendship through our lives. I would like to thank Dr. Jione Kang for her kind guidance during our Bible study. It has been a base of my faith. People I met at Caltech and ANC will be in my heart with deep appreciation for their kindness and support. I thank my family for their continuous support of my work. My parents have been role models for their sincerity. Finally, I thank God, my Lord, for this work wouldn't be accomplished without God's blessing. I know that God has led me here and I'm looking forward to where God will lead me!

**ABSTRACT**

Zeolite and molecular sieve materials are broadly used as ion-exchangers, adsorbents and catalysts in the chemical industry. Zeolites are typically synthesized by using organic molecules as structure-directing agents (SDA). The SDA should be removed from the pore cavity of the zeolite framework to create microporous void space before the zeolite can be used for further purposes. Porous zeolites have been prepared by calcination, or extraction in very limited cases. However, calcination has several undesired aspects mainly resulted from a high temperature. A combustion-free methodology is developed in this work by using a new concept for the SDAs. An organic molecule that can be easily cleaved into smaller fragments and subsequently recombined into the original molecule by simple treatments can be used as a 'recyclable SDA'. That is, after synthesizing a zeolite using this type of organic molecule as the SDA, the molecule can be fragmented in the pore cavity, and its fragments removed due to their smaller size. The recovered fragments are then recombined into the original SDAs, which can be used for further zeolite syntheses. The cyclic ketal molecule, 8,8-dimethyl-1,4-dioxo-8-azaspiro[4,5]decane, is used here to prove this new methodology. The ketal is fragmented into its corresponding ketone and diol molecules after structure-directing the synthesis of the zeolite, ZSM-5. The fragments are successfully removed by ion-exchange, and the prepared porous ZSM-5 shows equivalent porosity, catalytic activity and shape selectivity as conventional ZSM-5. In some cases, the SDA can be so tightly packed inside the pore cavity that the small reagent molecules required for fragmentation by acid hydrolysis have no access to the pore cavity. Therefore, the original methodology was expanded to provide a solution for this problem by utilizing two different kinds of organic

molecules, a SDA and a pore-filling agent (PFA), during the zeolite syntheses. The removal of the PFA by simple extraction generates the necessary space inside the pore cavity for agents necessary for the hydrolysis to transport into the zeolite. Using this methodology, ZSM-5, ZSM-12, VPI-8 and MOR are successfully synthesized with various ketal SDAs whose hydrolysis depends on the hydrophilicity and pore connectivity of the synthesized zeolites.

## TABLE OF CONTENTS

<b>Acknowledgements</b> .....	iii
<b>Abstract</b> .....	v
<b>Table of Contents</b> .....	vii
<b>List of Figures</b> .....	x
<b>List of Tables</b> .....	xiv
Chapter One. Introduction .....	1
1.1. Zeolites and Molecular Sieve Materials .....	2
1.1.1. Applications .....	2
1.1.2. Synthesis Procedures .....	4
1.1.3. Synthesis Mechanism.....	6
1.2. Strategies for Rational Design of Zeolite .....	7
1.2.1. Organic Structure-Directing Agents .....	8
1.2.2. Novel building blocks .....	11
1.2.3. Computational Calculations.....	13
1.3. Removal of Organic SDAs From the Zeolite Pores .....	15
1.3.1. Calcination .....	15
1.3.2. Extraction.....	16
1.3.3. Need for a New Strategy to Remove SDA .....	17
Chapter Two. Proposal of a New Methodology and Its Proof of Concept .....	31
2.1. Proposal of a Combustion-Free Methodology .....	32
2.2. Proof of Concept.....	34

2.3. Methods .....	37
2.3.1. Preparation of SDA (1) .....	37
2.3.2. Preparation of as-synthesized zeolite .....	37
2.3.3. Characterizations.....	38
Chapter Three. Modification of the Methodology Using Pore-Filling Agents.....	50
3.1. Need for Pore-Filling Agents .....	51
3.2. Experimental Section .....	53
3.2.1. Synthesis of SDA-1 .....	54
3.2.2. Synthesis of ZSM-5 with SDA-1.....	54
3.2.3. Synthesis of VPI-8 with SDA-1.....	55
3.2.4. Synthesis of ZSM-12 with SDA-1.....	55
3.2.5. Synthesis of ZSM-5 with SDA-1 and pore-filling agents, isobutylamine, or cyclopentylamine .....	55
3.3. Results and Discussions .....	56
3.3.1. Syntheses with SDA-1.....	57
3.3.2. Syntheses with SDA-1 and pore-filling agents.....	58
3.3.3. Cleavage attempts with SDA in unidimensional materials.....	59
3.3.4. Removal of PFAs and SDAs. ....	59
3.4. Conclusions .....	61
Chapter Four. Use of the Proposed Methodology for Synthesis of Various Zeolites ....	72
4.1. Using Various Ketal SDAs for Zeolite Synthesis .....	73
4.2. Experimental Section .....	75
4.2.1. Synthesis of Ketal Structure-Directing Agents.....	75

4.2.2. Zeolite Synthesis.....	78
4.2.3. Cleavage of SDAs in the Zeolite Pore Space.....	79
4.2.4. Analytical.....	80
4.3. Results and Discussion.....	81
4.3.1. Zeolite Synthesis.....	81
4.3.2. Cleavage reaction of ketal SDAs inside the pore space.....	83
4.3.3. Effect of organic contents.....	84
4.3.4. Effect of hydrophilicity.....	85
4.3.5. Effect of pore connectivity.....	86
4.4. Conclusions .....	88
Chapter Five. Concluding Remarks .....	103
5.1. Potential Applications of the New Methodology .....	104
5.2. Conclusions .....	108

## LIST OF FIGURES

### Chapter One

- Figure 1-1. Proposed mechanism for zeolite synthesis: Synthesis of ZSM-5 using tetrapropylammonium cations [1].....23
- Figure 1-2. The size effect of organic molecules in the synthesis zeolites [16].....24
- Figure 1-3. The effect of various shapes for zeolite synthesis in the case of small SDAs [16]. .....25
- Figure 1-4. Top: A schematic representation of ZSM-5 crystal structure. Bottom: The effect of the different SDAs on the crystal shape is quantified in a comparison of the aspect ratio of the crystals [height/depth and width/depth] synthesized in the presence of TPA, dimer-TPA, and trimer-TPA [17].....26
- Figure 1-5. Top: Energy scheme for the synthesis of two zeolite structure (Z) in the presence of a SDA starting from the same gel (G) and going through different nuclei (N). Middle: Proposed mechanism with a reversible nucleation followed by the crystallization. *Bottom*: Nuclei form when silicoalumina oligomers surround the SDA, giving an aggregate resembling a significant part of a structure [24].....27
- Figure 1-6. Typical temperature profile and gas flow for calcination.....28

### Chapter Two

- Figure 2-1. Schematic representations of new synthetic methodology. **a**, generalized scheme. step 1 : assemble the SDA with silica precursor, H<sub>2</sub>O, alkali metal ions, etc. for zeolite synthesis. step 2 : cleave the organic molecules inside the zeolite

pores. step 3 : remove the fragments. step 4 : recombine the fragments into the original SDA molecule. ....	42
Figure 2-2. Specific example of a proposed new synthetic methodology.....	43
Figure 2-3. SEM image of as-synthesized ZSM-5. This was performed with LEO 1550 VP field emission scanning electron microscope. ....	44
Figure 2-4. Powder X-ray diffraction patterns. <b>a</b> , as-synthesized ZSM-5. <b>b</b> , after treatment with 1M HCl solution. <b>c</b> , after ion-exchange with 0.01M NaOH + 1M NaCl solution. The ZSM-5 shows no structural degradation after the various treatments.....	45
Figure 2-5. <sup>13</sup> C CP MAS NMR spectra. <b>a</b> , intact <b>1</b> inside as-synthesized ZSM-5. <b>b</b> , after cleavage of <b>1</b> inside ZSM-5 pores using 1M HCl solution. <b>c</b> , after ion-exchange with 0.01M NaOH + 1M NaCl solution. The spinning rate was 4 kHz and contact time for cross polarization was 1ms for all cases. The notation of <b>1-1</b> denotes the peak corresponding to the carbon 1 of the organic molecule <b>1</b> in Scheme 1. The <sup>13</sup> C CP MAS NMR data show that <b>1</b> was cleaved into its desired fragments by acid treatment and successfully removed after ion-exchange.....	46
Figure 2-6. <sup>27</sup> Al MAS NMR for the ZSM-5 after the cleavage reaction and ion-exchange. This was performed with a Bruker DSX 500 MHz spectrometer at 14 kHz spinning rate with 1ms of (/8 pulse after dehydration for 3hrs at 120oC.....	47

### Chapter Three

Figure 3-1. Structure of SDA-1.....	64
Figure 3-2. Powder X-ray diffraction patterns of various materials synthesized using SDA-1. (a) VPI-8, (b) ZSM-12, (c) ZSM-5.....	65

- Figure 3-3. SEM images of VPI-8. (a)  $\text{LiOH}/\text{SiO}_2=0.05$ ,  $\text{SDA-1}/\text{SiO}_2=0.30$ . The VPI-8 is a very fine powder. (b)  $\text{LiOH}/\text{SiO}_2=0.25$ ,  $\text{SDA-1}/\text{SiO}_2=0.1$ . The VPI-8 has needle-like morphology. ....66
- Figure 3-4. . Schematic diagram of ZSM-5 containing both SDA and PFA and how they are removed. ....67
- Figure 3-5. Powder X-ray diffraction patterns for the ZSM-5 synthesized using SDA-1 and PFA. (a) SDA-1 only, (b) SDA-1 + isobutylamine as PFA, (c) SDA-1 + cyclopentylamine as PFA. ....68
- Figure 3-6.  $^{13}\text{C}$  cross polarization magic angle spinning (CP MAS) NMR spectra. (a) as-made ZSM-5 synthesized using SDA-1 and isobutylamine, (b) after the extraction of isobutylamine with dimethylformamide. The dotted line shows calcined ZSM-5 with impregnated dimethylformamide. The newly appearing peaks after contact with dimethylformamide are from its absorption during the extraction of isobutylamine, (c) After the cleavage reaction using 1N hydrochloric acid. ....69
- Figure 3-7.  $^{27}\text{Al}$  MAS NMR spectra. (a) as-made ZSM-5, (b) after cleavage reaction and subsequent ion-exchange with the mixture of NaOH and NaCl, (c) calcined ZSM-5. ....70

## Chapter Four

- Figure 4-1. Ketal structure-directing agents used in this work. ....92
- Figure 4-2. Powder X-ray diffraction patterns of ZSM-5 synthesized by using ketal-containing SDAs: (a) SDA : **II**, (b) SDA : **VII**, and (c) SDA : **VIII**. ....93
- Figure 4-3. Powder X-ray diffraction patterns of ZSM-12 synthesized by using ketal-containing SDAs: (a) SDA : **IV** (Al-ZSM-12), (b) SDA : **VIII** (Al-ZSM-

12), (c) SDA : <b>II</b> (B-ZSM-12), (d) SDA : <b>IV</b> (B-ZSM-12), and (e) SDA : <b>VIII</b> (B-ZSM-12).	94
Figure 4-4. Powder X-ray diffraction patterns of mordenite synthesized by using ketal-containing SDAs: (a) SDA : <b>III</b> , (b) SDA : <b>IV</b> , and (c) SDA : <b>VIII</b> .	95
Figure 4-5. Powder X-ray diffraction patterns of VPI-8 synthesized by using ketal-containing SDAs: (a) SDA : <b>II</b> , (b) SDA : <b>V</b> , (c) SDA : <b>VII</b> , and (d) SDA : <b>VIII</b> .	96
Figure 4-6. $^{13}\text{C}$ CP MAS NMR spectra for the ZSM-5 (SDA : <b>VIII</b> ) with organic content of 7.8%: (a) as-made ZSM-5 (b) after acidic treatment with 1N HCl at 80°C.	97
Figure 4-7. Thermogravimetric analysis results for: (a) as-made ZSM-5 with Si/Al=14.0, and (b) as-made ZSM-5 with Si/Al=40.8.	98
Figure 4-8. $^{13}\text{C}$ CP MAS NMR spectra for: (a) as-made ZSM-5 (SDA : <b>VIII</b> ), (b) after an acidic treatment by using 1H HCl at 80°C, (c) after an acidic treatment by using 1N HCl at 135°C, and (d) after further ion-exchange with NaCl/NaOH solution at 100°C.	99
Figure 4-9. $^{13}\text{C}$ CP MAS NMR spectra for: (a) as-made mordenite (SDA : <b>VIII</b> ), and (b) after an acidic treatment with 1N HCl at 135°C (c) after further ion-exchange with NaCl/NaOH at 100°C.	100

## Chapter Five

Figure 5-1. Removal of organic SDAs from organically functionalized zeolites.	113
Figure 5-2. Micropatterns prepared (a) by using zeolite nanoparticles [10], (b) by using pre-patterned substrates and functionalized zeolite microcrystals [12].	114

**LIST OF TABLES****Chapter One**

Table 1-1. Zeolites that were newly discovered by using unique organic molecules. .....	29
--	----

**Chapter Two**

Table 2-1. Comparisons of hydrocarbon product distributions for the conversion of methanol to higher hydrocarbons <sup>a</sup> . .....	48
Table 2-2. Comparisons between calcined and HCl-treated ZSM-5 <sup>a</sup> .....	49

**Chapter Three**

Table 3-1. Synthesis of VPI-8 using SDA-1 <sup>a</sup> .....	71
--	----

**Chapter Four**

Table 4-1. Zeolite syntheses using ketal-containing SDA's .....	101
Table 4-2. Properties of ZSM-5s with different organic contents and Si/Al ratios.	102

## **Chapter One**

### Introduction

## 1.1. Zeolites and Molecular Sieve Materials

Zeolites are defined as crystalline microporous aluminosilicates with three dimensionally connected pore structures. The porous structure consists of cavities and channels, and water or cations that counter-balance the negative ions of aluminum sites usually occupy the pore space. For example, zeolite A has a basic unit of  $\text{Na}_x[\text{SiAlO}_4] \cdot y\text{H}_2\text{O}$  where Na ions or water molecules reside in large cavities connected by small channels. The crystalline structure comprised of various combinations of tetrahedral  $\text{SiO}_4$  or  $\text{AlO}_4^-$  enables the zeolite to have monodisperse pore size distribution and better mechanical strength compared with amorphous materials. In addition to aluminosilicates, silicates with various heteroatoms, such as Ge, Ga, B, Zn, etc., aluminophosphates (AIPO), and silicaluminophosphates (SAPO) have been synthesized. When these materials have crystalline porous structures like zeolites, they are called as molecular sieve materials. Molecules can be taken up to the pores based on their size. While molecules smaller than the pore size can pass through, bigger molecules are rejected. Due to the crystallinity, the discrimination can occur so sharply that the molecules with even sub-Å size difference can be separated. This ‘molecular sieving’ effect is a unique and inherent character of zeolites and molecular sieve materials.

### 1.1.1. Applications

Traditionally, zeolitic materials have been used as ion-exchangers, adsorbents, separation agents, etc. Zeolites are the most widely used water softening agents in the detergent industry due to their high ion-exchange capability. Zeolites adsorb water or

small molecules very easily, and this property contributes to desiccation or gas purification. Molecular sieving effect enables zeolites to separate n-paraffin from i-paraffin, so it can separate the molecules with very small size difference. However, the most interesting application of zeolites is their use as catalysts in chemical industries. When a proton counterbalances the negative charge of aluminum, the proton can be acted as a Brønsted acid site. Zeolites have been utilized as heterogeneous acid catalysts in many commercial processes such as catalytic cracking, hydrocracking, selectoforming, hydroisomerization, dewaxing, alkylation, methanol to gasoline conversion, NO<sub>x</sub> reduction, etc. Zeolites are also used for shape selective catalysis resulting from the molecular sieving effect. For example, in the transalkylation reaction of 1,3-dimethylbenzene, the methyl group cannot access 5-position carbon of benzene (the part with no methyl groups) due to spatial confinement inside the crystalline pore. Hence, only 1,3,4-trimethylbenzene is formed instead of 1,3,5-trimethylbenzene.

The application of zeolitic materials has been actively expanded into new fields during the last decade. Kuznichi et al. reported that titanosilicate can control gas flow of nitrogen and methane. The material named as ETS-4 has small pore of 8MR (8 membered-ring; the number of oxygen around the pore is 8), and its pore shape is changed from circular to elliptical upon heat treatment. While both nitrogen and methane can pass through the circular pore, only nitrogen can pass through the elliptical pore. This material can provide new and more economical ways for the purification of natural gas containing large amounts of nitrogen. Various morphologies of zeolites, such as self-standing films, fibers, and micropatterns, have been synthesized. Especially, zeolite-based films are expected to have high potential as separation devices, membrane reactors, chemical sensors, and host for guest

species in optical applications. Porous zeolite films are considered to be a good alternative to dense silicate films as low-k materials in semiconductor device applications. Zeolites have higher mechanical strength than amorphous silicates, and the pores enables the k value of the zeolite film to be much lower than dense silicate films because the k value of air is 1 while the k value of SiO<sub>2</sub> is 4. Zeolitic materials have also been developed as contrast agents for magnetic resonance imaging (MRI). Gd<sup>+</sup> is an excellent contrast agent for MRI, but its toxicity forbids its use. When Gd<sup>+</sup> is impregnated in zeolites, the composite shows benign toxicity. In addition, zeolite can be used as a reactor for single-walled carbon nanotubes. The synthesized tube with 0.4nm diameter shows superconductivity.

### 1.1.2. Synthesis Procedures

Zeolitic materials are synthesized from a gel containing silica precursor, precursor compounds with heteroatoms such as Al, B, Zn, Ga, Ge, etc., organic or inorganic cations, mineralizing agents, and water. The crystalline phase of the obtained zeolite depends most strongly on the gel composition. By changing the organic or inorganic cations, heteroatoms, mineralizing agents, and the ratio of these compounds, different crystalline structures with various pore sizes and pore structures can be synthesized. So far, 161 crystalline structures have been discovered according to the International Zeolite Association (IZA). IZA recommends the use of a three letter code such as ABW, ACO, etc for zeolites with various structures. Detailed information about these crystalline structures can be found at the IZA website (<http://www.iza-structure.org>). Often new zeolite structures have been found by using novel shapes of organic cations. Although the shape of the produced pore is not exactly the same as the shape of the organic compound, the use of a particular organic compound directs the formation of

a specific crystalline porous structure. These organic compounds are called ‘structure-directing agents’, abbreviated as SDA. Because the host-guest relationship between the inorganic pore and the organic compound is not exactly matched, the term ‘template’ would be inappropriate in this case. Alkali-metal cations such as sodium or potassium are also the main components of the reactant mixture. They are known to accelerate the nucleation and crystal growth of zeolites [2], probably affecting the polymerization and depolymerization of the silicate species in the gel. When excessive amounts of alkali ions are used, layered silicates can be obtained. It seems that alkali-metal cations begin to compete with the organic molecules in a structure-directing role at high concentrations. When various heteroatoms are incorporated into the silicate framework, the bond length or bond angle of Si-O-X (X=heteroatom) is changed from the case for Si-O-Si, and different building blocks construct the crystalline structure. This new building block has also been applied to find new zeolite structures. Mineralizing agents are essential for zeolite synthesis as continual cleaving of Si-O bonds enables exploration of stable crystalline structures, since amorphous silicates would be obtained without mineralizing agents. OH<sup>-</sup> and F<sup>-</sup> are the only compounds employed as mineralizing agents. In addition, reacting time, temperature, seeds, aging, and status of reaction vessel (static or rotating) can influence the final zeolite structure. It can take from a few days to months to synthesize zeolites, also depending on the status of reactor, temperature, and seeds. When the reaction vessel is kept static in a convection oven, it takes longer than when the reaction vessel is rotated or stirred in the oven. Higher temperature syntheses usually require lower reacting time, and the use of seeds can also reduce the required reacting time. Different crystalline structures can be obtained by varying the time. For example, CIT-6 (3 days) and VPI-8 (7 days) evolve from the same gel in zincosilicate

synthesis[3, 4]. Thermodynamically, the most stable silicate, quartz, is often found after much longer reaction time. Typical temperatures for zeolite synthesis are 100~180°C. Open zeolite structures are synthesized more easily at lower temperature.

### 1.1.3. Synthesis Mechanism

The mechanism for zeolite synthesis is not fully understood. Recently, much effort has been concentrated to elucidate nucleation and crystal growth of zeolites, since zeolite nanoparticles have received much attention due to their various potential applications. About a decade ago, Davis et al. suggested the zeolite mechanism as shown in Fig.1-1. The simplest model for zeolite synthesis can be found in the synthesis of Si-ZSM-5 using tetrapropylammonium hydroxide (TPAOH). Only silica precursor (tetraethoxysilicate, TEOS), TPAOH, and water were used for the synthesis of Si-ZSM-5. TPA with intermediate hydrophobicity and hydrolyzed silica precursor have hydrophobic hydration sphere of ~1nm size. These two spheres overlap, driven by release of ordered water molecules around the spheres. The entropy increase is considered to be the main driving force to form aggregates consisting of TPA and silicate. The aggregates undergo further nucleation and crystal growth, and finally form zeolite. TPA is speculated to play a role in shaping the pore during the nucleation process. Recent work about the synthesis of silicate nanoparticles in the same condition found that particles with core-shell structure (silica at core and tetraalkylammonium at shell) are spontaneously formed [5]. These particles can be considered as primary units in Fig.1-1, but interestingly, the organic compounds occupy the shell. The exact mechanism of zeolite crystal nucleation should be investigated further. Also, it should be noted that zeolite synthesis is a kinetically controlled process, not thermodynamically controlled. The enthalpy change of pure

silica molecular sieves is in a range of 6.8~14.4kJ/mol less stable than that of quartz [6, 7]. This range (7.6kJ/mol) is comparable to twice the available thermal energy (6.2kJ/mol) at typical synthesis conditions. All known tetrahedrally coordinated SiO<sub>2</sub> polymorphs are only slightly metastable with respect to quartz. Therefore, the reaction pathway is critical for which crystalline phase can be obtained.

## 1.2. Strategies for Rational Design of Zeolite

All of the zeolites have effective pore sizes of less than 1nm. Presently, the maximum pore size for materials stable enough to be of commercial use is approximately 8Å [8]. This small pore size has restricted the applications of zeolites, hence the effort to synthesize zeolites with larger pores (especially 1~2nm) has been attempted for a long time. Zeolites with larger pores have huge potential in the areas of fine chemicals, pharmaceuticals, and nanotechnology. Phosphate-based materials such as VFI [9] or CLO [10], and mesoporous silicates such as M41S [11] or SBA [12] with amorphous character have been discovered in the middle of this effort. However, these materials are unstable in hydrothermal conditions unlike crystalline silicate materials, and they have insufficient acidity for application as catalysts. Silica-based crystalline materials with extra-large pores are still highly desired. Two general methodologies for the rational design of pore architecture and framework atom positioning have been applied to find these materials. First, the control of size, rigidity and hydrophobicity of the SDAs enables discovery of new zeolite structures. Second, the heteroatoms have been inserted to the gel in order to construct novel building blocks that can form new crystalline structures with larger pore volume. Additionally,

computational techniques have been adapted to assist the effort to synthesize zeolites with desired properties.

### 1.2.1. Organic Structure-Directing Agents

Liebau summarizes the conditions at which an organic guest will best form a clathrasil [13]. These conditions can be considered as requirements of SDAs for zeolite synthesis.

1. The molecule should have sufficient room within a particular cage or pore.
2. The molecule must be stable under the synthesis conditions.
3. The molecule should fit the inner surface of the cage with as many van der Waals contacts as possible, but with the least deformation.
4. The molecule should have only a weak tendency to form complexes with the solvent.
5. More rigid molecule will tend to form clathrasil easier than flexible molecules.
6. The tendency to form a clathrasil will increase with the basicity or polarizability of the guest molecule.

The first condition means that when the organic molecule is bigger than the polyhedral cage, steric forces inhibit the formation of the clathrasil. In the case of zeolite synthesis, the use of bigger SDAs often directs the formation of the zeolite with larger pores to a certain extent. For example, the SDAs of A, B, C, and D shown in Fig.1-2 directed the clathrasil nonasil, MTW, SSZ-31, and SSZ-31, respectively. When the reactant gel contained no organic molecules, quartz was synthesized [14]. As the size of the SDA increases, the synthesized product changes from a clathrasil to

a microporous large-pore molecular sieve. Secondly, the SDA should endure harsh conditions, often with high basicity and high temperature during zeolite synthesis. Decomposed SDA can easily affect the structure of the product. Thirdly, if the SDA should be deformed to accommodate inside a certain pore shape of a zeolite, the distortion tension will easily disrupt the formation of the crystalline structure. The organic molecules should be stabilized inside the inorganic crystalline phase via as many van der Waals interactions as possible. Fourthly, when the zeolite is synthesized in hydrothermal conditions with aqueous solution, the SDA should have intermediate hydrophobicity. To evaluate the hydrophobicity of the organic SDA, Zones has studied the transfer of different charged SDAs from an aqueous solution to a chloroform phase as a function of the  $C/N^+$  ratio [15]. He found that the percentage of transfer is low (less than 10%) for tetraethylammonium with  $C/N^+=8$  and that it is very large (more than 70%) for tetrabutylammonium with  $C/N^+=16$ . The various organic molecules with intermediate hydrophobicity of  $C/N^+=9\sim 15$  including tetrapropylammonium with  $C/N^+=12$  work well as SDAs yielding a variety of zeolitic materials. Fifthly, When the SDA is flexible, there will be many metastable states of inorganic-organic composites (such as aggregates shown in Fig.1-1) that the SDA conforms to. This will lead to competition among those metastable states, and additional factors such as addition of alkali ions and different temperatures might determine the final phase. In this case, the structure-directing effect of the organic molecules is considered to be weak. On the contrary, rigid organic molecules will have very limited conformational configurations and will produce the same crystalline phase across various synthesis conditions. Finally, higher pH has influence on the kinetics of silicate hydrolysis. The basicity of the organic molecules assists the silicate

hydrolysis, and their polarizability stabilizes the whole system with the electric field caused by the partial ionic character of the Si-O bonds.

The produced zeolite phase is known to depend more on the size and shape of the organic molecules rather than the chemical properties of the SDA[16]. When the SDA is small, the effect of the shape is not critical. The thermal motion of the SDA at high temperature easily covers the difference in the shape. The various organic molecules shown in Fig. 1-3 directed the same structure of DOH. When there is a good geometrical fit in the organic-inorganic composites by van der Waals contacts, the change in the shape of the organic molecules results in synthesizing different zeolite phases. For example, diethylamine and dipropylamine form ZSM-48 with linear 10MR pore structure, but triethylamine and tripropylamine form ZSM-5 with multidimensional 10MR pore structure. The transition from unidimensional to multidimensional zeolite has been achieved by changing the geometry of the organic SDA from linear to branched.

Table 1 shows zeolites discovered by using new SDAs: CIT-1 (CON) with 12MR and 3-dimensional pore structure (3-D), UTD-1 (DON) with 14MR and 1-D, CIT-5 (CFI) with 14MR and 1-D, STA-6 (SAS) with 8MR and 1-D, STA-7 (SAV) with 8MR and 3-D, SSZ-35 (STF) with 10MR and 1-D, SSZ-36 and SSZ-39 (Intergrowth of ITE and RTH) with 8MR and 2-D, SSZ-53 (SFH) with 14MR and 1-D, SSZ-55 (ATS) with 12MR and 1-D. It should be noted that organic (or organometallic) molecules were successfully used to find extra-large pore (with 14MR) pure silicate structures such as CIT-5 and UTD-1. Organic molecules with various sizes, shapes, and chemical properties have been studied to synthesize zeolites with larger pores in various research groups.

In addition to synthesizing new zeolite structures, organic SDAs have been used for controlling the crystal growth of zeolites. In the study to fabricate high-permeance, high-separation factor zeolite membrane, the crystal orientation of silicalite was controlled by modifying SDAs as shown in Fig. 1-4. The use of dimer-TPA or trimer-TPA as SDA enhances the growth of silicalite crystal in the b-direction significantly, and the membrane showed superior performance for the separation of organic mixtures with small differences in size and shape, such as xylene isomers[17]. Heteroepitaxial growth of a zeolite film with a patterned surface-texture has been achieved by controlled usage of SDA[18]. Large sodalite crystals were synthesized without using any organic component first, and then chabazite grew heteroepitaxially on the sodalite substrate by using a different reactant mixture containing TMA.

### 1.2.2. Novel building blocks

In addition to efforts to make zeolites with larger pore sizes, effort has also been concentrated on synthesizing zeolites with lower framework density (FD), defined as the number of tetrahedral atoms (T) per  $\text{nm}^3$ . It is known that the range of FD values in zeolites depends on the type and relative number of the smallest rings in the tetrahedral networks[19]. The frameworks of the lowest density are those with a maximum number of 4-rings. Piccione et al. also showed that molecular sieves consisting mostly of zero or one 4MR such as AFI, MTW, MFI, MEL, FER, and CFI are the most stable structures with higher FD, whereas those that contain mainly triple 4MR such as CHA, ISV, FAU, and AST are the least stable structures with lower FD[6]. Therefore, if zeolitic materials with low FD are to be synthesized, frameworks with T atoms mostly bonded to multiple 3, 4MR will have to be prepared. Double 4MR structure (D4MR) with cubic shape has been investigated as a novel building

block to synthesize zeolites with lower FD. The number of molecular sieve structures that contain D4MR units is very small (Zeolite A, octadecasil, and ISV). D4MRs can be stabilized by  $F^-$  media since  $F^-$  is located inside the D4MR and stabilizes this type of atomic arrangement.  $F^-$  can also replace  $OH^-$  in the zeolite synthesis as a mineralizing agent. The fluoride-based synthesis route combined with remarkably low concentration of water has led to many discoveries including the synthesis of all-silica molecular sieve materials for the first time and the synthesis of entirely novel framework structures[20]. D4MR can be additionally stabilized by incorporation of heteroatoms such as  $Ge^{4+}$ . When the D4MR is constructed by  $Si^{4+}$  alone, the Si-O-Si angle must be close to  $145^\circ$  for the tetrahedron to be regular. When  $Ge^{4+}$  is introduced, so that Ge-O-Si bond is formed, D4MRs become more relaxed, thus more stabilized. Pure polymorph C of zeolite beta which remained elusive for a long time has been synthesized using this strategy, named ITQ-24[21]. The stabilizing effect of  $Ge^{4+}$  for D4MR has led to the additional synthesis of three new structures, ITQ-15, ITQ-21, ITQ-22, all of which contain D4MRs. ITQ-15 is the first extra-large pore zeolite with intersecting 14- and 12- ring channels[22]. ITQ-21 has the largest void volume ever reported ( $0.24\text{cm}^3/\text{g}$ ) with a three-dimensional pore network containing 1.18nm diameter cavities, each of which is accessible through six circular, 0.74nm diameter windows. ITQ-22 is the first reported zeolite containing fully interconnected 8-, 10-, and 12-membered ring pores. On the other hand, synthesizing zeolites with 3MR has also been tried to create more open structures. The introduction of  $Be^{2+}$ ,  $Mg^{2+}$ ,  $Zn^{2+}$ , and even  $Li^+$  in framework positions can provide the necessary flexibility in one of the 3MR  $TO_4$  tetrahedral to stabilize its accommodation in a four-connected framework. Beryllsilicates with low FD were synthesized, such as OSB-1 with 3MR only ( $13.3\text{T}/\text{nm}^3$ ) or OSB-2 with dominantly 3MR ( $12.7\text{T}/\text{nm}^3$ ), but the high toxicity

of Be has induced active research for synthesizing zeolites with dominantly 3MR using other ions such as  $Zn^{2+}$ .

### 1.2.3. Computational Calculations

Computer modeling has been shown to be a valuable tool for investigating the structure and reactivity of zeolites. As with experimental studies, work has concentrated on the location and diffusion of molecules within the pores. Recently, computational techniques have been actively used to evaluate the effectiveness of SDAs for rational design of particular zeolite structures. Also, the stability of the zeolite framework itself has been studied by using various simulation techniques.

The crystallization rate of zeolites in the presence of different SDAs has been correlated with calculated interaction energies of the SDA with the framework. Lewis et al. demonstrated that for successful structure-direction, the favorable nonbonding interaction between the SDA and the framework must be maximized, and the SDA molecules must be able to pack efficiently within the framework[23]. They calculated nonbonded interaction energy and stabilization energy of SDAs in various zeolite frameworks (e.g. tetraalkylammonium cations (TMA, TEA, TPA, TBA) in ZSM-5, ZSM-11, and  $\beta$  or bis-quaternary amines (tri, tetra, penta, hexa, hepta, octamethonium) in EU-1 and ZSM-23). Sastre et al. also studied the stability of  $\beta$ , EU-1, ZSM-11 and ZSM-12 when cyclohexylalkyl pyrrolidinium salts are used as the SDA[24]. They found that the stabilization of intermediate species during nucleation appears to orient the final synthesis result. Fig.1-5 shows how a balance between kinetic and thermodynamic factors can contribute to the synthesis outcome throughout the nucleation and crystallization processes. Path 1 requires less activation energy for the nucleation (kinetically favorable), and path 2 gives the most stable final structure

(thermodynamically favorable). Since energy difference in different nuclei ( $E(Z_1\text{-SDA})-E(Z_2\text{-SDA})$ ) is sometimes slight, small changes in the properties of an SDA can result in different final products. The same authors later successfully controlled the produced zeolite structure by estimating zeolite-SDA interaction when related structures compete and small difference in this interaction may shift the synthesis toward one or the other structure[25]. Two closely related zeolitic structures, ISV and BEC, that strongly compete during the crystallization process were synthesized separately by using modified SDAs that had been predicted by *a priori* computational results. Additionally, molecular dynamics studies have been done on the role of tetramethylammonium cations in the stability of the silica octamers  $\text{Si}_8\text{O}_{20}^{8-}$  in solution to elucidate the nucleation step[26].

The stability of porous zeolite frameworks themselves have also been studied to give practical advice for actual synthesis. Zwijnenburg et al. showed how the topology and energetics of the constituent cages can lead to estimating the stability of large pore/channel materials[8]. Zeolites were decomposed into space-filling sets of face-sharing polyhedral units to evaluate their stability. They found that large pores require compensation by small faces and extra-large pore zeolites should consist of large polyhedra to be more energetically stable. Hence, steering the synthesis mixture toward small rings and large cages most likely offers a route to extra-large pore zeolites. Curtis and Deem also pointed that the flatness of rings can represent the stability of zeolites[27]. Comparison of the flatness distribution of known zeolites to those of the hypothetical zeolites shows that it should be possible to synthesize zeolites containing at least somewhat flat rings with greater than 12 members. They suggested that the main stumbling factor in the formation of large pores is not thermodynamics but rather identification of suitable SDAs.

### **1.3. Removal of Organic SDAs From the Zeolite Pores**

After the synthesis of zeolite and molecular sieve materials, the resulting solid is non-porous because the organic SDAs are trapped in the cavities of the solid. To obtain a completely porous solid, it is necessary to remove the SDA from the as-made materials. Factors such as pore size, size of SDA, and interaction of the SDA and zeolite framework can affect the removal of the SDA. The methods that have been used to remove the organic SDA are shown and their limitations are discussed below.

#### **1.3.1. Calcination**

The most common method to remove the organic components from the pores is calcination. The organic species are removed by combustion at high temperature in a flow of oxygen or air. Fig. 1-6 shows typical conditions used for calcination of crystalline inorganic materials. The final temperature can easily go up to 700°C in some cases. During this calcination, high local temperature and water formation may occur, and therefore extra-framework species may be formed. This is the case for some aluminosilicates where extra-framework aluminum species can be detected after removal of the template by calcination. For example, when zeolite  $\beta$  is calcined and steamed severely, a substantial portion of the framework aluminum is completely hydrolyzed, and non-framework aluminum species are generated[28]. This leads to significant reduction in its catalytic activity. There can also be a high exotherm when the organic compound burns inside the pore. The exotherm may destroy the inorganic framework, and this often occurs for weaker inorganic crystalline materials with open

frameworks. Besides, the organic components are completely destroyed into  $\text{CO}_2$ ,  $\text{NO}_x$ , and  $\text{H}_2\text{O}$  by calcination. This is a waste of expensive organic species. The cost of organic molecules contributes up to 25% of overall zeolite synthesis cost in industry. As the effort to find extra-large pore zeolites is being done by using larger and more complicated organic molecules, the cost of organic molecules in zeolite synthesis would be a bigger problem for industrial applications. Even if new zeolites with desired properties are synthesized by a new, but expensive SDA, the new discovery may remain an academic concern only due to low economical efficiency. Additionally, there are  $\text{NO}_x$ -containing gas effluents during calcination since nitrogen containing compounds such as amines or ammonium ions are usually used as SDAs. This  $\text{NO}_x$  must be treated further to meet environmental regulation in industry, and this can be an additional cost for zeolite synthesis. As novel applications of zeolitic materials emerge, high temperature procedures become undesirable due to incompatibility with other procedures.

### 1.3.2. Extraction

The other way to remove organic SDAs from zeolitic materials is extraction. Many novel methods such as microwave-assisted template removal, extraction with supercritical  $\text{CO}_2$ , and ozone treatment have been successfully used to remove organic templates from mesoporous silica such as MCM-41 and SBA-15[29]. Those methods can remove the organic components more easily due to larger pore sizes and weak framework-surfactant interaction of mesoporous materials. The organic template and MCM-41 is bound by electrostatic interaction while van der Waals or hydrogen bonding interaction is a main force connecting organic species and SBA-15. Hence, the organic molecules inside SBA-15 are more easily removed than inside MCM-41.

In the case of zeolitic materials, however, the pore size is much smaller, pore channel often has a smaller diameter than pore cage, and the electrostatic interaction between SDA and framework is stronger. Therefore, there are limited cases where the SDA can be removed by extraction. Jones et al. reported SDA removal by extraction from MFI or BEA structure[30]. The amount of SDA that could be removed by extraction was found to be dependent on the size of the SDA and the strength of its interaction with the molecular sieve framework. The effect of strength of interaction was estimated by using BEA with different heteroatoms such as Zn, B, and Al. However, the SDA was only partly extracted except TEA from pure silica zeolite  $\beta$ , and heteroatoms were removed from the framework during extraction. For instance, 60% of boron was removed from the framework during solvent extraction with aqueous acetic acid.

### 1.3.3. Need for a New Strategy to Remove SDA

As explained in the previous sections, calcination and extraction are the only two methods able to remove SDAs, and they have many undesired aspects. A new method to remove SDAs completely without using high temperature procedures is highly desired. A combustion-free methodology to synthesize zeolite and zeolite-like materials was proposed, and it was shown that the methodology can be used to prepare porous zeolites in the following chapter. The limitation of the proposed methodology was described and an additional strategy to overcome the problem was provided in Chapter 3. The methodology has been applied to synthesize various structures of zeolites and the important factors for success of the proposed methodology were investigated in Chapter 4. Potential applications of the methodology were suggested in Chapter 5.

## References

1. P.P.E.A. de Moor, T.P.M. Beelen, B.U. Komanschek, O. Diat, and R.A.V. Santen, Imaging the assembly process of the organic-mediated synthesis of a zeolite, *Chem. Eur. J.* 5 (1999) 2083.
2. M. Goepper, H.X. Li, and M.E. Davis, A possible role of alkali metal ions in the synthesis of pure-silica molecular sieves, *Journal of the Chemical Society, Chemical Communications* (1992) 1665.
3. T. Takewaki, L.W. Beck, and M.E. Davis, Synthesis of CIT-6, a zincosilicate with the \*BEA topology, *Topics in Catalysis* 9 (1999) 35.
4. T. Takewaki, L.W. Beck, and M.E. Davis, Zincosilicate CIT-6: A precursor to a family of \*BEA-type molecular sieves, *J. Phys. Chem. B* 103 (1999) 2674.
5. J. Fedeyko, J.D. Rimer, R.F. Lobo, and D. Vlachos, The spontaneous formation of silica nanoparticles in basic solution of small tetraalkylammonium cations, *J. Phys. Chem. B* In print (2005)
6. P.M. Piccione and M.E. Davis, Thermochemistry of pure-silica zeolites, *J. Phys. Chem. B* 104 (2000) 10001.
7. P.M. Piccione, S. Yang, A. Navrotsky, and M.E. Davis, Thermodynamics of pure-silica molecular sieve synthesis, *J. Phys. Chem. B* 106 (2002) 3629.
8. M.A. Zwijnenburg, S.T. Bromley, J.C. Jansen, and T. Maschmeyer, Toward understanding extra-large-pore zeolite energetics and topology: A polyhedral approach, *Chem. Mater.* 16 (2004) 12.
9. M.E. Davis, C. Saldarriaga, C. Montes, J. Garces, and C. Crowder, A molecular sieve with eighteen-membered rings, *Nature* 331 (1988)

10. M. Estermann, L.B. McCusker, C. Baerlocher, A. Merrouche, and H. Kessler, A synthetic gallophosphate molecular sieve with a 20-tetrahedral-atom pore opening, *Nature* 352 (1991) 320.
11. C.T. Kresge, M.E. Leonowicz, W.J. Roth, J.C. Vartuli, and J.S. Beck, Ordered mesoporous molecular sieves synthesized by a liquid-crystal template mechanism, *Nature* 359 (1992) 710.
12. Q. Huo, D.I. Margolese, U. Ciesia, P. Feng, T.E. Gier, P. Sieger, R. Leon, P.M. Petroff, F. Schuth, and G.D. Stucky, Generalized synthesis of periodic surfactant/inorganic composite materials, *Nature* 368 (1994) 317.
13. F. Liebau, *Structural Chemistry of Silicates*. 1985, Berlin: Springer-Verlag. 242.
14. Y. Nakagawa and S.I. Zones, in *Synthesis of Microporous Materials*, M.L. Occelli and H. Robson, Editors. 1992, Van Nostrand Reinhold: New York. p. 222.
15. M.E. Davis and S.I. Zones, *A perspective on zeolite synthesis : How do you know what you'll get?*, in *Synthesis of Porous Materials : Zeolites, Clays, and Nanostructures*, M.L. Occelli and H. Kessler, Editors. 1997, Dekker. p. 1.
16. R.F. Lobo, S.I. Zones, and M.E. Davis, Structure-direction in zeolite synthesis, *Journal of Inclusion Phenomena and Molecular Recognition in Chemistry* 21 (1995) 47.
17. Z. Lai, G. Bonilla, I. Diaz, J.G. Nery, K. Sujaoti, M.A. Amat, E. Kokkoli, O. Terasaki, R.W. Thompson, M. Tsapatsis, and D.G. Vlachos, Microstructural optimization of a zeolite membrane for organic vapor separation, *Science* 300 (2003) 456.

18. T. Wakihara, S. Yamakita, K. Iezumi, and T. Okubo, Heteroepitaxial growth of a zeolite film with a patterned surface-texture, *J. Am. Chem. Soc.* 125 (2003) 12388.
19. G.O. Brunner and W.M. Meier, Framework density distribution of zeolite-type tetrahedral nets, *Nature* 337 (1989) 146.
20. S.I. Zones, S.-j. Hwang, S. Elomari, I. Ogino, M.E. Davis, and A.W. Burton, The fluoride-based route to all-silica molecular sieves; a strategy for synthesis of new materials based upon close-packing of guest-host products, *C.R. Chimie* in print (2005)
21. A. Corma, M.T. Navarro, F. Rey, J. Rius, and S. Valencia, Pure polymorph C of zeolite beta synthesized by using framework isomorphous substitution as a structure-directing mechanism, *Angew. Chem. Int. Ed.* 40 (2001) 2277.
22. A. Corma, M.J. Diaz-Cabanas, F. Rey, S. nicolopoulos, and B. Boulayha, ITQ-15: The first ultralarge pore zeolite with a bi-directional pore system formed by intersecting 14- and 12-ring channels, and its catalytic implications, *Chem. Commun.* 12 (2004) 1356.
23. D.W. Lewis, C.M. Freeman, and C.R.A. Catlow, Predicting the templating ability of organic additives for the synthesis of microporous materials, *J. Phys. Chem.* 99 (1995) 11194.
24. G. Sastre, S. Leiva, M.J. Sabater, I. Gimenez, F. Rey, S. Valencia, and A. Corma, Computational and experimental approach to the role of structure-directing agents in the synthesis of zeolites : The case of cyclohexyl alkyl pyroliidinium salts in the synthesis of beta, EU-1, ZSM-11, and ZSM-12 zeolites, *J. Phys. Chem. B* 107 (2003) 5432.

25. G. Sastre, A. Cantin, M.j. Diaz-Cabanas, and A. Corma, Searching organic structure directing agents for the synthesis of specific zeolitic structures: An experimentally tested computational study, *J. phys. Chem. B* (2005)
26. S. Caratzoulas, D.G. Vlachos, and M. Tsapatsis, Molecular dynamics studies on the role of tetramethylammonium cations in the stability of the silica octamers Si<sub>8</sub>O<sub>20</sub>(8-) in solution, *J. Phys. Chem. B* In print (2005)
27. R.A. Curtis and M.W. Deem, A statistical mechanics study of ring size, ring shape, and the relation to pores found in zeolites, *J. Phys. Chem. B* 107 (2003) 8612.
28. G.H. Kuehl and H.K.C. Timken, Acid sites in zeolite beta : Effects of ammonium exchange and steaming, *Micropor. Mesopor. Mater.* 35-36 (2000) 521.
29. j. Patarin, mild methods for removing organic templates from inorganic host materials, *Angew. Chem. Int. Ed.* 43 (2004) 3878.
30. C.W. Jones, K. Tsuji, T. Takewaki, L.W. Beck, and M.E. Davis, Tailoring molecular sieve properties during SDA removal via solvent extraction, *Microporous and Mesoporous Mater.* 48 (2001) 57.
31. R.F. Lobo and M.E. Davis, CIT-1: A New Molecular Sieve with Intersecting Pores Bounded by 10- and 12- Rings, *J. Am. Chem. Soc.* 117 (1995) 3766.
32. C.C. Freyhardt, M. Tsapatsis, R.F. Lobo, K.J. Balkus, and M.E. Davis, A high-silica zeolite with a 14-tetrahedral-atom pore opening, *Nature* 381 (1996) 295.
33. P. Wagner, M. Yoshikawa, M. Lovallo, K. Tsuji, M. Tsapatsis, and M.E. Davis, CIT-5 : a high-silica zeolite with 14-ring pores, *Chem. Commun.* (1997) 2179.

34. R. Garcia, E.F. Philip, A.M.Z. Slawin, P.A. Wright, and P.A. Cox, Nickel complexed within an azamacrocycle as a structure directing agent in the crystallization of the framework metalloaluminophosphates STA-6 and STA-7, *Journal of Materials Chemistry* 11 (2001) 1421.
35. P.A. Wright, M.J. Maple, A.M.Z. Slawin, V. Patinec, R.A. Aitken, S. Welsh, and P.A. Cox, Cation-directed syntheses of novel zeolite-like metalloaluminophosphates STA-6 and STA-7 in the presence of azamacrocycle templates, *J. Chem. Soc., Dalton Trans.* (2000) 1243.
36. P. Wagner, Y. Nakagawa, G.S. Lee, M.E. Davis, S. Elomari, R.C. Medrud, and S.I. Zones, Guest/host relationships in the synthesis of the novel cage-based zeolites SSZ-35, SSZ-36, and SSZ-39, *J. Am. Chem. Soc.* 122 (2000) 263.
37. S.I. Zones and S.-J. Hwang, Synthesis of high silica zeolites using a mixed quaternary ammonium cation, amine approach : Discovery of zeolite SSZ-47, *Chem. Mater.* 14 (2002) 313.
38. A. Burton, S. Elomari, C.Y. Chen, R.C. Medrud, I.Y. Chan, L.M. Bull, C. Kibby, T.V. Harris, S.I. Zones, and E.S. Vittoratos, SSZ-53 and SSZ-59: two novel extra-large pore zeolites, *Chem. Eur. J.* 9 (2003) 5737.
39. M.G. Wu, M.W. Deem, S.A. Elomari, R.C. Medrud, S.I. Zones, T. Maesen, C. Kibby, C.-Y. Chen, and I.Y. Chen, Synthesis and structure determination by ZEFSAII of SSZ-55 : A new high-silica large-pore zeolite, *J. Phys. Chem. B* 106 (2002) 264.

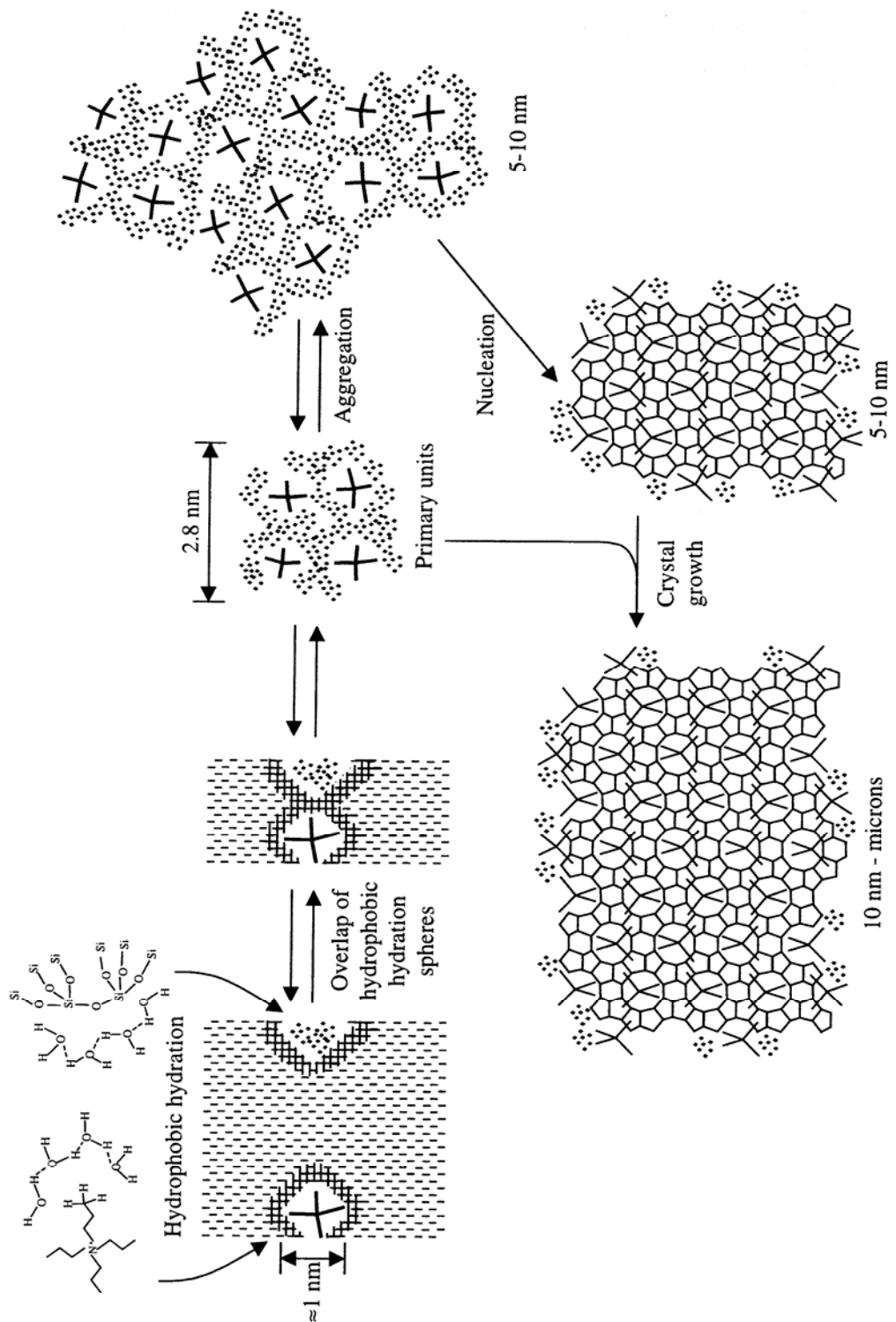


Figure 1-1. Proposed mechanism for zeolite synthesis: Synthesis of ZSM-5 using tetrapropylammonium cations [1].

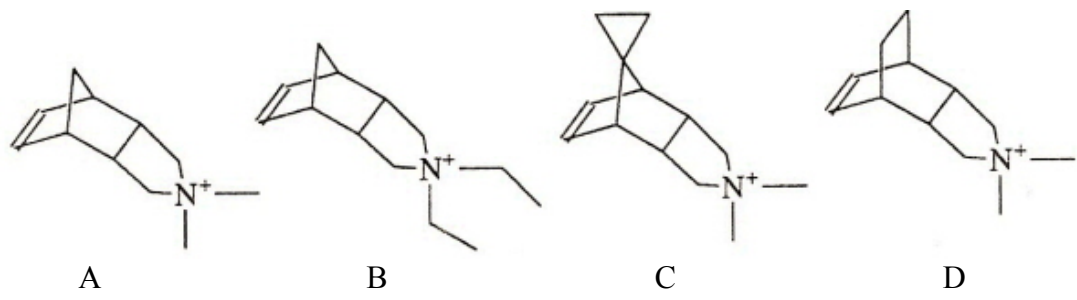


Figure 1-2. The size effect of organic molecules in the synthesis zeolites [16].

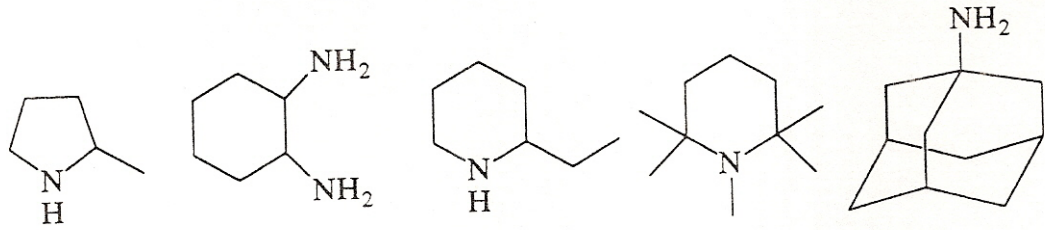


Figure 1-3. The effect of various shapes for zeolite synthesis in the case of small SDAs [16].

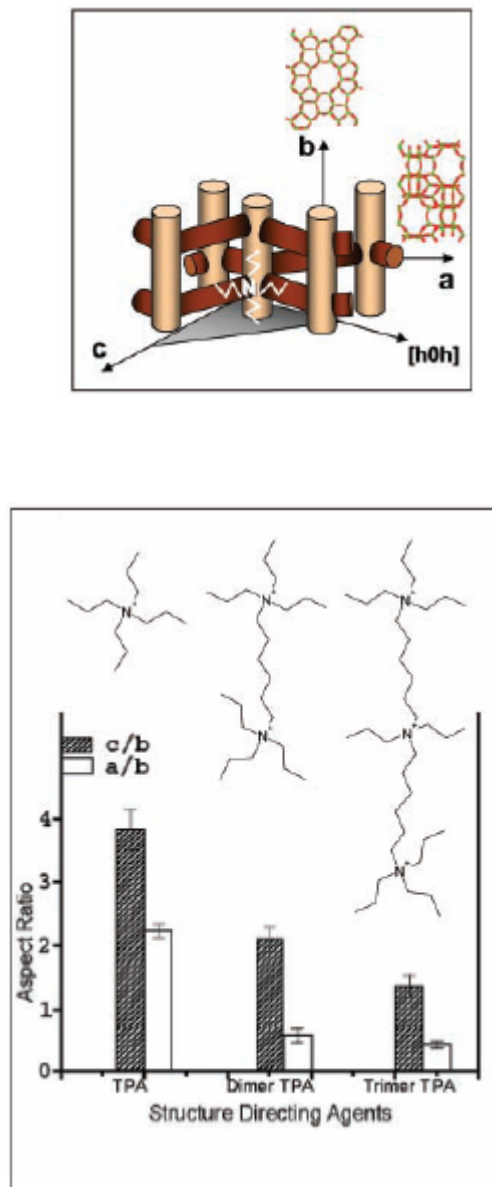


Figure 1-4. Top: A schematic representation of ZSM-5 crystal structure. Bottom: The effect of the different SDAs on the crystal shape is quantified in a comparison of the aspect ratio of the crystals [height/depth and width/depth] synthesized in the presence of TPA, dimer-TPA, and trimer-TPA [17].

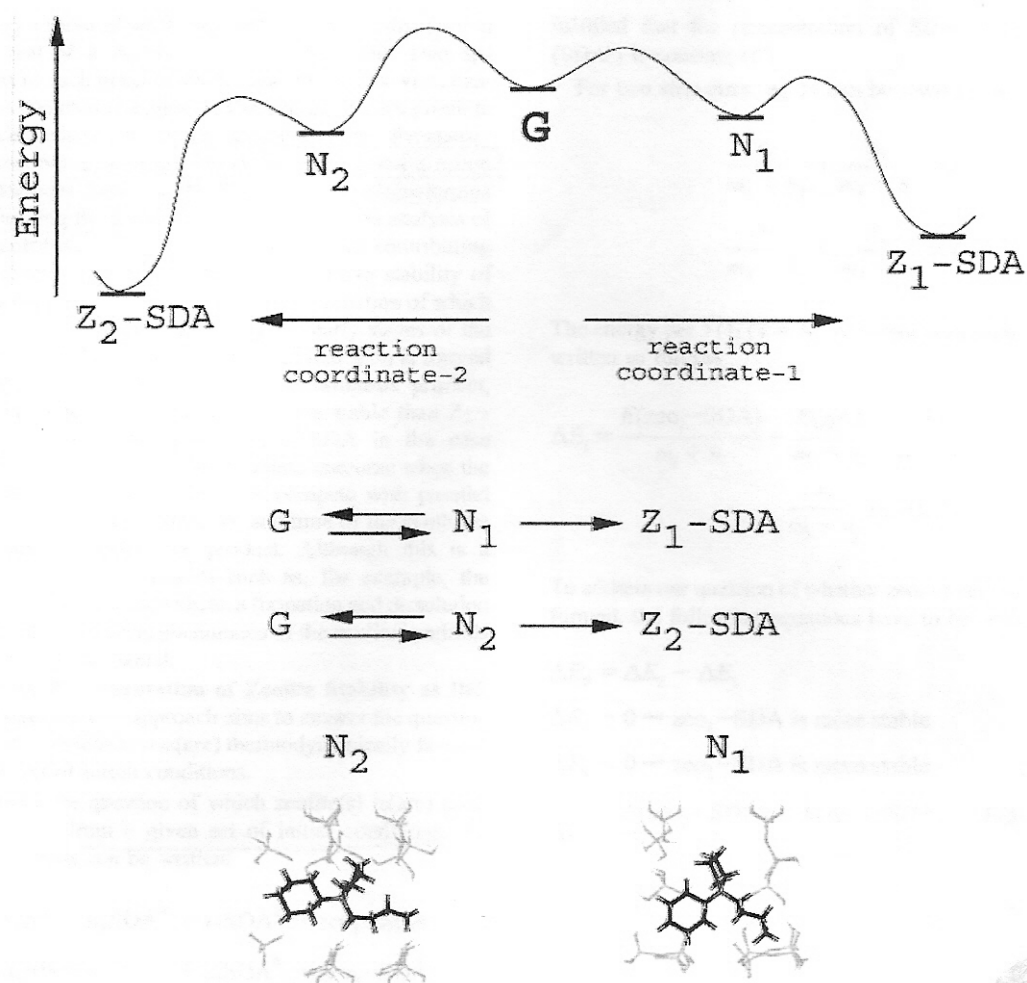


Figure 1-5. Top: Energy scheme for the synthesis of two zeolite structure (Z) in the presence of a SDA starting from the same gel (G) and going through different nuclei (N). Middle: Proposed mechanism with a reversible nucleation followed by the crystallization. *Bottom*: Nuclei form when silicoalumina oligomers surround the SDA, giving an aggregate resembling a significant part of a structure [24].

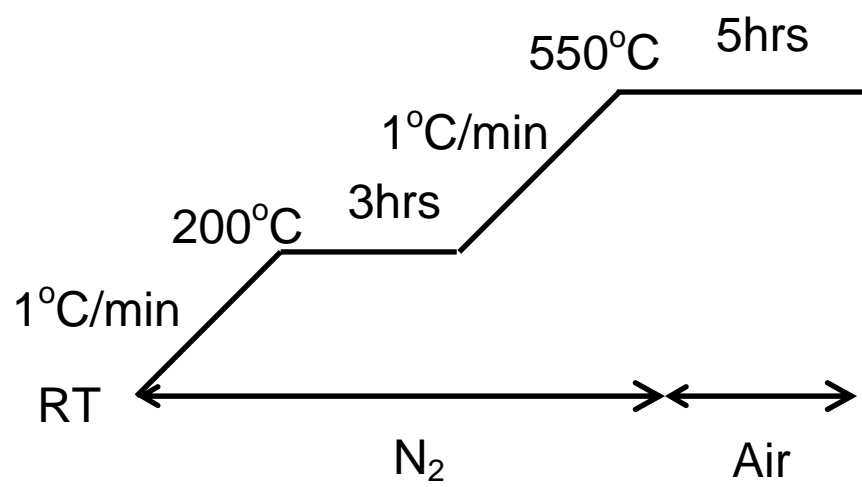


Figure 1-6. Typical temperature profile and gas flow for calcination.

Table 1-1. Zeolites that were newly discovered by using unique organic molecules.

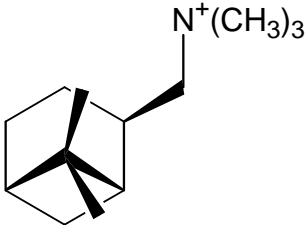
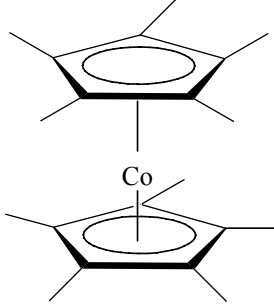
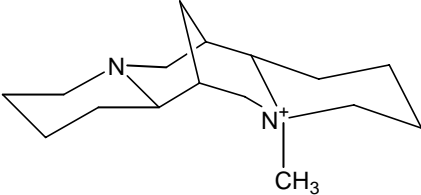
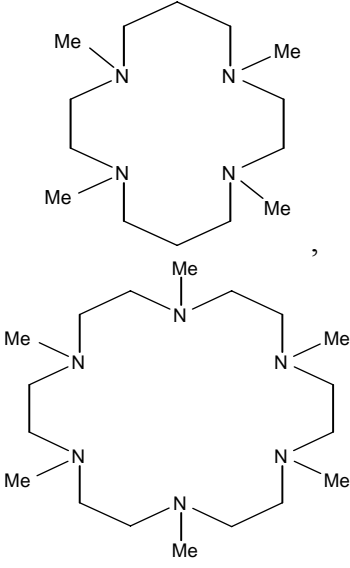
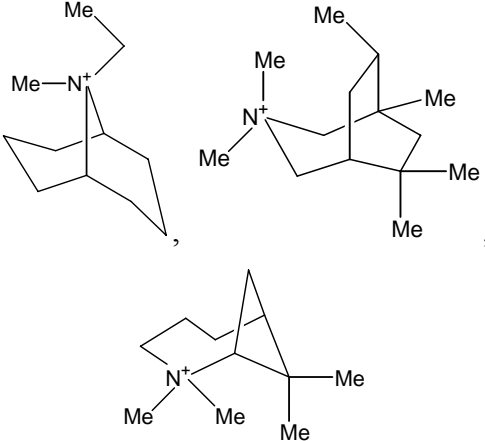
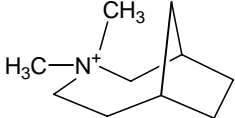
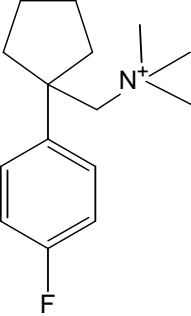
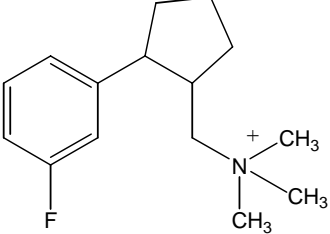
Zeolite	Structure-Directing Agents	Year	Ref.
CIT-1 (CON)		1995	[31]
UTD-1 (DON)		1996	[32]
CIT-5 (CFI)		1997	[33]
STA-6 (SAS), STA-7 (SAV)		2000	[34, 35]

Table 1. Cont'd

Zeolite	Structure-Directing Agents	Year	Ref.
SSZ-35 (STF), SSZ-36 (ITE- RTH), SSZ-39 (AEI)		2000	[36]
SSZ-47		2002	[37]
SSZ-53 (SFH)		2003	[38]
SSZ-55 (ATS)		2002	[39]

## **Chapter Two**

Proposal of a New Methodology and Its Proof of Concept

(Modified from ‘H. Lee., S. I. Zones, and M. E. Davis, A Combustion-Free Methodology for Synthesizing Zeolite and Zeolite-like Materials, *Nature* 425, 395-398 (2003)’)

## 2.1. Proposal of a Combustion-Free Methodology

Zeolites are mainly used for the adsorption and separation of ions and small molecules, and as heterogeneous catalysts. More recently, these materials are receiving attention in other applications such as medical diagnosis and as components in electronic devices<sup>1</sup>. Modern synthetic methodologies for preparing zeolites and zeolite-like materials typically involve the use of organic molecules that direct the assembly pathway and ultimately fill the pore space<sup>2-6</sup>. Removal of these enclathrated species normally requires high temperature combustion that destroys this high cost component, and the associated energy release in combination with the formed water can be extremely detrimental to the inorganic structure<sup>7</sup>. Here, we report a new synthetic methodology that avoids the aforementioned difficulties by creating organic structure-directing agents (SDAs) that can be disassembled within the zeolite pore space to allow removal of their fragments for use again by reassembly. The methodology is shown for the synthesis of zeolite ZSM-5 using a SDA that contains a cyclic ketal group that is removed from the SDA while it is inside the zeolite without destruction of the inorganic framework. This new methodology will have broad applications for the synthesis of a wide variety of inorganic and organometallic structures.

The elimination of high temperature treatments for SDA removal from crystalline structures is very desirable for many reasons in addition to the loss of the expensive SDA. For example, zeolite films that are used as molecular sieving membranes are susceptible to cracking at high temperature treatments for SDA removal because of mechanical stresses placed on the membrane by thermal expansion mismatches with supporting substrates. Newer, molecular sieve low dielectric components<sup>8</sup> may also

benefit from the ability to remove the “guest” organic molecule using only moderate heating, rather than combustion. This is because they require air to fill the microporous space in order to achieve their desired properties and will be components of devices that may not be compatible with high temperature processing steps<sup>1</sup>.

Ordered, mesoporous materials can be prepared using organic components such as surfactants that can form organized aggregates that contain large numbers of molecules that ultimately fill the pore space of the as-synthesized solids<sup>9,10</sup>. Unlike crystalline microporous materials, the mesoporous solids allow for the extraction of the organic structure-directing components<sup>11-13</sup>. This is due to the fact that the individual molecules that form the assembled structure-directing components are held together by weak forces that are easily disrupted and are each sufficiently small to be removed through the relatively large mesopores. Additionally, the interaction energies between the organic and inorganic fractions in the ordered, mesoporous materials are not as large as with microporous materials where SDA molecules-framework interactions can be quite strong, e.g. interaction enthalpies between the silica framework and the organic SDA have been measured as large as  $-181 \pm 21$  kJ/mol SDA<sup>14</sup>. The ability to remove and recycle the organic components allows for low-cost preparation of ordered, mesoporous materials.

Our new synthetic strategy for microporous crystalline molecular sieves (Fig. 2-1) eliminates any high temperature processing steps and the destruction of the SDA. Conceptually, the strategy is to assemble a SDA from at least two components using covalent bonds and/or non-covalent interactions that are able to survive the conditions for assembly of the zeolite, and yet be reversed inside the microporous void space. The fragments formed from the SDA in the zeolite can then be removed from the inorganic framework and be re-combined for use again. This procedure differs from

that employed with mesoporous materials in that the number of components used to create the SDA is small, e.g. less than five, and the SDA is a homogeneous, well-defined entity.

## 2.2. Proof of Concept

We demonstrate our synthetic methodology with a new SDA that contains a cyclic ketal and use it to assemble the zeolite ZSM-5 (Fig.2-2). Commercially available 1,4-dioxo-8-azaspiro[4,5]decane was quaternized using methyl iodide to give **1** (Scheme 1). Using **1** in its hydroxide form, the following reaction composition gave ZSM-5 (sub-micron crystals observed in SEM – see Figure 2-3) ; 0.033 **1** : 0.238 KOH : 0.056 Al(OH)<sub>3</sub> : 42.23 H<sub>2</sub>O : 1.0 SiO<sub>2</sub> (Fig. 2-4a). In the absence of the SDA, this reaction mixture does not yield ZSM-5. As-synthesized ZSM-5 has an elemental composition of 40.27 wt% Si, 2.31 wt% Al, 2.25 wt% K, 3.45 wt% C, 0.97 wt% H, 0.45 wt% N. The SiO<sub>2</sub>/Al<sub>2</sub>O<sub>3</sub> ratio was estimated from these analyses to be 33.5.

The choice of using a cyclic ketal was to provide for a SDA that would remain intact at zeolite synthesis conditions (high pH) and be cleavable at conditions that would not destroy the assembled zeolite (low pH). **1** was expected to be cleaved into **2** and ethylene glycol under acidic condition. Figure 2-5 shows the <sup>13</sup>C cross polarization magic angle spinning (CP MAS) NMR spectra from the ZSM-5 after various treatments. The spectrum in Fig. 2-5a shows that the as-synthesized material contains intact **1**. When the ZSM-5 was contacted with 1M HCl solution at 80°C for 20 hrs, the <sup>13</sup>C CP MAS NMR spectrum obtained (Fig. 2-5b) is consistent with the presence of the ketone fragment as illustrated in Scheme 1. The carbonyl of **2** was also detected by IR (1741cm<sup>-1</sup>), and the weight of the organic components as assessed

by thermogravimetric weight losses at temperatures between 200 and 700°C decreased from 6.2 wt% to 4.6 wt% (consistent with the loss of ethylene glycol). The HCl solution after the cleavage reaction was collected, concentrated, and then analyzed by  $^{13}\text{C}$  NMR. Only ethylene glycol was detected at 62.8ppm. The powder X-ray diffraction pattern of the treated sample reveals that the ZSM-5 remains intact after HCl treatment (Fig. 2-4b). Alternatively, a gas-phase cleavage reaction was performed using  $\text{H}_2\text{O}$ -saturated  $\text{HCl}(\text{g})$  at 120°C for 3hrs. The  $^{13}\text{C}$  CP MAS NMR spectrum of the treated ZSM-5 was the same as that shown in Fig. 2-5b except that ethylene glycol was also detected. These results showed that **1** can be cleaved into the desired pieces inside the zeolite pore space.

While ethylene glycol can be extracted easily, **2** remains inside the pores because of strong ionic interaction with the anionic framework. Ion-exchange was used to remove these positively charged organic fragments. Exposure to a mixture of 0.01M NaOH and 1M NaCl at 100°C for 72 hrs removed **2** (Fig. 2-5c and no carbonyl peak observed in IR). Additionally, the ion-exchanged ZSM-5 now has porosity ( $\text{N}_2$  adsorption capacity of 0.14 cc liquid  $\text{N}_2$  /g dry ZSM-5) that was not present prior to this treatment (as-synthesized ZSM-5 showed no microporosity while the calcined ZSM-5 gave 0.15 cc/g). When the as-synthesized solid was not treated with HCl solution, the ion-exchange step did not cause the removal of **1**. Thus, the fragmentation of **1** is essential for its removal from the zeolite pores. **2** was detected in the solution after the ion-exchange by electrospray mass spectrometry. After NaOH/NaCl treatment, the powder X-ray diffraction data show no loss in structural integrity of the ZSM-5 (Fig. 2-4c). Additionally, the  $^{27}\text{Al}$  NMR spectrum from the NaOH/NaCl treated material (Fig. 2-6) contains only the resonance for framework aluminum at 55.1ppm. No extra-framework aluminum is detected. For numerous

synthetic preparations that have been treated by either the liquid phase HCl method or the vapor phase HCl method, the measured  $\text{SiO}_2/\text{Al}_2\text{O}_3$  ratios are  $30\pm 4$ . Thus, within the error reported for the  $\text{SiO}_2/\text{Al}_2\text{O}_3$  ratio, the composition of the samples did not vary over the treatment regimes. The catalytic activity of this ZSM-5 was evaluated using the conversion of methanol to higher hydrocarbons (MTG) as the test reaction. The product slate of individual hydrocarbons was the same (within experimental errors) in distribution to that obtained from a vendor sample of ZSM-5 (see Table 2-1). Additionally, the constraint index (CI) that measures the relative cracking rates of n-hexane and 3-methylpentane<sup>15</sup> was determined for the ammonium forms of our synthesized ZSM-5 that was calcined or processed through the new organic removal procedure outlined above. This test reaction should be more discerning than the MTG reaction in terms of differences in acid strength and number of sites when comparing zeolite samples. The samples show similar rates and CIs (see Table 2-2). Additionally, these data compare well to those obtained from a vendor sample of ZSM-5<sup>15,16</sup>.

Here, we have provided the essential results necessary for the demonstration of our proposed new synthetic methodology. The recombination of the fragments of **1** is not illustrated, however, this reaction is well-known. We have successfully synthesized other zeolites (ZSM-11, ZSM-12) using this generalized methodology. In addition to ketals like those illustrated here, acetals and ortho ester functionalities have the appropriate properties (hydrolytically acid labile and base stable)<sup>17</sup> for use in the outlined synthesis methodology. Currently, we are applying this methodology to the preparation of larger SDAs and testing these organics in a broad selection of zeolite synthesis conditions.

## 2.3. Methods

### 2.3.1. Preparation of SDA (1)

4.00g of 1,4-dioxo-8-azaspiro[4,5]decane (98%, Aldrich), 8.01g of tributylamine (99%, Aldrich), and 30ml of MeOH (Burdick & Jackson) were mixed in a flask. 12.20g of iodomethane (99.5%, Aldrich) was added dropwise over a period of 10min. The mixture was refluxed for 5 days at room temperature. Yellow solids were produced. After adding ethyl ether to the mixture, the produced solids were filtered and washed with ethyl ether. The solids were recrystallized from hot acetone/MeOH. Iodine salts were converted to the corresponding hydroxide form in 90.2% yield using Bio-Rad AG1-X8 anion exchange resin.

### 2.3.2. Preparation of as-synthesized zeolite.

0.2g of potassium hydroxide (85+%, Aldrich) and 0.083g of aluminum hydroxide (Reheis F-2000) were added to the mixture of 0.094g of **1** and 11.4g of water, and stirred to obtain a clear solution. 0.9g of silica (CabOSil M5) were added to the solution and the mixture was stirred for 2 hrs to prepare a homogeneous gel. The resulting mixture was charged into a rotating teflon lined autoclave (100rpm) and heated at 175°C for 6 days. After crystallization, the autoclave was cooled to room temperature. The solid product was collected by filtration, repeatedly washed with deionized water and finally dried overnight.

### 2.3.3. Characterizations.

<sup>13</sup>C CP MAS NMR measurement was performed with a Bruker Avance 200 MHz spectrometer. Solution <sup>13</sup>C NMR spectrum was obtained with a Varian Mercury 300 MHz spectrometer. Powder X-ray diffraction pattern was collected on a Scintag XDS 2000 diffractometer using CuK $\alpha$  radiation at the rate of 2.5°/min. Elemental analysis was obtained by Quantitative Technologies INC., Whitehouse, NJ. IR spectroscopy was performed on a Nicolet Nexus 470 FT-IR. Thermogravimetric analysis was performed on a NETZSH STA 449C analyzer. Nitrogen adsorption capacity was measured using an Omnisorp 100 sorption apparatus. Mass spectrum was measured with a Perkin Elmer/Sciex API 365 electrospray mass spectrometer.

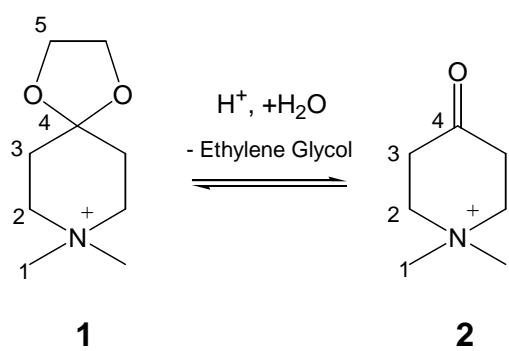
### Reference

1. Davis, M. E. Ordered porous materials for emerging applications. *Nature* **417**, 813-821 (2002).
2. Freyhardt, C. C., Tsapatsis, M., Lobo, R. F., Balkus, K. J. & Davis, M. E. A high-silica zeolite with a 14-tetrahedral-atom pore opening. *Nature* **381**, 295-298 (1996).
3. Wagner, P. et al. CIT-5 : a high-silica zeolite with 14-ring pores. *Chem. Commun.*, 2179-2180 (1997).
4. Wagner, P. et al. Guest/host relationships in the synthesis of the novel cage-based zeolites SSZ-35, SSZ-36, and SSZ-39. *J. Am. Chem. Soc.* **122**, 263-273 (2000).

5. Wright, P. A. et al. Cation-directed syntheses of novel zeolite-like metalloaluminophosphates STA-6 and STA-7 in the presence of azamacrocyclic templates. *J. Chem. Soc., Dalton Trans.*, 1243-1248 (2000).
6. Corma, A., Diaz-Cabanas, M. J., Martinez-Triguero, J., Rey, F. & Rius, J. A large-cavity zeolite with wide pore windows and potential as an oil refining catalyst. *Nature* **418**, 514-517 (2002).
7. Kuehl, G. H. & Timken, H. K. C. Acid sites in zeolite beta : Effects of ammonium exchange and steaming. *Microporous and Mesoporous Mater.* **35-36**, 521-532 (2000).
8. Wang, Z., Wang, H., Mitra, A., Huang, L. & Yan, Y. Pure-silica zeolite low-k dielectric thin films. *Adv. Mater.* **13**, 746-749 (2001).
9. Kresge, C. T., Leonowicz, M. E., Roth, W. J., Vartuli, J. C. & Beck, J. S. Ordered mesoporous molecular sieves synthesized by a liquid-crystal template mechanism. *Nature* **359**, 710-712 (1992).
10. Corma, A. From microporous to mesoporous molecular sieve materials and their use in catalysis. *Chem. Rev.* **97**, 2373-2419 (1997).
11. Whitehurst, D. D. in *U. S. Patent 5,143,879* (1992).
12. Chen, C. Y., Li, H. X. & Davis, M. E. Studies on mesoporous materials I. Synthesis and characterization of MCM-41. *Microporous Mater.* **2**, 17-26 (1993).
13. Tanev, P. T. & Pinnavaia, T. J. A neutral templating route to mesoporous molecular sieves. *Science* **267**, 865-867 (1995).
14. Piccione, P. M., Yang, S., Navrotsky, A. & Davis, M. E. Thermodynamics of pure-silica molecular sieve synthesis. *J. Phys. Chem. B* **106**, 3629-3638 (2002).

15. Frillette, V. J., Haag, W. O. & Lago, R. M. Catalysis by crystalline aluminosilicates : Characterization of intermediate pore-size zeolites by the "constraint index". *J. Catal.* **67**, 218-222 (1981).
16. Zones, S. I. & Harris, T. V. The constraint index test revisited : anomalies based upon new zeolite structure types. *Microporous and Mesoporous Mater.* **35-36**, 31-46 (2000).
17. Srinivasachar, K. & David M. Neville, J. New protein cross-linking reagents that are cleaved by mild acid. *Biochemistry* **28**, 2501-2509 (1989).

Scheme 1.



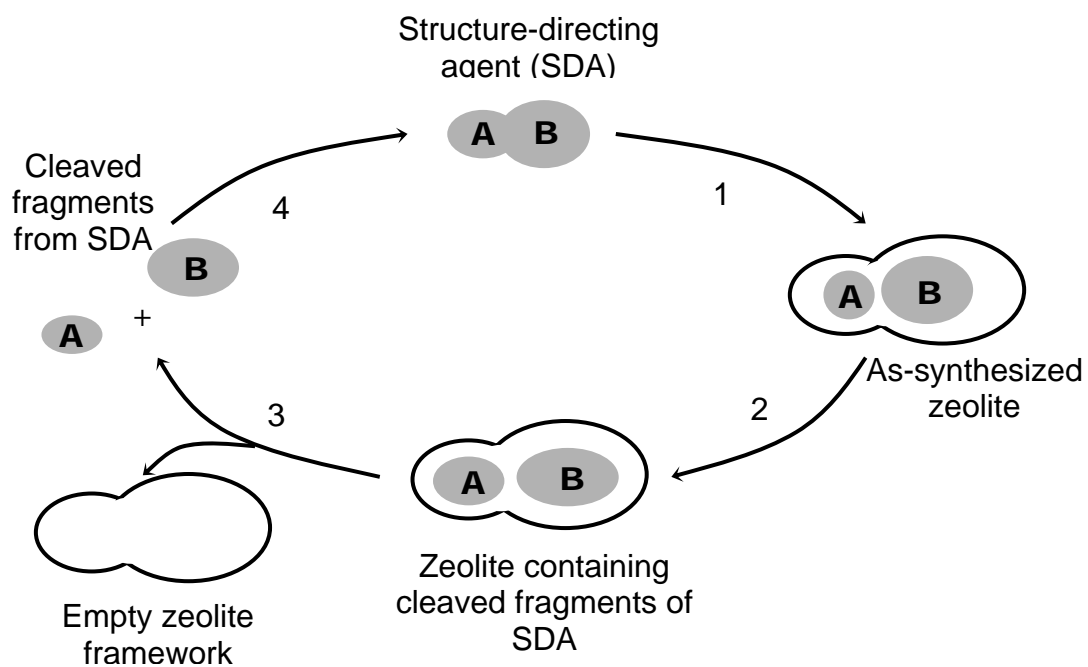


Figure 2-1. Schematic representations of new synthetic methodology. **a**, generalized scheme. step 1 : assemble the SDA with silica precursor, H<sub>2</sub>O, alkali metal ions, etc. for zeolite synthesis. step 2 : cleave the organic molecules inside the zeolite pores. step 3 : remove the fragments. step 4 : recombine the fragments into the original SDA molecule.



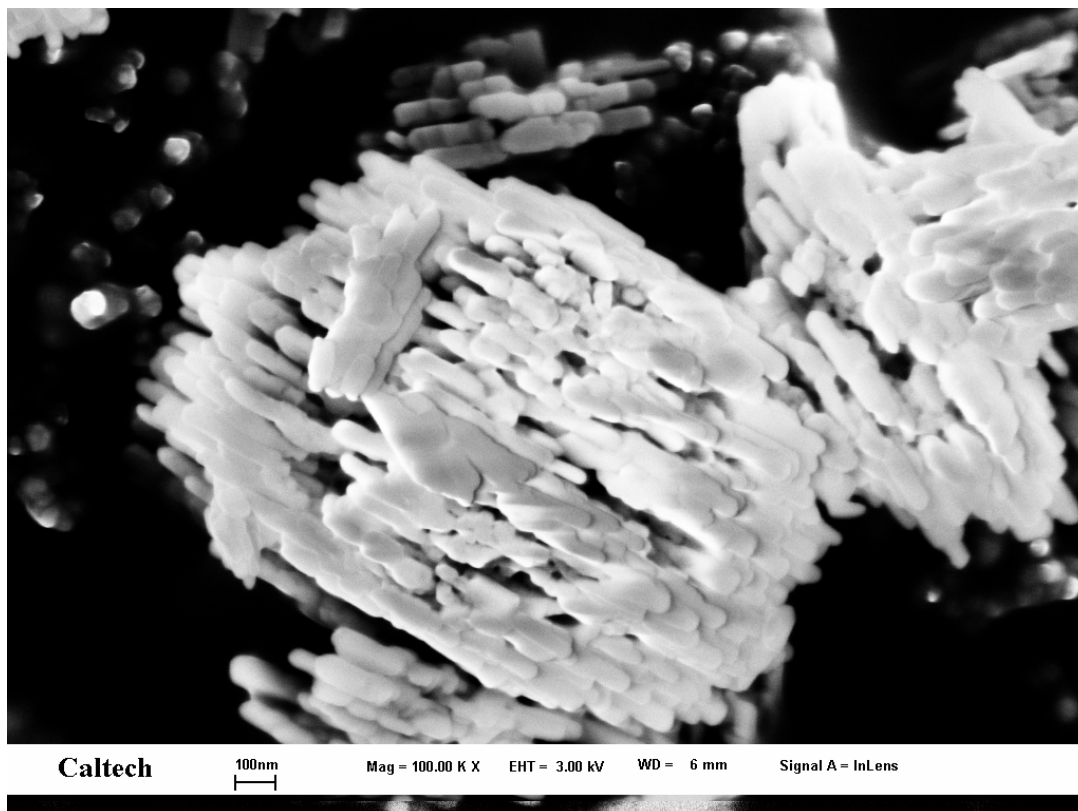


Figure 2-3. SEM image of as-synthesized ZSM-5. This was performed with LEO 1550 VP field emission scanning electron microscope.

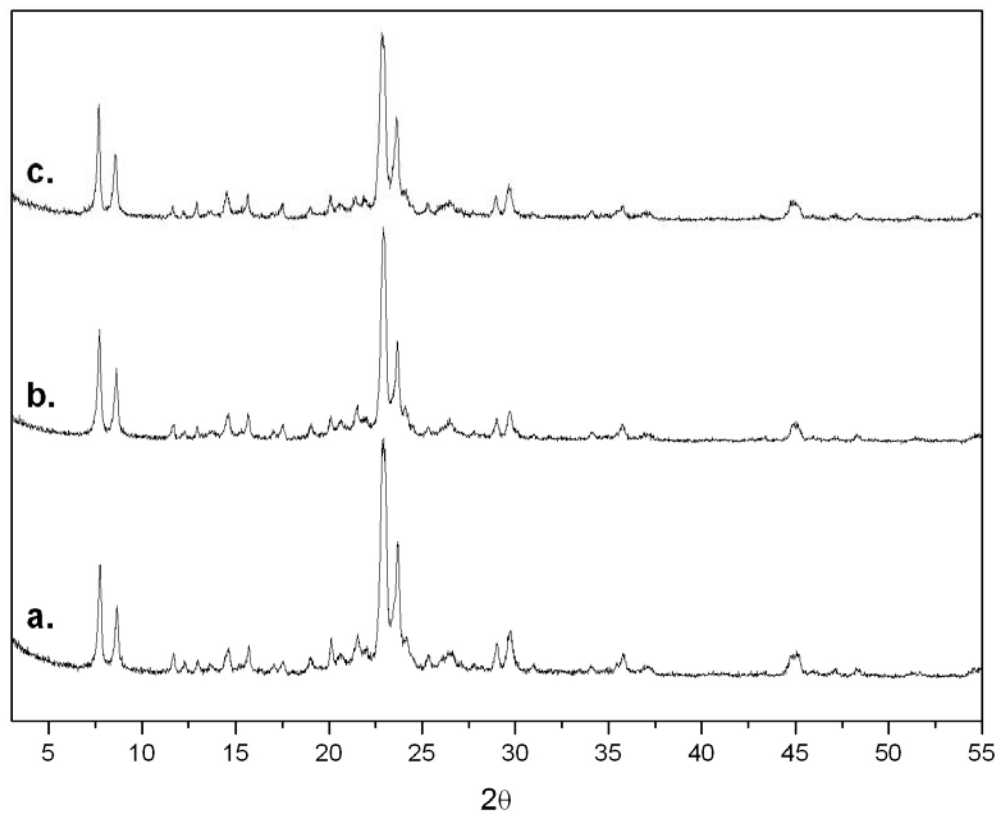


Figure 2-4. Powder X-ray diffraction patterns. **a**, as-synthesized ZSM-5. **b**, after treatment with 1M HCl solution. **c**, after ion-exchange with 0.01M NaOH + 1M NaCl solution. The ZSM-5 shows no structural degradation after the various treatments.

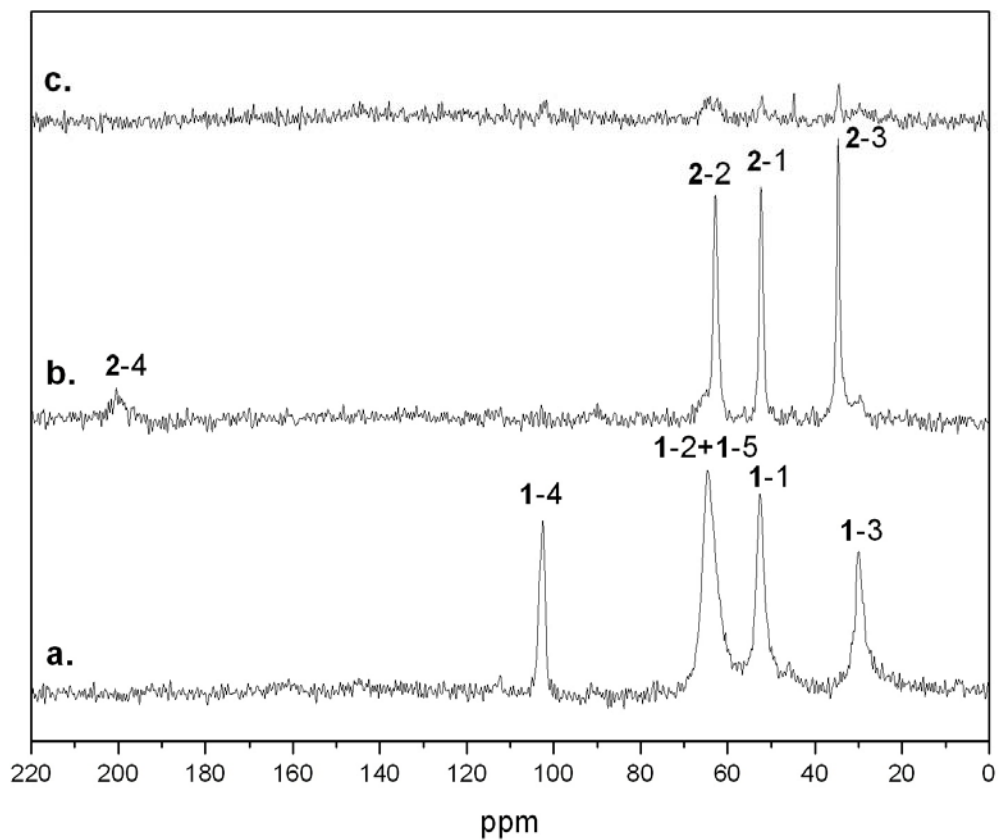


Figure 2-5.  $^{13}\text{C}$  CP MAS NMR spectra. **a**, intact **1** inside as-synthesized ZSM-5. **b**, after cleavage of **1** inside ZSM-5 pores using 1M HCl solution. **c**, after ion-exchange with 0.01M NaOH + 1M NaCl solution. The spinning rate was 4 kHz and contact time for cross polarization was 1ms for all cases. The notation of **1-1** denotes the peak corresponding to the carbon 1 of the organic molecule **1** in Scheme 1. The  $^{13}\text{C}$  CP MAS NMR data show that **1** was cleaved into its desired fragments by acid treatment and successfully removed after ion-exchange.

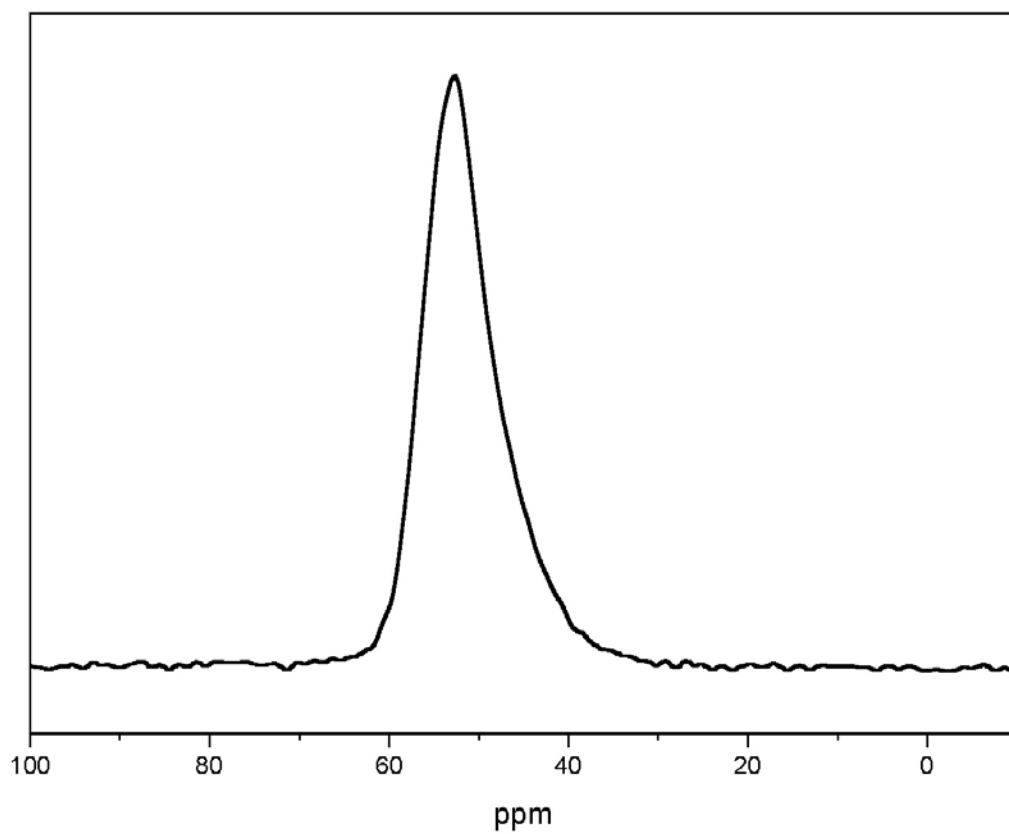


Figure 2-6.  $^{27}\text{Al}$  MAS NMR for the ZSM-5 after the cleavage reaction and ion-exchange. This was performed with a Bruker DSX 500 MHz spectrometer at 14 kHz spinning rate with 1ms of  $\pi/8$  pulse after dehydration for 3hrs at 120oC.

Table 2-1. Comparisons of hydrocarbon product distributions for the conversion of methanol to higher hydrocarbons<sup>a</sup>.

	Vendor ZSM-5	HCl-treated ZSM-5
Temp	370°C	400°C
Feed (% methanol in water)	100	22
Conversion	99	97
Hydrocarbon <sup>b</sup>	Hydrocarbon distribution (wt %)	
C1	0.5	0.6
C2	7	7.5
C3	17	23
C4	26	24
C5+	22	20
Ar6	1.5	0.4
Ar7	3	1
Ar8	8	6
Ar9	3	10.5
Ar10	3	3

<sup>a</sup> The ZSM-5 we produced was ion-exchanged with  $\text{NH}_4^+$  cations and then tested for catalytic activity using the conversion of methanol to higher hydrocarbons. 45mg of the catalyst sample was packed in a fixed bed reactor bracketed by alundum and glass wool. The experimental design is the same as in : Yuen, L. T., Zones, S. I., Harris, T. V., Gallegos, E. J. & Auroux, A. Product selectivity in methanol to hydrocarbon conversion for isostructural compositions of AFI and CHA molecular sieves. *Microporous Materials* 2, 105-117 (1994). The catalyst was tested at 400°C with a feed of 22% methanol in water and a feed rate of 1.6 cc/hr (along with a carrier of 20 cc/min  $\text{N}_2$ ) at atmospheric pressure.

<sup>b</sup>  $\text{C}_i$  denotes all non-aromatic hydrocarbons of  $i$  carbon number.  $\text{Ar}_i$  denotes all aromatic hydrocarbons of  $i$  carbon number.

Table 2-2. Comparisons between calcined and HCl-treated ZSM-5<sup>a</sup>

	Calcined ZSM-5	HCl-treated ZSM-5
n-hexane Conv, %	93.5	89.4
3-methylpentane Conv. %	41	33.9
Feed Conv. %	67.3	61.7
CI <sup>b</sup>	5.18	5.43

<sup>a</sup> Conversion at 10 min, 700°F. The experimental design is the same as in ref. [16] except that 0.1g of samples were used, respectively.

<sup>b</sup> 2-methylpentane from isomerization was excluded for CI calculation.

## Chapter Three

### Modification of the Methodology Using Pore-Filling Agents

(Modified from ‘H. Lee, S. I. Zones, and M. E. Davis, Zeolite Synthesis Using Degradable Structure-Directing Agents and Pore-Filling Agents, *J. Phys. Chem. B* **109**, 2187-2191 (2005)’)

### 3.1. Need for Pore-Filling Agents

Zeolites and molecular sieves are used on large scale as adsorption materials, ion exchangers and catalysts.[1] Newer applications of these materials include their use as MRI contrast agents and blood clotting substances.[2] Several zeolites and molecular sieves are commercially available, and there are numerous others that remain laboratory scale materials. One impediment to the commercialization of zeolites and molecular sieves is cost. Modern synthetic methodologies for preparing zeolites and molecular sieves involve the use of organic molecules that direct the assembly pathways.[3] These so called structure-directing agents (SDAs) must be removed after the synthesis of zeolites and molecular sieve materials in order to create the microporous void spaces that are needed for their application. The removal of these enclathrated molecules normally requires high temperature processes such as calcinations that destroy the high costing organic and lead to environmental processing steps for the removal of combustion products like nitrogen oxides. Additionally, the high temperature processing steps can lead to detrimental effects on the inorganic materials themselves such as the change of structure[4] and/or loss of framework elements[5], e.g., de-alumination. Recently, zeolites and molecular sieves are being studied as components in systems such as membrane reactors[6], separation devices[7] and sensors[8], and in electronic devices as low k barriers.[9] When used as a component of a system, the processing of the zeolite is often not compatible with the other materials contained within the system. High temperature oxidations like those used in calcinations steps for SDA removal are not always compatible with device manufacture. Also, inorganic-organic framework materials are now receiving greater attention and a way to treat these materials at a mild condition becomes highly

desirable. Organic functionalized molecular sieves[10] and metal-organic frameworks[11-13] are synthesized using SDAs that are organic molecules, and attempts to remove the templates by calcinations are not likely to yield success because they also destroy components of the framework.

The removal of organic SDAs via extraction has been reported[10,14,15]. However, successful extraction is limited into just a few cases, i.e., tetraethylammonium ions from zeolite beta. In order to have a reasonable change of SDA content after extraction, the SDA should have a smaller size than the pore opening of the zeolite and weak interaction with the zeolite framework[15].

We recently reported a new methodology to remove organic SDAs from zeolites and molecular sieves without the use of a high temperature process.[16] We created SDA that can be disassembled and reassembled easily. The SDA was cleaved into fragments within the zeolite pore space by a change of reaction condition such as pH after synthesizing zeolite. Their fragments were removed from zeolite pore for possible use again by reassembly. The methodology is very general and should open avenues to the commercialization of zeolite products that were heretofore too costly to produce because of the loss of the organic and to the use of zeolite components in devices that can not be exposed to high temperature processing. The key to the application of this new methodology is the proper design of the SDA. First, the SDA should be able to synthesize zeolites. In other words, the organic molecules should be intermediate in hydrophobicity and of size appropriate to structure-direct a microporous material. If the organic is too hydrophobic, it tends to aggregate in aqueous media and not interact with the inorganic species. On the contrary, if the organic is too hydrophilic, it will not interact with hydrated silica species. Historically, organic species that contain quaternary ammonium ions work well as

SDAs and have yielded a variety of new high-silica molecular sieves.[3] Second, the SDA should be stable during the zeolite synthesis, and then be easily cleaved by relatively simple changes in environmental conditions such as pH. One class of organic molecules that satisfy these conditions is ketal-containing species that are very stable at high pH, and can be cleaved into ketones and diols by lowering the pH. These ketal molecules will be intact during zeolite synthesis that typically occurs at high pH, and fragmented into pieces by lowering the pH. We used a ketal-containing SDA to provide the first demonstration of our new synthetic methodology.

The objective of our work is to explore whether the ketal-containing SDA used in our initial report is able to crystallize other microporous solids and to extend our methodology to its use in combination with pore filling agents (PFA). A pore filling agent is an organic molecule that by itself can not cause the zeolite to crystallize but yet can be occluded in the pore space during the synthesis when using SDAs. Zones and co-workers have shown that the use of SDAs and PFAs can lead to lower cost materials since the PFAs can be low cost components relative to the SDAs.[17,18] Here, we use the concept of a PFA to create pore space to provide avenues for reagents to contact and react with the SDA. Specifically, we use amine PFAs that can be extracted from the as-synthesized zeolite to create intrazeolitic pore space prior to cleavage reactions on the SDA. This enhanced procedure creates further generality in our methodology.

### **3.2. Experimental Section**

### 3.2.1. Synthesis of SDA-1

SDA-1, 8,8-dimethyl-1,4-dioxaspiro[4,5]decane, was synthesized as follows (Fig. 3-1). 1,4-dioxaspiro[4,5]decane (Aldrich, 98%) 19.43g, 37.72g of tributylamine (Aldrich, 99%) and 140mL of MeOH were mixed in a flask and 57.81g of iodomethane (Aldrich, 99.5%) added dropwise for 30min. The solution was stirred with a magnetic bar for one week at room temperature while in the dark. After adding ethyl acetate to the mixture, the solids produced were filtered and washed with more ethyl acetate. The solids were recrystallized from hot acetone/MeOH ( $^1\text{H}$  NMR (Methanol- $d_4$ ) 4.1(singlet), 3.7(J=6Hz, triplet), 3.3(singlet), 2.2(broad singlet) ppm.  $^{13}\text{C}$  NMR ( $\text{D}_2\text{O}$ ) 106.2, 67.3, 63.7, 54.1, 31.9 ppm). The iodide salt was dissolved in DI water for ion-exchange into the corresponding hydroxide ion. 30g of Bio-Rad AG1-X8 anion exchange resin were mixed with the solution overnight, and the degree of the ion-exchange was measured by a titration with a 0.01N HCl standard solution. The ion-exchange was repeated once. The yield of the ion-exchanges to place the organic into the hydroxide form was 93.0%.

### 3.2.2. Synthesis of ZSM-5 with SDA-1.

0.189g of SDA-1 and 0.908g of KOH (Aldrich, 45%) were dissolved in 22.313g of water. Then, 0.168g of aluminum hydroxide (Reheis F-2000, 79.3%) were mixed and stirred to obtain a clear solution. 1.813g of silica (Cab-O-Sil M5) were added to the solution and the mixture was aged for 2hrs to get a homogeneous gel. The gel was charged into rotating Teflon-lined stainless steel autoclave (100rpm) and heated at 170°C for 6days. The autoclave was cooled to room temperature after crystallization.

The solid product was collected by filtration, repeatedly washed with DI water and finally dried overnight at 110°C.

### 3.2.3. Synthesis of VPI-8 with SDA-1.

0.019g of LiOH (Fisher) were dissolved in a mixture of SDA-1 0.849g and water 6.002g, then 0.100g of zinc acetate dehydrate (Aldrich, 98+%) were dissolved in the solution completely. 2.996g of silica (Ludox HS-30) were added to the mixture, and then it was stirred for 2 hrs to obtain a clear solution. The mixture was charged into Teflon-lined autoclaves and heated statically at 150°C for 5 days in a convection oven. The product was filtered, washed, and dried in the same way as the ZSM-5 above.

### 3.2.4. Synthesis of ZSM-12 with SDA-1.

The synthesis mixture was prepared by dissolving 0.018g of LiOH (Fisher) and 0.851g of SDA-1 in 6.006g of water, adding 3.017g of silica (Ludox HS-30), and then stirring the mixture for 2 hrs to obtain a clear solution. The mixture was charged into Teflon-lined stainless steel autoclaves and heated statically at 150°C for 5 days in a convection oven. The product was filtered, washed, and dried.

### 3.2.5. Synthesis of ZSM-5 with SDA-1 and pore-filling agents, isobutylamine or cyclopentylamine.

0.20g of isobutylamine (Aldrich, 99%) (or 0.23g of cyclopentylamine (Aldrich, 99%)) were added to 0.746g of SDA-1 solution (0.662mmol SDA-1/g solution). 0.196g of potassium hydroxide (Aldrich, 85%) and 0.084g of aluminum hydroxide

(Reheis F-2000, 79.3%) were added to the mixture and the mixture stirred to obtain a clear solution. 0.9g of silica (CabOSil M5) were added to the solution and it was aged for 2 hrs to obtain a homogeneous gel. The gel was charged into a rotating Teflon lined autoclave (100rpm) and heated at 170°C for 6 days. The solid product was collected by filtration, repeatedly washed with DI water and dried overnight at 110°C.

### 3.2.6. Analysis.

Powder X-ray diffraction patterns were collected on a Scintag XDS 2000 diffractometer using  $\text{CuK}\alpha$  radiation. Scanning electron microscopy images were recorded using a LEO 1550 VP field emission scanning electron microscope.  $^{13}\text{C}$  cross polarization magic angle spinning (CP MAS) NMR measurements were performed with a Bruker Advance 200 MHz spectrometer. The contact time was 1millisecond, and the recycle delay was 1second. The zirconia rotor with 7mm diameter was used at the spinning rate of 4kHz.  $^{27}\text{Al}$  MAS NMR was performed with a Bruker DSX 500 MHz spectrometer at 14 kHz spinning rate with 1millisecond of  $\pi/8$  pulse. Elemental analyses were performed by Quantitative Technologies Inc., NJ. Inductively coupled plasma (ICP) spectroscopy was used for the inorganic analysis. Thermogravimetric analyses (TGA) were done with a NETZSH STA 449C instrument. The temperature was increased at the rate of 1°C/min, and helium was used as carrier gas. Mass spectra were measured with a Perkin Elmer/Sciex API 365 electrospray mass spectrometer.

## 3.3. Results and Discussions

### 3.3.1. Syntheses with SDA-1.

Figure 3-2 shows the powder X-ray diffraction patterns of various crystalline solids synthesized using SDA-1. We reported before that SDA-1 can be used with an aluminosilicate reaction mixture to crystallize ZSM-5.[16] The same ZSM-5 was synthesized when the silica source was changed from fumed silica to colloidal silica (Ludox). In the case that tetraethoxysilane was used as silica precursor, a mixture of amorphous silica and ZSM-5 was obtained. When the organic component was excluded from the reactant gel, ZSM-5 was not formed at all. Also, when 1,1-dimethylpiperidinium (absence of ketal group compared to SDA-1) was used as a structure-directing agent instead of SDA-1, ZSM-5 was not synthesized either.

SDA-1 is also useful in synthesizing different crystalline materials by varying the reaction conditions and inorganic compositions. When zinc acetate dihydrate was used as a framework element together with silica, VPI-8 (one dimensional pore structure) is formed.[19, 20] Table 3-1 lists the compositions from which VPI-8 is obtained. Only narrow range of 0.3~0.35 SDA-1/SiO<sub>2</sub> ratios directly produce VPI-8 with 0.05 LiOH/SiO<sub>2</sub>. For the ratio of 0.25 SDA-1/SiO<sub>2</sub>, a mixture of ZSM-12 and VPI-8 is obtained, and as the reaction time is extended, more VPI-8 is observed. When the ratio of SDA-1/SiO<sub>2</sub> is larger than 0.4, only amorphous solids are obtained. Figure 3-3 shows SEM images of VPI-8 prepared using different compositions. Interestingly, the VPI-8 produced with low Li/SiO<sub>2</sub> and high SDA-1/SiO<sub>2</sub> (fourth line of Table 3-1) in the reactant gel consists of very fine particles, and indicates a high rate of nucleation at this synthesis condition. These particles could only be collected by centrifugation. The reactant gel with a higher Li/SiO<sub>2</sub> (first line of Table 3-1) produced VPI-8 crystals that are larger and have needle-like morphology (Fig. 3-3b). The content of the SDA-1 inside VPI-8 was measured to be 10.8 wt% for fine particle

shape and 9.3 wt% for needle shape by TGA. In addition to preparing VPI-8 (contains Zn) and ZSM-5 (contains Al), SDA-1 can structure-direct the formation of pure-silica ZSM-12 in the absence of the heteroatoms zinc or aluminum. A gel with the composition of 0.05 LiOH : 0.3 SDA-1 : SiO<sub>2</sub> : 30 H<sub>2</sub>O successfully synthesized ZSM-12 in 5 days at 150°C. The SDA-1 content was measured as 10.8 wt% by TGA.

### 3.3.2. Syntheses with SDA-1 and pore-filling agents.

Pore-filling agents (PFAs) have no influence on the structure of zeolite formed but simply occupy pore space. Zones et al. previously reported the use of PFAs together with SDAs in zeolite synthesis to reduce the required amount of valuable SDAs.[17, 18] Figure 3-4 shows a schematic of how we envision the use of PFAs, and how they contribute to the successful removal of all organic species from the microporous void space. Because PFAs are usually small and have weak interactions with the inorganic framework, they are easily extracted. Consequently, the void space created from the extraction process can be used to access the SDA for the cleavage reaction to occur. As an example of this methodology and to show its feasibility, we synthesized ZSM-5 using both SDA-1 and PFAs. Figure 3-5 illustrates the powder X-ray diffraction patterns of the solids obtained from pure SDA-1 or SDA-1 used in combination with the PFAs such as isobutylamine or cyclopentylamine (at these synthesis conditions the use of either isobutylamine or cyclopentylamine in the absence of SDA-1 produces no crystalline solids). The use of a PFA does not change the zeolite phase obtained from the one crystallized with SDA-1 alone.

### 3.3.3. Cleavage attempts with SDA in unidimensional materials.

Previously, we have shown that SDA-1 can be cleaved inside ZSM-5 by contact with aqueous HCl or HCl(g).[16] ZSM-5 has a multidimensional pore system. Attempts to cleave SDA-1 at the same conditions as those used for ZSM-5 with one dimensional pore structure materials (VPI-8 and ZSM-12) were not successful. Treatments involved either 1N hydrochloric acid or HCl(g).  $^{13}\text{C}$  CP MAS NMR and TGA results confirm that SDA-1 remains intact inside the pore space of either VPI-8 or ZSM-12. It is not surprising that the unidimensional pore systems will present a greater challenge[21] for the cleavage reaction. More rigorous conditions will be attempted in the future.

### 3.3.4. Removal of PFAs and SDAs.

For the synthesis of ZSM-5 with PFAs and SDA-1, the PFAs are removed by reflux in dimethylformamide (DMF) for 20hrs. The  $^{13}\text{C}$  CP MAS NMR spectra of ZSM-5 prepared with SDA-1 and isobutylamine is shown in Fig. 3-6a. Both SDA-1 and isobutylamine are encapsulated during ZSM-5 synthesis. Figure 3-6b shows the  $^{13}\text{C}$  peaks of isobutylamine (19.2, 27.6, 48.6ppm) are significantly reduced after the extraction in DMF. Even though most of the isobutylamine was extracted by reflux in DMF, the SDA-1 remained inside ZSM-5 pores. The extracted isobutylamine was detected in the DMF solution by positive ion electrospray mass spectrometry.

The acid treatment was performed for the cleavage reaction of SDA-1 inside ZSM-5 pores. Using the ZSM-5 formed with SDA-1 and isobutylamine, and isobutylamine extracted prior to the acid treatment, the tertiary carbon peak (103.1ppm) in the  $^{13}\text{C}$  CP MAS NMR spectrum of SDA-1 disappears and new peaks for the cleaved piece,

1,1-dimethyl-4-oxopiperidinium, appear at 63.9, 53.5, and 35.8 ppm after the treatment with 1N hydrochloric acid at 90°C for 20hrs (Fig 3-6c ; the other peaks are from small amounts of the remaining isobutylamine(27.5, 19.3ppm) and DMF(46.2, 36.3ppm)). The carbonyl peak of the SDA-1 fragment was also observed by IR at 1734.5cm<sup>-1</sup>. The ZSM-5 before the acid treatment showed no IR peak at that position. These data show that most of the SDA-1 molecules inside the zeolite pores are fragmented by the cleavage reaction. The cleavage reaction has also been performed on the ZSM-5 when it contained both the SDA-1 and the PFA(isobutylamine). Hydrogen chloride gas was bubbled through water, and the H<sub>2</sub>O-saturated HCl(g) passed through a reactor where the zeolite sample was residing at 120°C for 3hr. The outlet HCl(g) was neutralized in a NaOH scrubber. The SDA-1 remained intact after the HCl(g) treatment without the extraction of isobutylamine. These results show that the extraction of isobutylamine is essential for the successful cleavage of SDA-1. After cleavage of SDA-1, the organic fragments can be removed by ion-exchange with the mixture of NaOH and NaCl following the procedures described previously.[16] The ZSM-5 synthesized using SDA-1 and isobutylamine contains 41.91% Si, 2.23% Al, 0.91% K, 5.19% C, 0.88% H, and 1.15% N according to elemental analyses. Weight losses of 2.2% in the low temperature region of 100~280°C are assigned to removal of isobutylamine while losses of 5.1% from the high temperature region of 280~520°C are assigned to the SDA-1 by TGA. Based on elemental analyses and TGA results, the numbers of SDA-1 and isobutylamine molecules per unit cell are estimated to be 2.9 and 2.8, respectively. Therefore, the extraction of isobutylamine can open significant pore space relative to the space occupied by SDA-1.

Figure 3-7 shows the  $^{27}\text{Al}$  magic angle spinning NMR spectra for as-made ZSM-5, the ZSM-5 after the cleavage reaction and ion-exchange, and calcined ZSM-5. The spectra were normalized by the sample masses and scan repetition numbers. The area beneath the peak was 0.93 for the ZSM-5 after the cleavage reaction and ion-exchange, and 0.83 for the calcined ZSM-5 when normalizing the value from as-made ZSM-5 to 1.00. Thus the acid treatment caused less leaching of aluminum from the framework than calcination. The removal of SDA via extraction was reported to be successful for pure-silica analogues of zeolite beta[10, 15] or Zn-beta (CIT-6)[19] and attempts with aluminosilicate were unsuccessful.[15] When Fajula and coworker used the extraction method to remove tetraethylammonium hydroxide from aluminosilicate zeolite beta, they extracted the SDA and caused complete dealumination rather than preserving the framework aluminum that gives catalytic sites. Here, we show that our methodology allows for the maintenance of framework aluminum and complete adsorption capacity.[16] Previously, we also showed that the ZSM-5 exposed to the treatments of cleavage reaction with acid and ion-exchange preserve the catalytic activity to the level of a vendor ZSM-5.[16] Therefore, the method showed in this study can provide an unprecedented opportunity to remove SDAs while preserving framework aluminum for use as catalytic sites.

### **3.4. Conclusions**

The use of degradable SDAs can allow for zeolite and molecular sieve synthesis to occur and with subsequent processing create microporous materials that have avoided high temperature treatments. The degradable SDAs can be fragmented into smaller pieces by a chemical reaction inside zeolite pores, and the pieces readily removed to

create microporosity. Ketal-containing molecule, SDA-1, can be used for the synthesis of ZSM-5, VPI-8 and ZSM-12. Thus, SDA-1 can be employed to prepare different zeolite and molecular sieve structures by changing the composition of gel, synthesis temperature and time. PFAs can be used with SDA-1 to crystallize ZSM-5. Because the PFA is small and has a weak interaction with the inorganic framework, it can be easily extracted. The extraction of the PFA provides a pathway for HCl and H<sub>2</sub>O to travel through to reach the ketal-containing SDA-1. Cleavage of SDA-1 and extraction of its fragments gives a microporous ZSM-5 that has never been exposed to high temperature treatments. The success of the combined PFA and SDA-1 synthesis of ZSM-5 provides motivation for seeking other PFA/SDA combinations for preparing numerous other zeolites and molecular sieves. Commercial zeolites that are highly suitable for use of this methodology are zeolite beta and MCM-22.

## References

1. Dyer, A., *An Introduction to Zeolite Molecular Sieves*. 1988: John Wiley & Sons.
2. Davis, M.E., *Nature* 417 (2002) 813.
3. Lobo, R.F., S.I. Zones, and M.E. Davis, *Journal of Inclusion Phenomena and Molecular Recognition in Chemistry* 21 (1995) 47.
4. Cheetham, A.K., G. Ferey, and T. Loiseau, *Angew. Chem. Int. Ed.* 38 (1999) 3268.
5. Kuehl, G.H. and H.K.C. Timken, *Micropor. Mesopor. Mater.* 35-36 (2000) 521.
6. Wan, Y.S.S., J.L.H. Chau, A. Gavriilidis, and K.L. Yeung, *Microporous and Mesoporous Mater.* 42 (2001) 157.

7. Lai, Z., G. Bonilla, I. Diaz, J.G. Nery, K. Sujaoti, M.A. Amat, E. Kokkoli, O. Terasaki, R.W. Thompson, M. Tsapatsis, and D.G. Vlachos, *Science* 300 (2003) 456.
8. Tess, M.E. and J.A. Cox, *Journal of pharmaceutical and biomedical analysis* 19 (1999) 55.
9. Wang, Z., H. Wang, A. Mitra, L. Huang, and Y. Yan, *Adv. Mater.* 13 (2001) 746.
10. Jones, C.W., K. Tsuji, and M.E. Davis, *Nature* 393 (1998)
11. Chui, S.S.-Y., S.M.-F. Lo, J.P.H. Charmant, A.G. Orpen, and I.D. Williams, *Science* 283 (1999) 1148.
12. Li, H., M. Eddaoudi, M. O'Keeffe, and O.M. Yaghi, *Nature* 402 (1999) 276.
13. Inagaki, S., S. Guan, T. Ohsuna, and O. Terasaki, *Nature* 416 (2002) 304.
14. Lami, E.B., F. Fajula, D. Anglerot, and T.D. Courieres, *Microporous Mater.* 1 (1993) 237.
15. Jones, C.W., K. Tsuji, T. Takewaki, L.W. Beck, and M.E. Davis, *Microporous and Mesoporous Mater.* 48 (2001) 57.
16. Lee, H., S.I. Zones, and M.E. Davis, *Nature* 425 (2003) 385.
17. Zones, S.I., S.-J. Hwang, and M.E. Davis, *Chem. Eur. J.* 7 (2001) 1990.
18. Zones, S.I. and S.-J. Hwang, *Chem. Mater.* 14 (2002) 313.
19. Takewaki, T., L.W. Beck, and M.E. Davis, *Topics in Catalysis* 9 (1999) 35.
20. Serrano, D.P., R.v. Grieken, M.E. Davis, J.A. Melero, A. Garcia, and G. Morales, *Chem. Eur. J.* 8 (2002) 5153.
21. Skoulidas, A.I. and D.S. Sholl, *J. Phys. Chem. A* 107 (2003) 10132.

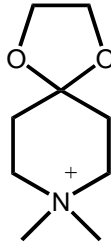


Figure 3-1. Structure of SDA-1.

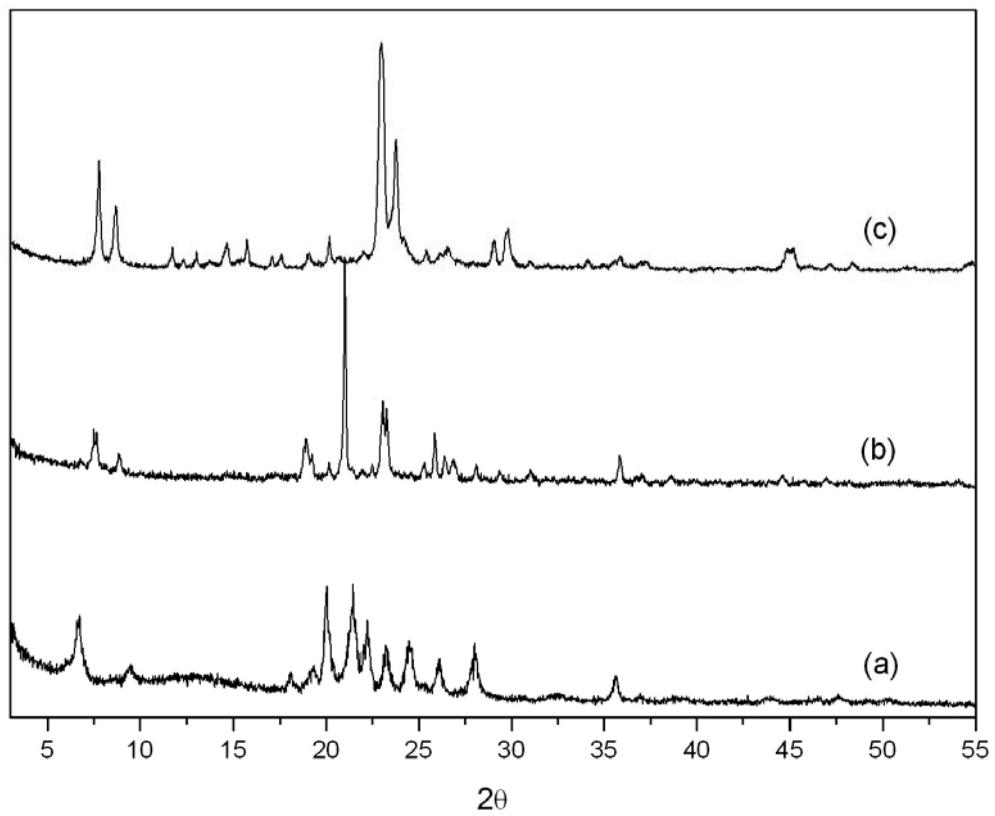


Figure 3-2. Powder X-ray diffraction patterns of various materials synthesized using SDA-1. (a) VPI-8, (b) ZSM-12, (c) ZSM-5.

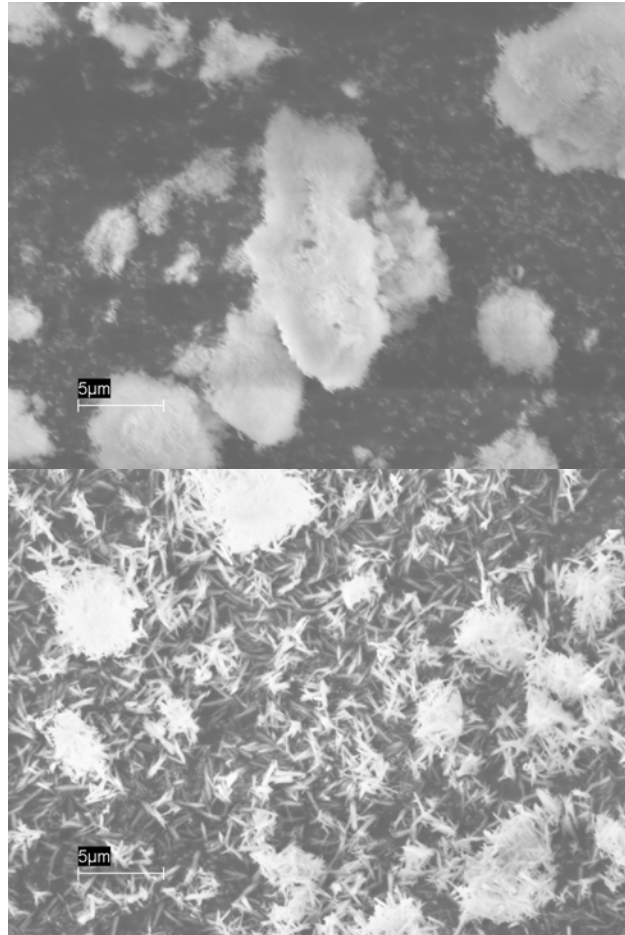


Figure 3-3. SEM images of VPI-8. (a)  $\text{LiOH}/\text{SiO}_2=0.05$ ,  $\text{SDA-1}/\text{SiO}_2=0.30$ . The VPI-8 is a very fine powder. (b)  $\text{LiOH}/\text{SiO}_2=0.25$ ,  $\text{SDA-1}/\text{SiO}_2=0.1$ . The VPI-8 has needle-like morphology.

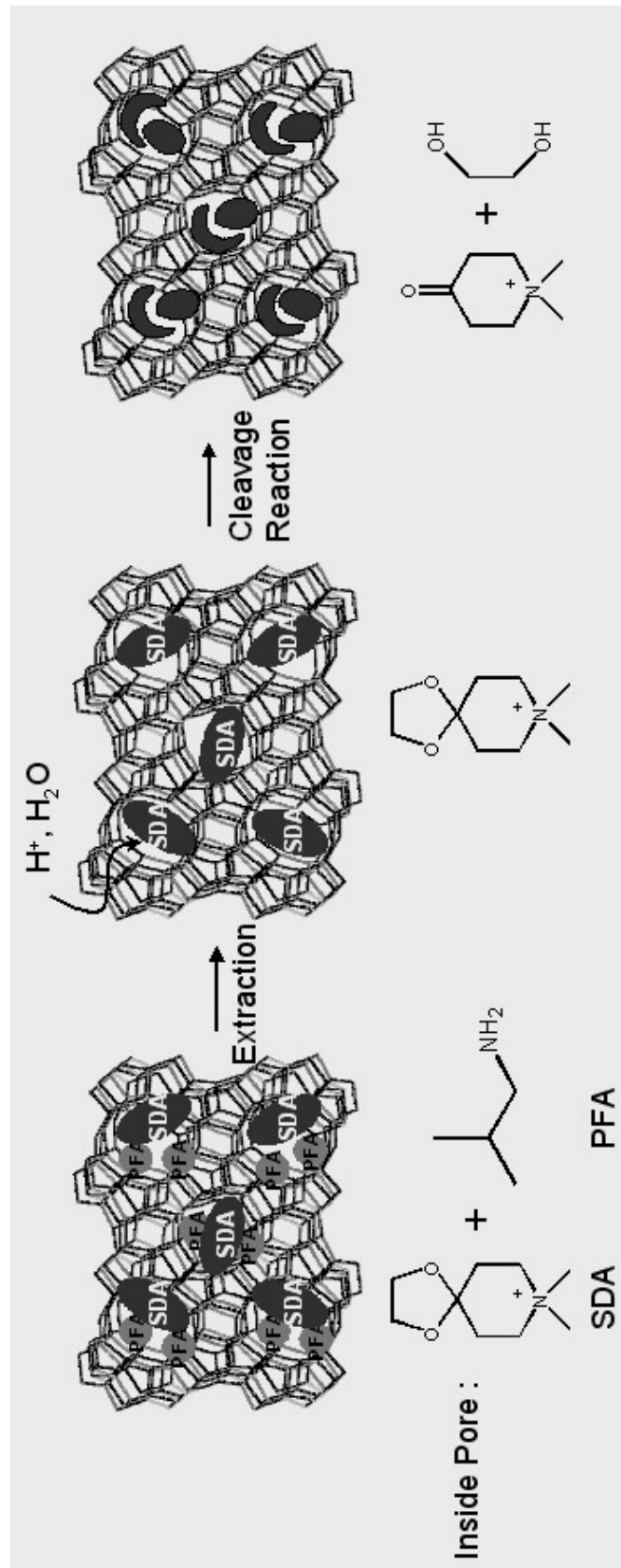


Figure 3-4. . Schematic diagram of ZSM-5 containing both SDA and PFA and how they are removed.

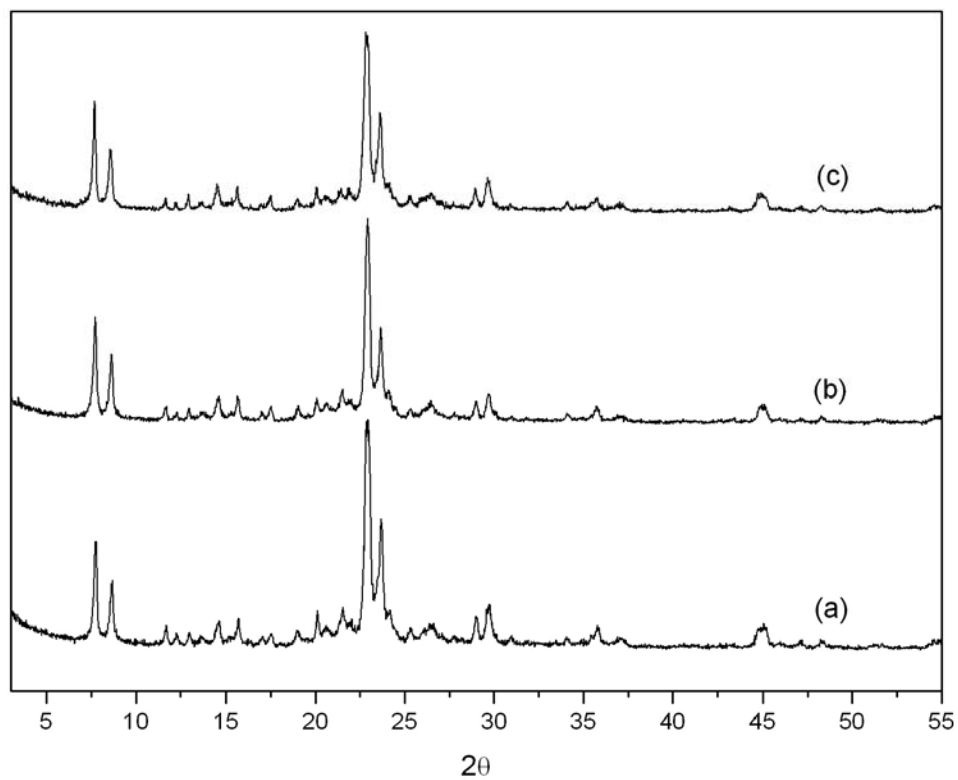


Figure 3-5. Powder X-ray diffraction patterns for the ZSM-5 synthesized using SDA-1 and PFA. (a) SDA-1 only, (b) SDA-1 + isobutylamine as PFA, (c) SDA-1 + cyclopentylamine as PFA.

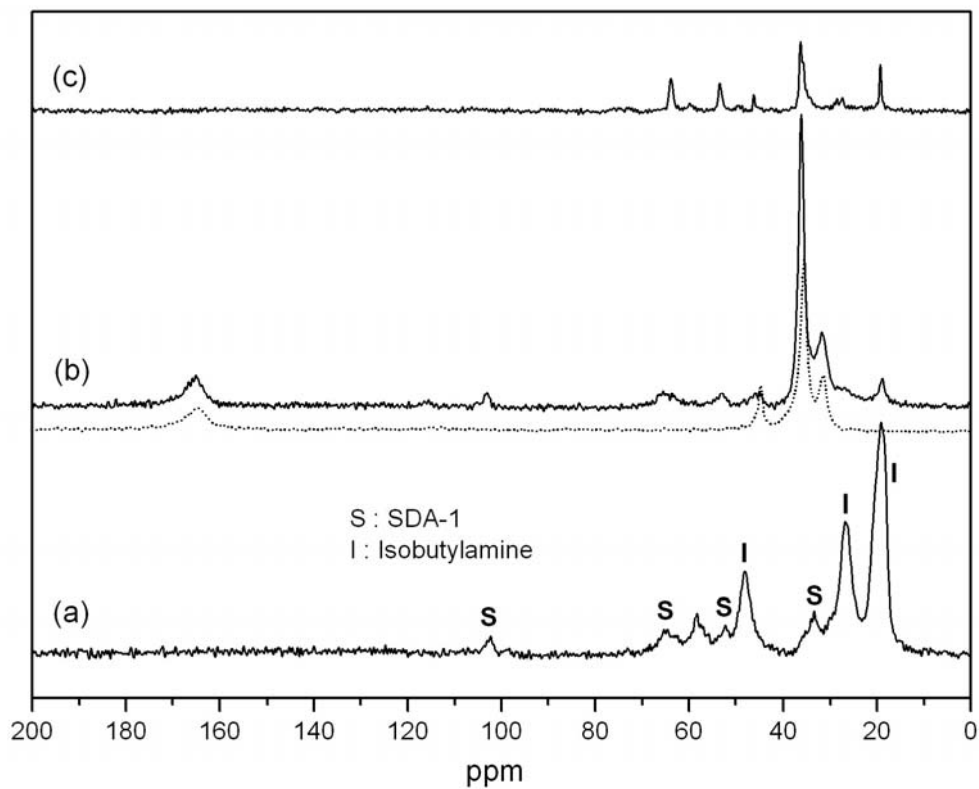


Figure 3-6.  $^{13}\text{C}$  cross polarization magic angle spinning (CP MAS) NMR spectra. (a) as-made ZSM-5 synthesized using SDA-1 and isobutylamine, (b) after the extraction of isobutylamine with dimethylformamide. The dotted line shows calcined ZSM-5 with impregnated dimethylformamide. The newly appearing peaks after contact with dimethylformamide are from its absorption during the extraction of isobutylamine, (c) After the cleavage reaction using 1N hydrochloric acid.

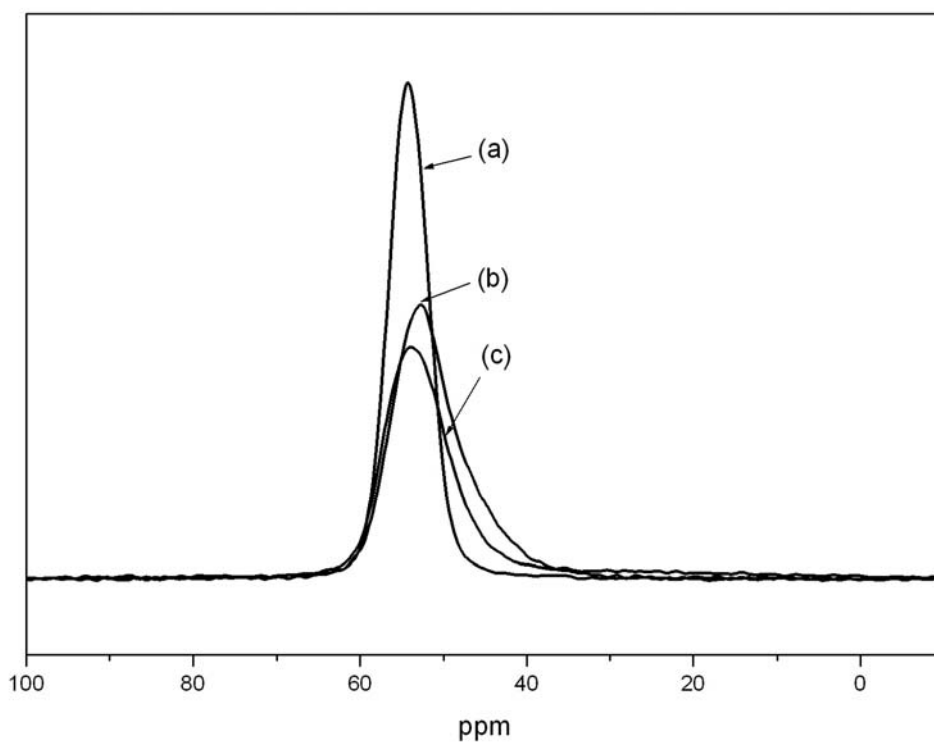


Figure 3-7.  $^{27}\text{Al}$  MAS NMR spectra. (a) as-made ZSM-5, (b) after cleavage reaction and subsequent ion-exchange with the mixture of NaOH and NaCl, (c) calcined ZSM-

Table 3-1. Synthesis of VPI-8 using SDA-1<sup>a</sup>

a	b	C	Starting mixture	T(°C)	Time	Results
0.25	0.1	0.03	White gel	150	5 days	VPI-8
0.15	0.1	0.03	White gel	150	5 days	VPI-8
0.05	0.3	0.03	Clear	150	5 days	VPI-8
0.05	0.35	0.03	Clear	150	5 days	VPI-8

<sup>a</sup> Gel composition; aLiOH : bSDA-1 : cZn(CH<sub>3</sub>COO)<sub>2</sub> · 2H<sub>2</sub>O : SiO<sub>2</sub> : 30 H<sub>2</sub>O

## **Chapter Four**

Use of the Proposed Methodology for Synthesis of Various Zeolites

(Modified from ‘H. Lee, S. I. Zones, and M. E. Davis, Synthesis of Zeolites Using Ketal Structure-Directing Agents and Their Degradation Inside the Zeolite Pore Space, Submitted to *Microporous and Mesoporous Materials* (2005)’)

#### 4.1. Using Various Ketal SDAs for Zeolite Synthesis

Zeolite and molecular sieve materials have been traditionally used in the chemical industry as catalysts, catalyst supports, ion-exchangers, etc.[1, 2]. Many zeolites require the use of organic molecules called structure-directing agents (SDA) for their synthesis. These SDAs direct the formation of zeolite with a specific structure although the shape of organic molecules is not exactly the same as the shape of the produced pore space [3, 4]. The organic molecules must be removed for further use, and calcination is the standard method for this purpose. Calcination, which burns out the organic molecules at very high temperature of 500~600°C, often destroys the catalytic activity or even the framework structure of the produced inorganic materials [5, 6]. Recently, applications of zeolite and molecular sieve materials have also expanded into film patterning, low-k materials, fuel cell composite materials, etc. [7-10]. These new applications often require properties not considered to be important for traditional uses of zeolitic materials. For example, when the zeolitic materials are used as low-k materials, the procedure for preparing a porous zeolite film on a silicon wafer must be compatible with the other semiconductor manufacturing processes. Conventional hydrothermal procedures used for zeolite synthesis might not be the desirable route to film preparation. While one of the key properties for the low-k application is the porosity of the zeolite, calcination at high temperatures of 500~600°C in highly oxidizing environments is likely not useful for the integration with other components of the semiconductor fabrication. When organic functionalized zeolites (organic functional groups are anchored on the silicate framework) are used as proton conductivity media in fuel-cell composite materials, it is crucial to make the zeolites porous while preserving the organic functional groups[11]. Since organically

functionalized zeolites are synthesized with organic SDAs, calcination for removal of the SDA would destroy both the SDA and the incorporated functional groups. Therefore, methodologies for preparing porous zeolitic materials without using calcination are highly desirable, especially for use in some of their newer applications.

We previously reported a new synthesis method to avoid the undesired high temperature calcinations procedure by using degradable structure-directing agents[12, 13]. When the SDA consists of two (or many) parts that can be easily cleaved and recombined, the SDA can be fragmented into smaller pieces after structure-directing a specific zeolite. Then, the pieces can be removed more easily, and the recovered pieces can be recombined into the original SDA for further zeolite synthesis. Because this methodology excludes the high temperature procedure, it may provide benefits to many applications of zeolitic materials.

In this work, various zeolites are synthesized using degradable SDAs. Quaternary ammonium cations that contain various ketal groups are used here as SDAs (See Scheme 1). It should be noted that there are many other possibilities for preparing degradable SDAs. Among the steps of this methodology: 1) synthesis of the zeolite, 2) degradation of the SDAs inside the zeolite pore space, and 3) removal of the fragments from the pores, the degradation of SDAs is often the most difficult step [12, 13]. The factors affecting a successful cleavage of the SDA are investigated here. When using ketal groups as the cleavable moiety, access of  $\text{H}_2\text{O}$  and  $\text{H}^+$  to the ketal group of the SDA is essential for the hydrolysis reaction to occur. If this access is prohibited, the SDAs will remain intact despite the chemical treatment. The properties of the synthesized zeolite such as organic content, hydrophilicity, and pore connectivity can have significant influence on the mass transfer of  $\text{H}_2\text{O}$  and  $\text{H}^+$

through the porous structure. Here, these parameters are evaluated for the degradation of ketal-containing SDAs inside zeolites with various properties.

## 4.2. Experimental Section

### 4.2.1. Synthesis of Ketal Structure-Directing Agents.

Fig. 4-1 shows the ketal-containing SDAs synthesized in this work.

**Synthesis of 2,3,8,8-tetramethyl-1,4-dioxo-8-azoniaspiro[4,5]decane hydroxide(I).** 7.68g (0.05mol) of 4-piperidone monohydrate hydrochloride were dissolved in 100mL of cyclohexane. 9.01g (0.1mol) of *meso*-2,3-butanediol and 0.10g of *p*-toluenesulfonic acid monohydrate were added to the solution and refluxed in Dean-Stark apparatus at 130°C until no more water was distilled. After cooling, the cyclohexane solution was decanted. The residue was dissolved in 50mL of chloroform, and then treated with 6.00g of potassium carbonate and 6mL of water with stirring. The chloroform layer was separated. The aqueous solution was extracted with chloroform several times. The extracts were combined and the chloroform was evaporated in a rotavapor to give a 2,3-dimethyl-1,4-dioxo-8-azaspiro[4,5]decane (P1);  $^{13}\text{C}$  NMR ( $\text{CDCl}_3$ )  $\delta = 15.5, 33.2, 36.1, 42.9, 43.1, 74.1, 104.0$  ppm. 6.81g (0.04mol) of P1, 11.12g (0.06mol) of tributylamine were dissolved in 50mL of methanol. 17.03g (0.12mol) of iodomethane were added to the solution dropwise for 30min. The solution was refluxed for one week at room temperature. The methanol was evaporated in a rotavapor. The residue was redissolved in chloroform and the desired product was precipitated by addition of ethyl acetate;  $^{13}\text{C}$  NMR of **I** iodide salt ( $\text{D}_2\text{O}$ )  $\delta = 17.0, 32.0, 34.6, 54.2, 63.7, 77.5, 105.0$  ppm.  $\text{C}_{11}\text{H}_{22}\text{O}_2\text{NI}$  Anal. Calcd: C,

40.38; N, 4.28; H, 6.78; O, 9.78. Found: C, 40.27; N, 4.19; H, 6.70; O, 10.02. The exchange of the iodide salt into a corresponding hydroxide was accomplished as follows: 6.9g of the iodide salt of **I** (21.1mmol) were dissolved in 150mL of distilled water and refluxed with 30.1g of Bio-Rad AG1-X8 anion exchange resin for a day. The solution was filtered and concentrated to 4.26g of OH- form **I**/16.84g solution. The conversion of iodide to hydroxide was 96.3% based on titration of the resultant solution.

**Synthesis of 2-ethyl-8,8-dimethyl-1,4-dioxo-8-azoniaspiro[4,5]decane hydroxide(II).** The synthesis of **II** was carried out by reacting 1,2-butanediol with 4-piperidone followed by reaction with iodomethane as described above for **I**.  $^{13}\text{C}$  NMR of 2-ethyl-1,4-dioxo-8-azoniaspiro[4,5]decane ( $\text{CDCl}_3$ )  $\delta = 9.8, 26.4, 33.6, 34.8, 43.1, 43.2, 69.1, 77.5, 105.5$  ppm.  $^{13}\text{C}$  NMR of **II** iodide salt ( $\text{D}_2\text{O}$ )  $\delta = 11.5, 28.0, 31.9, 32.9, 53.7, 54.4, 63.6, 71.3, 80.6, 106.2$  ppm.  $\text{C}_{11}\text{H}_{22}\text{O}_2\text{NI}$  Anal. Calcd: C, 40.38; N, 4.28; H, 6.78; O, 9.78. Found: C, 40.43; N, 4.12; H, 6.73; O, 9.51.

**Synthesis of 8,8-dimethyl-2-phenyl-1,4-dioxo-8-azoniaspiro[4,5]decane hydroxide(III).** The synthesis of **III** was carried out by reacting 1-phenyl-1,2-ethanediol with 4-piperidone followed by reaction with iodomethane as described above for **I**.  $^{13}\text{C}$  NMR of 2-phenyl-1,4-dioxo-8-azoniaspiro[4,5]decane ( $\text{CDCl}_3$ )  $\delta = 34.0, 34.6, 43.2, 43.3, 71.4, 77.9, 106.6, 126.1, 127.7, 128.3, 138.2$  ppm.  $^{13}\text{C}$  NMR of **III** iodide salt ( $\text{CD}_3\text{OD}$ )  $\delta = 31.4, 32.0, 52.5, 62.7, 72.8, 79.7, 105.8, 127.6, 129.5, 129.8, 139.6$  ppm.  $\text{C}_{15}\text{H}_{22}\text{O}_2\text{NI}$  Anal. Calcd: C, 48.01; N, 3.73; H, 5.91; O, 8.52. Found: C, 47.15; N, 3.50; H, 5.85; O, 8.20.

**Synthesis of 9,9-dimethyl-1,5-dioxo-9-azoniaspiro[5,5]undecane hydroxide(IV).** The synthesis of **IV** was carried out by reacting 1,3-propanediol with 4-piperidone followed by reaction with iodomethane as described above for **I**. **IV** was

finally purified by recrystallization with methanol/acetone.  $^{13}\text{C}$  NMR of 1,5-dioxa-9-azoniaspiro[5,5]undecane ( $\text{D}_2\text{O}$ )  $\delta = 27.3, 32.3, 43.7, 62.5, 97.6$  ppm.  $^{13}\text{C}$  NMR of **IV** iodide salt ( $\text{D}_2\text{O}$ )  $\delta = 27.2, 30.2, 54.2, 62.2, 62.7, 96.6$  ppm.  $\text{C}_{10}\text{H}_{20}\text{O}_2\text{NI}$  Anal. Calcd: C, 38.35; N, 4.47; H, 6.44; O, 10.22. Found: C, 38.48; N, 4.37; H, 6.39; O, 9.86.

**Synthesis of 2,9,9-trimethyl-1,5-dioxa-9-azoniaspiro[5,5]undecane hydroxide(V).** The synthesis of **V** was carried out by reacting 1,3-butanediol with 4-piperidone followed by reaction with iodomethane as described above for **I**. **V** was finally purified by recrystallization with methanol/acetone.  $^{13}\text{C}$  NMR of 2-methyl-1,5-dioxa-9-azoniaspiro[5,5]undecane ( $\text{CDCl}_3$ )  $\delta = 22.2, 28.7, 33.0, 38.6, 42.5, 42.6, 59.3, 64.3, 96.2$  ppm.  $^{13}\text{C}$  NMR of **V** iodide salt ( $\text{DMSO}$ )  $\delta = 21.8, 22.9, 32.3, 32.3, 50.0, 51.3, 58.7, 59.0, 59.3, 64.5, 93.5$  ppm.  $\text{C}_{11}\text{H}_{22}\text{O}_2\text{NI}$  Anal. Calcd: C, 40.38; N, 4.28; H, 6.78; O, 9.78. Found: C, 40.62; N, 4.15; H, 6.77; O, 9.51.

**Synthesis of 3,3-dimethyl-7,12-dioxa-3-azoniaspiro[5,6]dodecane hydroxide(VI).** The synthesis of **VI** was carried out by reacting 1,4-butanediol with 4-piperidone followed by reaction with iodomethane as described above for **I**.  $^{13}\text{C}$  NMR of 7,12-dioxa-3-azoniaspiro[5,6]dodecane ( $\text{CDCl}_3$ )  $\delta = 29.7, 34.7, 43.3, 61.5, 99.2$  ppm.  $^{13}\text{C}$  NMR of **VI** iodide salt ( $\text{D}_2\text{O}$ )  $\delta = 31.1, 31.4, 54.1, 63.0, 65.8, 99.8$  ppm.  $\text{C}_{11}\text{H}_{22}\text{O}_2\text{NI}$  Anal. Calcd: C, 40.38; N, 4.28; H, 6.78; O, 9.78. Found: C, 40.56; N, 4.11; H, 6.65; O, 9.32.

**Synthesis of 2,8,8-trimethyl-1,4-dioxa-8-azoniaspiro[4,5]decane hydroxide(VII).** The synthesis of **VII** was carried out by reacting 1,2-propanediol with 4-piperidone followed by reaction with iodomethane as described above for **I**. **VII** was finally purified by recrystallization with methanol/acetone.  $^{13}\text{C}$  NMR of 2-methyl-1,4-dioxa-8-azoniaspiro[4,5]decane(P7) ( $\text{CDCl}_3$ )  $\delta = 18.6, 36.0, 37.2, 44.0, 44.1, 70.4, 71.7, 107.2$  ppm.  $^{13}\text{C}$  NMR of **VII** iodide salt ( $\text{D}_2\text{O}$ )  $\delta = 17.6, 32.1, 33.2,$

53.8, 54.5, 63.7, 73.1, 75.8, 106.4 ppm.  $C_{10}H_{20}O_2NI$  Anal. Calcd: C, 38.35; N, 4.47; H, 6.44; O, 10.22. Found: C, 39.87; N, 4.17; H, 6.61; O, 11.79.

**Synthesis of 8,8-dimethyl-1,4-dioxo-8-azoniaspiro[4,5]decane (VIII).** VIII was synthesized by following the procedure explained elsewhere [13].

#### 4.2.2. Zeolite Synthesis.

Table 4-1 shows the zeolite synthesis conditions utilized for testing the ketal-containing SDAs. All of the SDA molecules were ion-exchanged into their hydroxide forms for zeolite synthesis. The SDAs are denoted as ROH below. The ZSM-5 was synthesized from reaction mixtures of composition,  $0.04ROH : 0.24KOH : 0.06Al(OH)_3 : 40H_2O : SiO_2$ . Aluminum hydroxide ( $Al(OH)_3 \cdot 1.13H_2O$ , Reheis F-2000) was used as aluminum source, and fumed silica (Cab-O-Sil grade M-5) was used as silica source. The prepared gel was aged for 2 hours and then placed into Teflon-lined autoclaves that were rotated at 60rpm for 7 days at  $170^\circ C$ . After the crystallization, the solid product was recovered by filtration, washed, and dried at  $100^\circ C$ . The ZSM-12 was synthesized with the gel with the composition of  $0.15ROH : 0.15NaOH : 0.055Al : 27H_2O : SiO_2$ . NaY (sodium zeolite Y) with silica to alumina ratio of 6 (SAR=6) was used to provide aluminum to reactant gel. Fumed silica (Cab-O-Sil) was also used as silica source. The remaining procedure was the same as the case of ZSM-5. The temperature, time and rotation speed (rpm) used for the syntheses are given in Table 4-1. The B-ZSM-12 was prepared from a gel with the composition of  $0.2ROH : 0.1NaOH : 0.01Na_2B_4O_7 : 44H_2O : SiO_2$ . Sodium tetraborate decahydrate (Fisher Scientific) was used as boron source and fumed silica (Cab-O-Sil) was used as silica source. Mordenite was synthesized by using the gel composition with an excessive amount of alkali ions. Two different gel compositions of  $0.3ROH :$

1.33KF : 0.067Al(OH)<sub>3</sub> : 45H<sub>2</sub>O : SiO<sub>2</sub> and 0.14ROH : 0.06Al : 0.53Na : 32H<sub>2</sub>O : SiO<sub>2</sub> were used. In first case, KF•2H<sub>2</sub>O (Mallinckrodt) was used to provide alkali ions, and Al(OH)<sub>3</sub>•1.13H<sub>2</sub>O (Reheis F-2000) and fumed silica (Cab-O-Sil) were used as aluminum and silica source, respectively. In second case, NaY with SAR 6 was used as aluminum source and sodium silicate solution (Aldrich, 27% SiO<sub>2</sub> 14% NaOH) was used as sodium and silica source. Colloidal silica (Ludox HS-40) was also used as an additional silica source. The zincosilicate VPI-8 was synthesized from a gel composition of 0.3ROH : 0.05LiOH : 0.03Zn(CH<sub>3</sub>COO)<sub>2</sub> : 30H<sub>2</sub>O : SiO<sub>2</sub>. Zinc acetate (Zn(CH<sub>3</sub>COO)<sub>2</sub>•2H<sub>2</sub>O, Aldrich) was used to provide zinc to the reactant gel. Colloidal silica (Ludox HS-30) was used as silica source.

#### 4.2.3. Cleavage of SDAs in the Zeolite Pore Space.

Different conditions were used for the cleavage reactions of the SDAs in zeolite pore spaces. First, 0.2g of synthesized zeolite were refluxed with 50mL of 1N HCl solution at 80°C for 12hrs. Then, the zeolite was washed with ~200mL of water and dried at room temperature. Second, 0.2g of synthesized zeolite were placed in Teflon-lined autoclave with 35ml of 1N HCl solution at 135°C for 20hrs. After cooling the reactors, the zeolite was collected by filtration, washed with ~200mL of water, and then dried at 100°C. Also, an acetic acid solution (5mL acetic acid/30mL water) was used for the acidic treatment. 0.2g of synthesized zeolite were placed in Teflon-lined autoclave with the acetic acid solution at 135°C for 2 days. After cooling the reactors, the zeolite was collected by filtration or centrifugation, washed with ~200mL of water, and then dried at 100°C. The cleaved fragments were removed from the pore space by ion-exchange with 0.01NaOH/1N NaCl solution at 100°C for 1 day. The resulting

zeolite was collected by filtration, washed with ~200ml of water, and then dried at 100°C.

#### 4.2.4. Analytical.

Powder X-ray diffraction (XRD) patterns were collected on a Scintag XDS 2000 diffractometer using  $\text{CuK}\alpha$  radiation and a solid-state Ge detector. The diffraction profiles were scanned over the range of  $3^\circ < 2\theta < 55^\circ$  in the rate of  $2.5^\circ/\text{min}$ . Fluorophlogopite mica (Standard Reference Material 675, National Bureau of Standards) was used as an external standard. Fourier-Transform infrared (FT-IR) spectroscopy was carried out on a Nicolet Nexus 470. The samples were prepared by using the KBr pellet technique. Liquid NMR spectra were collected on a Varian Mercury 300MHz spectrometer.  $^{13}\text{C}$  solid-state NMR measurements were performed with a Bruker Advance 200 MHz spectrometer. The cross polarization, magic angle spinning (CP MAS) technique was used. The spectra were recorded with a pulse length of  $4\mu\text{s}$  and a spinning rate of 4kHz and were referenced to an adamantane standard (downfield resonance at  $-38.47\text{ppm}$ ). The contact time was 1ms, and the recycle delay was 1s. The zirconia rotor was used as a sample holder. Elemental analyses were performed by Quantitative Technologies Inc., NJ and Galbraith Laboratories, Inc., TN. ICP was used for the inorganic analysis. Thermogravimetric analyses were done with a NETZSH STA 449C instrument at the rate of  $10^\circ\text{C}/\text{min}$ , and air was used as carrier gas. Mass spectra were measured with a Perkin Elmer/Sciex API 365 liquid chromatography electrospray mass spectrometer.

## 4.3. Results and Discussion

### 4.3.1. Zeolite Synthesis

Various zeolite synthesis conditions were used to investigate the abilities of the ketal-containing SDAs to direct the formation of various zeolites and molecular sieves. Table 4-1 shows the conditions at which the SDAs were used for zeolite synthesis, and the structures of zeolitic materials that were obtained at these conditions. Experiments where amorphous or dense phases were obtained, or where the SDA was degraded during the synthesis are not included in the table. The gel with the composition of  $0.04\text{ROH} : 0.24\text{KOH} : 0.06\text{Al}(\text{OH})_3 : 40\text{H}_2\text{O} : \text{SiO}_2$  produced ZSM-5 after 7 days at  $170^\circ\text{C}$ . The SDAs, **II**, **VII**, and **VIII** structure-direct the formation of ZSM-5. Fig. 4-2 shows the powder XRD patterns of those ZSM-5s. The side groups on the ketal ring such as methyl and ethyl groups had little influence on the structure of the synthesized zeolite. These SDAs remain intact during the zeolite syntheses (verified by  $^{13}\text{C}$  CP MAS NMR). The organic molecules inside the zeolite pore space have the  $^{13}\text{C}$  NMR resonances at the same position as solution  $^{13}\text{C}$  NMR spectra. When the SDAs with larger ketal rings such as **IV** and **VI** were used for zeolite synthesis, those organic molecules were degraded at the synthesis condition. The ZSM-5s with various properties were also synthesized as shown in Table 4-2. **VIII** was used as SDA for the cases listed. When the ratio of  $\text{ROH}/\text{SiO}_2$  in the gel was increased from 0.04 to 0.10, the content of organic molecules in the ZSM-5 also increased from 6.4% to 7.8%. The ZSM-5 synthesized with the ratio of  $\text{ROH}/\text{SiO}_2$  larger than 0.1 showed little differences in the organic content of the final solid. The two ZSM-5s with different organic content have the same Si/Al ratio (13.8 and 14.0

as shown in Table 4-2). The ZSM-5s with different hydrophilicity were also synthesized by controlling Si/Al ratio. When the ratio of  $\text{Al}(\text{OH})_3/\text{SiO}_2$  in the reactant gel was varied in the range of 0~0.1, ZSM-5 was synthesized for only  $x = 0.06$ . The Si/Al ratio of the product ZSM-5 was ~14. ZSM-5 with higher Si/Al ratio was obtained by using a different gel composition of  $0.15\text{ROH} : 0.1\text{NaOH} : 0.02\text{Al}(\text{OH})_3 : 44\text{H}_2\text{O} : \text{SiO}_2$ . The ZSM-5 produced with this gel composition at  $170^\circ\text{C}$ , 7days, and 60rpm had the Si/Al ratio of 40.8. As shown in cases 2 and 3 of Table 4-2, the ZSM-5s with the same organic contents (7.8% and 7.7%) have the different Si/Al ratios of 14.0 and 40.8, respectively. The ZSM-5s with various properties were used later to test the effect of organic content and hydrophilicity on the degradation of SDA inside the pores.

ZSM-12 was synthesized when NaY with SAR of 6 was used as an aluminum source. The aluminum in zeolite Y was released slowly from the framework to the reactant gel as an aluminum source during the zeolite synthesis. Only **IV** and **VIII** structure-directed the formation of Al-ZSM-12. B-ZSM-12 was also synthesized from the gel containing a boron source. **II**, **IV** and **VIII** structure-directed the formation of B-ZSM-12. Fig. 4-3 shows the powder XRD patterns of the synthesized ZSM-12s with various SDAs.

Mordenite was synthesized with **III**, **IV**, and **VIII** as SDA. **III** was used as SDA with the gel composition of  $0.3\text{ROH} : 1.33\text{KF} : 0.067 \text{Al}(\text{OH})_3 : 45\text{H}_2\text{O} : \text{SiO}_2$ , and **IV** and **VIII** were used as SDA when the sodium silicate was used as a silica source. Fig. 4-4 shows powder XRD patterns of the synthesized mordenites. Because a lot of alkali ions were used in the synthesis, there is the possibility that the mordenite is synthesized without utilizing the organic SDA. When the syntheses of mordenite were tried with the same gels in the absence of the SDA, mordenite was not obtained but

rather dense crystalline phase was obtained. Also, the intact SDA was observed inside the mordenite pores by  $^{13}\text{C}$  CP MAS NMR. These results suggest that the organic SDAs are essential for the synthesis of mordenite at the given conditions.

Zincosilicate, VPI-8, was synthesized from a gel composition of  $0.3\text{ROH} : 0.05\text{LiOH} : 0.03\text{Zn}(\text{CH}_3\text{COO})_2 : 30\text{H}_2\text{O} : \text{SiO}_2$  when the SDA, **II**, **V**, **VII**, and **VIII** were used. Figure 4-5 shows the powder XRD patterns of the synthesized VPI-8s. **II**, **V**, **VII**, **VIII** were intact inside the VPI-8 pores (verified by  $^{13}\text{C}$  CP MAS NMR).

The ketal-containing SDAs studied here appear to have weak structure-directing effects based on the observation that the produced zeolite phases were mainly determined by gel compositions. However, the zeolites were not synthesized without organic SDAs and only particular SDAs could produce the corresponding zeolites as shown in Table 4-1. The various synthesized zeolites were used to study the degradation of the organic SDAs inside the pores as described next.

#### 4.3.2. Cleavage reaction of ketal SDAs inside the pore space.

Scheme 1 shows the cleavage reaction of the ketal-containing SDA into smaller fragments. There are many factors that affect the cleavage reaction of the organic molecules that are enclathrated inside the pore space during zeolite synthesis. In this study, the effects of organic content, hydrophilicity and pore connectivity of the synthesized zeolites on the successful degradation of the SDAs are investigated. Different acidic treatment conditions were used for the cleavage reaction. First, 1N HCl solution was used to degrade the SDA at  $80^\circ\text{C}$ . Second, the same HCl solution was used at higher temperature of  $135^\circ\text{C}$ . Acetic acid solution (5mL acetic acid/30mL water) was also used at  $135^\circ\text{C}$ . Because  $135^\circ\text{C}$  is higher than the boiling point of the solutions, a pressurized autoclave reactor was utilized. The pressure was higher than



#### 4.3.4. Effect of hydrophilicity.

When the synthesized zeolite is hydrophobic, the access of water molecules necessary for hydrolysis of the ketal-containing SDAs might be hindered. Hence, the hydrophilicity of the zeolite can have impact on the degradation of ketal-containing SDAs. ZSM-5s with different hydrophilicity were synthesized as shown in case 2 and case 3 of Table 4-2 using **VIII** as a SDA. The ZSM-5 in case 2 has lower Si/Al ratio of 14.0 while the ZSM-5 in case 3 has higher Si/Al ratio of 40.8. Figure 4-7 provides data that show that the ZSM-5 with lower Si/Al ratio contains more water than the ZSM-5 with higher Si/Al ratio, based on the weight loss in the range of 100~250°C. This TGA pattern reveals that the ZSM-5 with lower Si/Al ratio has more hydrophilic character while the ZSM-5 with higher Si/Al ratio has more hydrophobic character. When the cleavage reaction was attempted with the more hydrophilic ZSM-5 using 1N HCl solution at 80°C, the SDA was easily cleaved into smaller fragments. On the other hand, when the cleavage reaction was carried out for the more hydrophobic ZSM-5 at the same conditions, the SDA remained unchanged as shown by the data in Fig. 4-8(b). The ketal-containing SDA appears to be preserved inside the pore space despite the acidic treatment (compare to <sup>13</sup>C NMR spectrum of as-made ZSM-5 in Fig. 4-8(a)). However, when the harsher condition was applied by using higher temperature of 135°C in the autoclave, the NMR spectrum showed a chemical change of organic molecules inside the pore as observed in Fig. 4-8(c). The SDAs were cleaved to smaller fragments by the access of H<sub>2</sub>O and H<sup>+</sup>, and the remaining fragments in the pore were further removed by ion-exchange with NaCl/NaOH solution. As depicted in Fig. 4-8(d), <sup>13</sup>C CP MAS NMR data show that no organic compound was observed after the ion-exchange in the hydrophobic ZSM-5. The crystalline framework of the ZSM-5 was preserved after the HCl treatment at 135°C

according to powder XRD. While the SDA in the hydrophilic ZSM-5 was easily degraded, the same SDA in the more hydrophobic ZSM-5 required harsher condition of higher temperature and pressure. Therefore, the hydrophilicity of the synthesized zeolite plays a significant role in determining the conditions necessary for the successful degradation of the SDA.

#### 4.3.5. Effect of pore connectivity.

Zeolites with different pore connectivity were investigated for the cleavage reaction. ZSM-5, mordenite, and ZSM-12 were used to evaluate this effect. The ZSM-5 has three-dimensionally connected 10 membered-ring (10MR; the number of oxygen atoms that make up the pore is 10) pore structure. Mordenite has one-dimensional structure with 12MR large pore, viewed on the 001 plane, and also another limited access from 8MR pore, viewed on the 010 plane [14]. ZSM-12 has one dimensional structure with 12MR large pore. As shown previously, the SDA inside the ZSM-5 was easily cleaved by 1N HCl at 80°C. The same cleavage reaction was also tried for mordenite. The Si/Al ratio of the mordenite was 14.7, which is very similar to the ratio in the hydrophilic ZSM-5. The SDA (**VIII**) inside the mordenite showed no chemical change after the acidic treatment with 1N HCl solution at 80°C. On the other hand, when the same solution was used at 135°C, the SDA was degraded as shown by the data given in Fig. 4-9(b). It is considered that the higher temperature and pressure enhance the mass transfer of H<sub>2</sub>O and H<sup>+</sup> to the SDA, which is essential for the cleavage reaction. According to FT-IR spectra before and after the cleavage reaction, the IR peak for the ketone fragment appeared at 1735.0cm<sup>-1</sup> after the treatment at higher temperature. The remaining fragments in the pores were removed by ion-exchange with NaCl/NaOH solution at 100°C by using autoclave. No organic

compound was observed after the ion-exchange as depicted in the data listed in Fig. 4-9(c). The cleavage reaction was also attempted for the SDA inside ZSM-12. The ZSM-12s with different heteroatoms such as aluminum or boron were tested with both 1N HCl solution at 80°C and 135°C. The Si/Al ratio for Al-ZSM-12 was 23.8, and the Si/B ratio for B-ZSM-12 was 52.3. Even when the higher temperature conditions were applied, the SDA still remained intact in all cases. The higher ratio of Si/B might hinder the cleavage reaction further due to the more hydrophobic character. But as shown for Al-ZSM-12 with Si/Al of 23.8, the low pore connectivity certainly contributes to making the cleavage reaction of the SDA inside the pores more difficult compared with ZSM-5 with Si/Al of 14.0 and mordenite with Si/Al of 14.7. After the acidic treatment, boron content (Si/B) showed no difference from as-made B-ZSM-12 based on elemental analysis results. Another zeolite with one-dimensional pore structure, VPI-8, showed the same results as ZSM-12. When the VPI-8 with Si/Zn ratio of 31.5 was tested with the acid treatments, the SDA inside the VPI-8 pores remained intact even after the treatment at higher temperature. However, it might be possible to cleave the SDAs inside one-dimensional pore structure by using much harsher conditions than those used here. On the other hand, acetic acid solution was used to fragmentize the SDA(VIII) in the hydrophobic ZSM-5 at 135°C. Most of the fragments were removed from the zeolite framework after prolonged time of 2 days of the acetic acid treatment. This is due to concurrent ion-exchange of the SDA fragments with acetic acid protons. The cleaved fragments with MW 128.1 (ketone fragment) and 146.1 (water was added to the ketone fragment) were observed in the acetic acid solution collected after the treatment by LC electrospray mass spectrometer. Organic molecules were hardly observed inside the zeolite according to  $^{13}\text{C}$  CP MAS NMR. The SDA(VIII) inside the mordenite was also cleaved by the

acetic acid solution at 135°C. In this case, the fragments remained in the pore after 2 days of the acidic treatment. The cleaved fragments in the mordenite stay inside the pores while most of the fragments in the ZSM-5 were removed. While the fragments could be removed more easily from three-dimensionally connected ZSM-5 framework, the same fragments remained inside two-dimensional pore structure of mordenite probably due to less effective mass transfer. From the observations mentioned thus far, the SDAs inside the zeolite with higher pore connectivity were more easily cleaved and this is likely due to better mass transfer of small molecules necessary for the cleavage reaction. Also, the SDA fragments were more easily removed from the zeolite with higher pore connectivity.

#### **4.4. Conclusions**

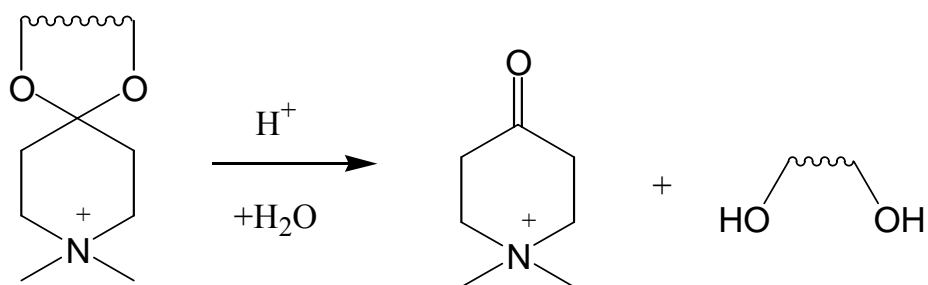
Quaternary ammonium cations containing a variety of ketal groups were synthesized and used as degradable structure-directing agents for zeolite and molecular sieve syntheses. The ketal-containing SDAs directed the formation of ZSM-5, mordenite, ZSM-12 and VPI-8. ZSM-5s with different organic contents and Si/Al ratios were synthesized. Changes in the structure of the ketal group had a small impact on the type of zeolite prepared. The ketal-containing SDAs inside the zeolite pore space were degraded into smaller fragments by acidic treatments using 1N HCl solution at 80°C and 135°C or acetic acid solution at 135°C. The hydrophilicity and pore connectivity of the synthesized zeolites had large influence on the successful degradation of the organic SDAs. The hydrophilic character of the zeolites likely enabled the access of water molecules necessary for hydrolysis of the ketal molecules. The zeolites with higher pore connectivity showed easier degradation of the organic

SDAs and is probably due to better mass transfer into and out of the zeolite pore space when compared to zeolites with one-dimensional pore structure.

## References

1. M.E. Davis and S.I. Zones, *A perspective on zeolite synthesis : How do you know what you'll get?*, in *Synthesis of Porous Materials : Zeolites, Clays, and Nanostructures*, M.L. Occelli and H. Kessler, Editors. 1997, Dekker. p. 1.
2. A. Dyer, *An Introduction to Zeolite Molecular Sieves*. 1988: John Wiley & Sons.
3. R.F. Lobo, S.I. Zones, and M.E. Davis, Structure-direction in zeolite synthesis, *Journal of Inclusion Phenomena and Molecular Recognition in Chemistry* 21 (1995) 47.
4. G. Sastre, S. Leiva, M.J. Sabater, I. Gimenez, F. Rey, S. Valencia, and A. Corma, Computational and experimental approach to the role of structure-directing agents in the synthesis of zeolites : The case of cyclohexyl alkyl pyroliidinium salts in the synthesis of beta, EU-1, ZSM-11, and ZSM-12 zeolites, *J. Phys. Chem. B* 107 (2003) 5432.
5. S.A. Schunk and F. Schuth, *Synthesis of zeolite-like inorganic compounds*, in *Molecular Sieves Science and Technology : Synthesis*, H.G. Karge and J. Weitkamp, Editors. 1998, Springer. p. 229.
6. G.H. Kuehl and H.K.C. Timken, Acid sites in zeolite beta : Effects of ammonium exchange and steaming, *Micropor. Mesopor. Mater.* 35-36 (2000) 521.

7. B.A. Holmberg, S.-J. Hwang, M.E. Davis, and Y. Yan, Synthesis and proton conductivity of sulfonic acid functionalized zeolite BEA nanocrystals, *Micropor. Mesopor. Mater.* 80 (2005) 347.
8. B.A. Holmberg, H. Wang, J.M. Norbeck, and Y. Yan, Nafion/acid functionalized zeolite nanocomposite fuel cell membranes, *Polymer* 45 (2004) 24.
9. S. Li, Z. Li, and Y. Yan, Ultra-low-k pure-silica zeolite MFI films using cyclodextrin as porogen, *Adv. Mater.* 15 (2003) 1528.
10. Z. Wang, H. Wang, A. Mitra, L. Huang, and Y. Yan, Pure-silica zeolite low-k dielectric thin films, *Adv. Mater.* 13 (2001) 746.
11. B.A. Holmberg, S.-J. Hwang, M.E. Davis, and Y.S. Yan, Synthesis and proton conductivity of sulfonic acid functionalized zeolite BEA nanocrystals, *Micropor. Mesopor. Mater.* 80 (2005) 347-356
12. H. Lee, S.I. Zones, and M.E. Davis, A combustion-free methodology for synthesizing zeolites and zeolite-like materials, *Nature* 425 (2003) 385.
13. H. Lee, S.I. Zones, and M.E. Davis, Zeolite synthesis using degradable structure-directing agents and pore-filling agents, *J. Phys. Chem. B* 109 (2005) 2187.
14. C. Baerlocher, W.M. Meier, and D.H. Olson, *Atlas of zeolite framework types*. 2001: Elsevier. p. 190.



Scheme 1. Cleavage reaction of ketal-containing SDA into smaller fragments.

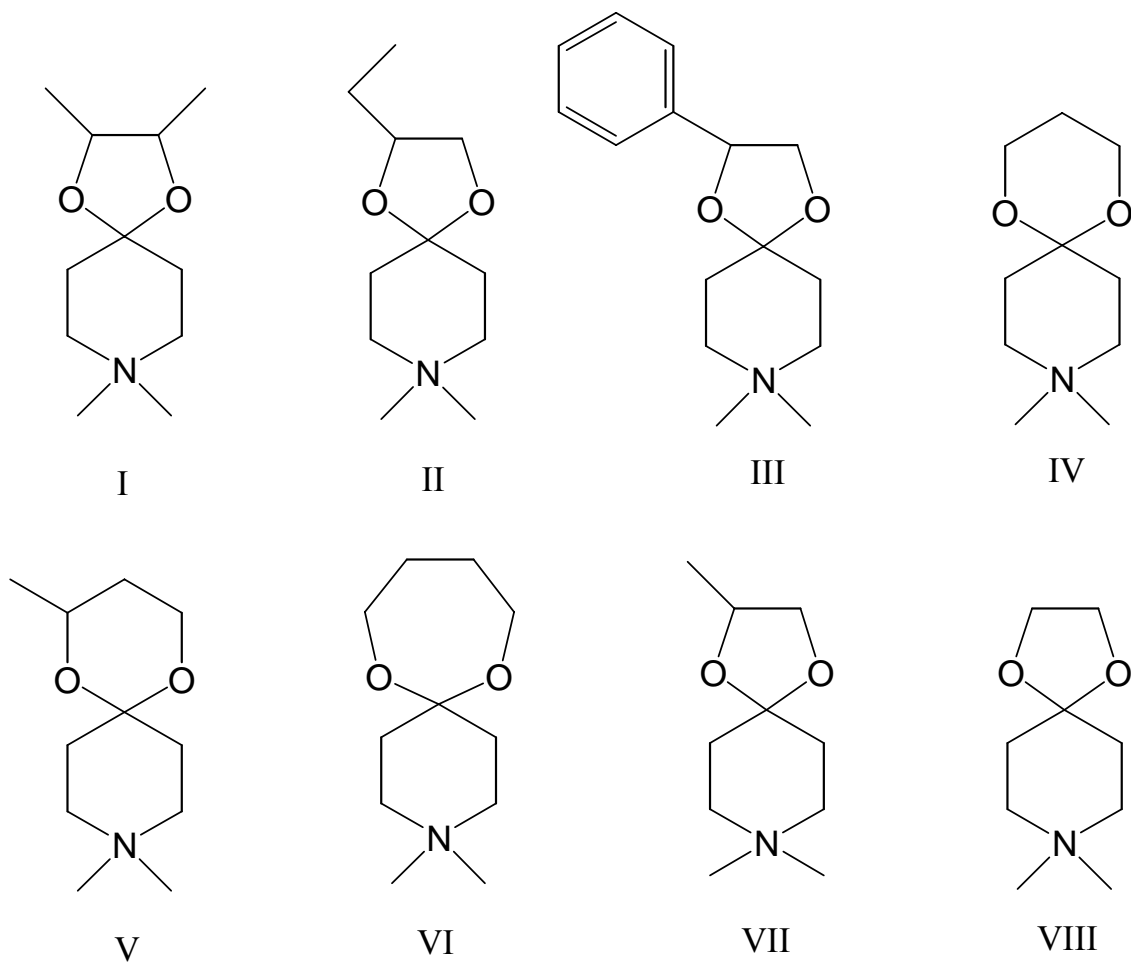


Figure 4-1. Ketal structure-directing agents used in this work.

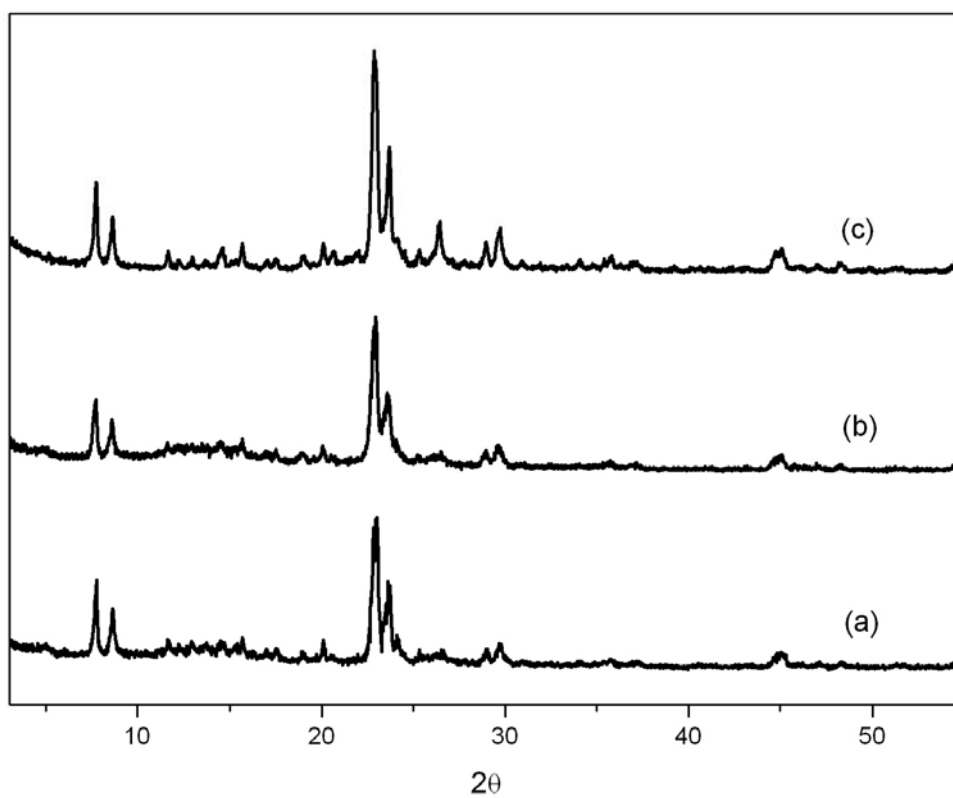


Figure 4-2. Powder X-ray diffraction patterns of ZSM-5 synthesized by using ketal-containing SDAs: (a) SDA : **II**, (b) SDA : **VII**, and (c) SDA : **VIII**.

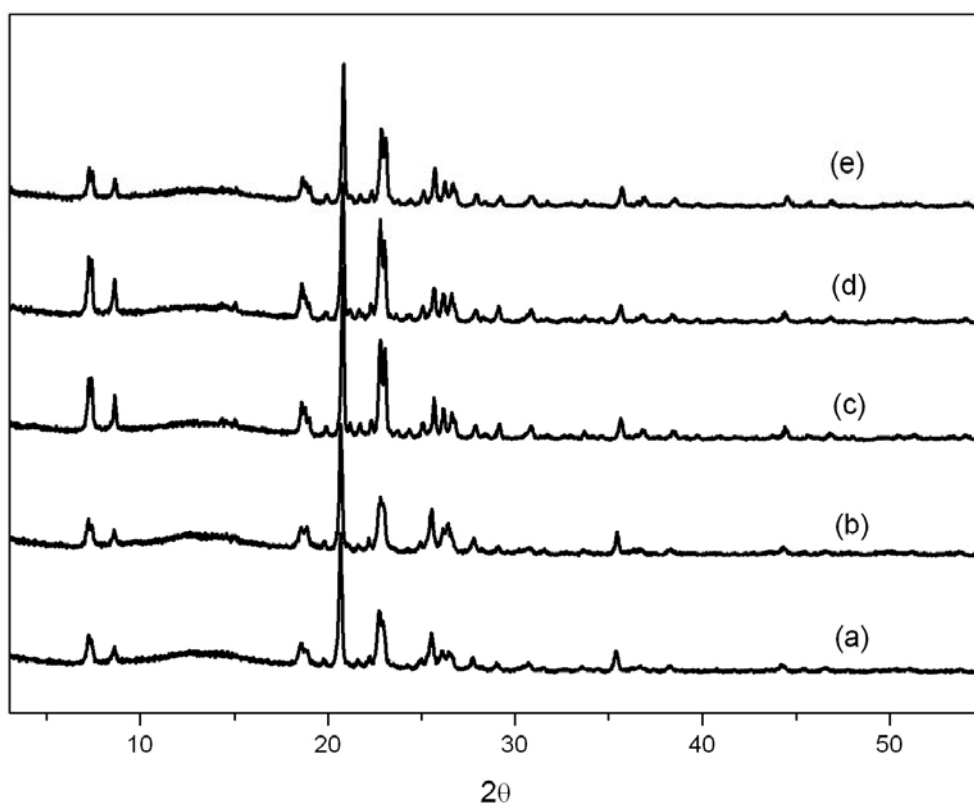


Figure 4-3. Powder X-ray diffraction patterns of ZSM-12 synthesized by using ketal-containing SDAs: (a) SDA : **IV** (Al-ZSM-12), (b) SDA : **VIII** (Al-ZSM-12), (c) SDA : **II** (B-ZSM-12), (d) SDA : **IV** (B-ZSM-12), and (e) SDA : **VIII** (B-ZSM-12).

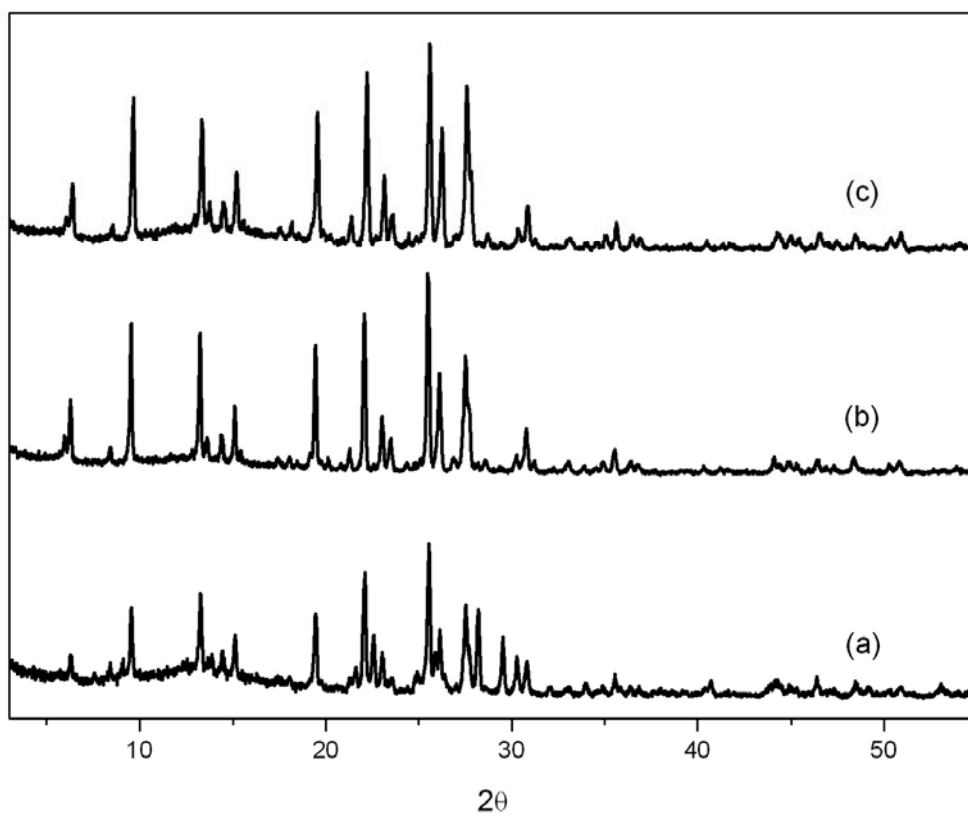


Figure 4-4. Powder X-ray diffraction patterns of mordenite synthesized by using ketal-containing SDAs: (a) SDA : **III**, (b) SDA : **IV**, and (c) SDA : **VIII**.

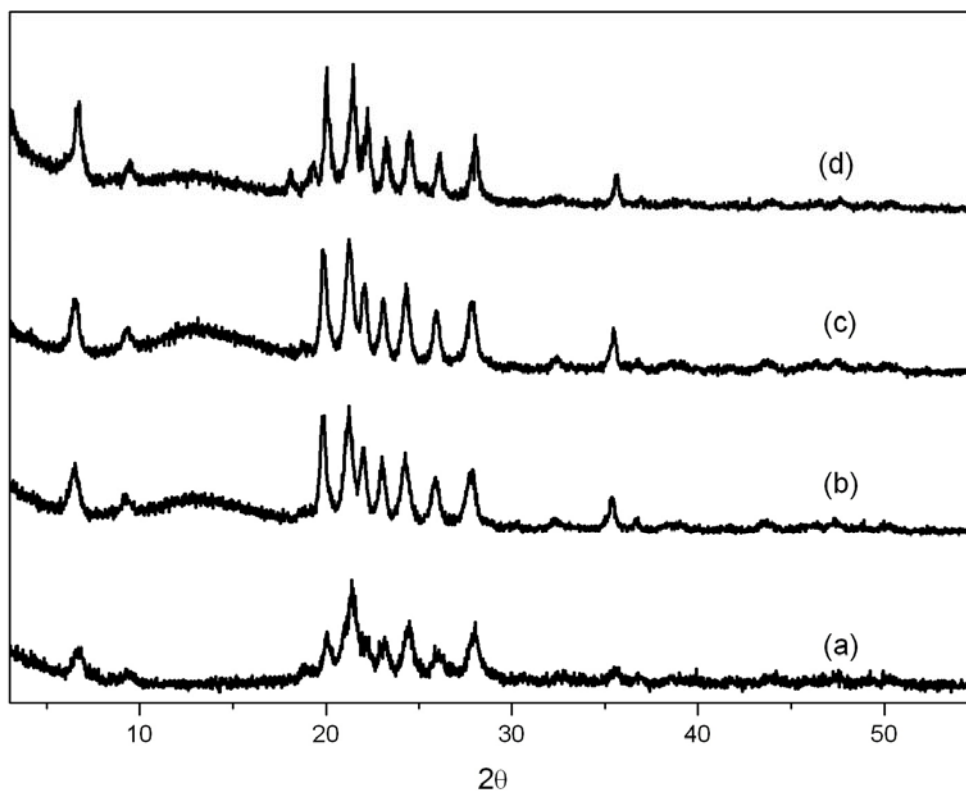


Figure 4-5. Powder X-ray diffraction patterns of VPI-8 synthesized by using ketal-containing SDAs: (a) SDA : **II**, (b) SDA : **V**, (c) SDA : **VII**, and (d) SDA : **VIII**.

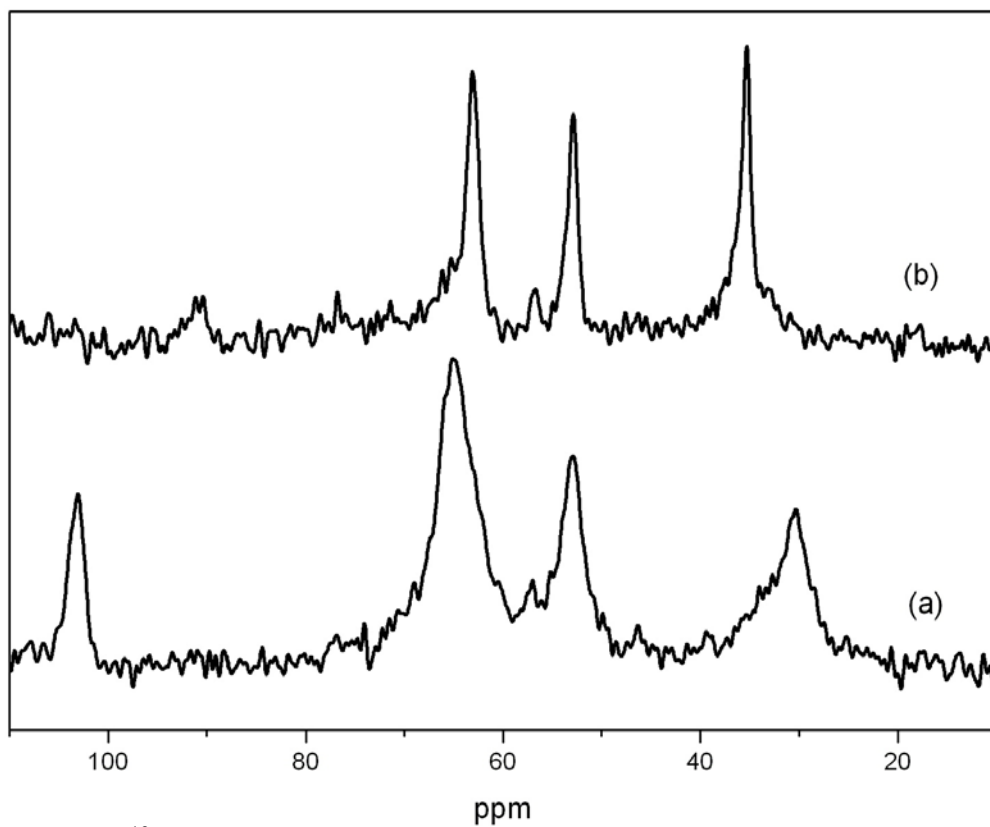


Figure 4-6.  $^{13}\text{C}$  CP MAS NMR spectra for the ZSM-5 (SDA : VIII) with organic content of 7.8%: (a) as-made ZSM-5 (b) after acidic treatment with 1N HCl at 80°C.

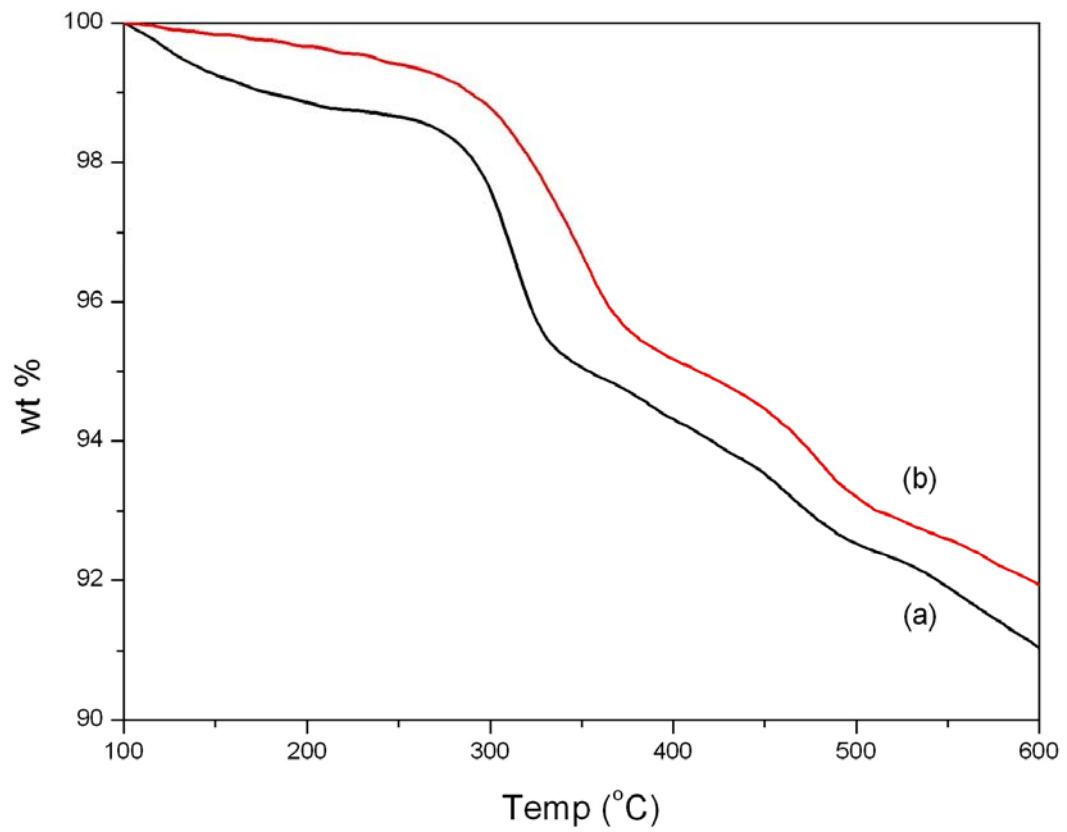


Figure 4-7. Thermogravimetric analysis results for: (a) as-made ZSM-5 with Si/Al=14.0, and (b) as-made ZSM-5 with Si/Al=40.8.

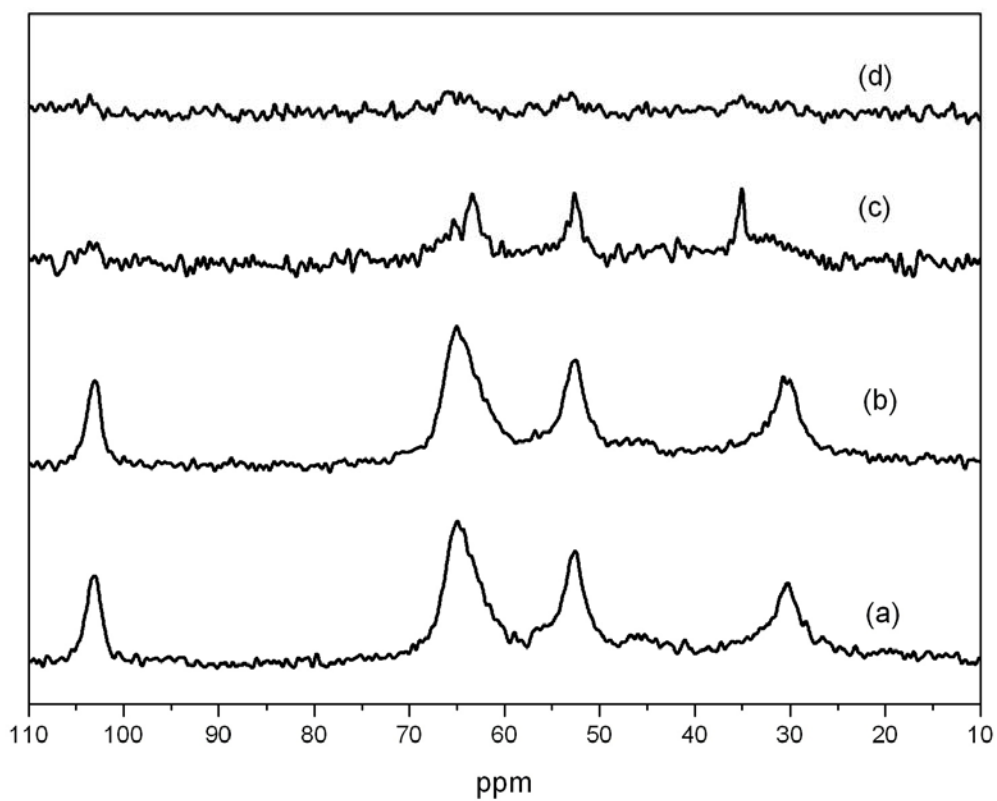


Figure 4-8.  $^{13}\text{C}$  CP MAS NMR spectra for: (a) as-made ZSM-5 (SDA : **VIII**), (b) after an acidic treatment by using 1N HCl at  $80^\circ\text{C}$ , (c) after an acidic treatment by using 1N HCl at  $135^\circ\text{C}$ , and (d) after further ion-exchange with NaCl/NaOH solution at  $100^\circ\text{C}$ .

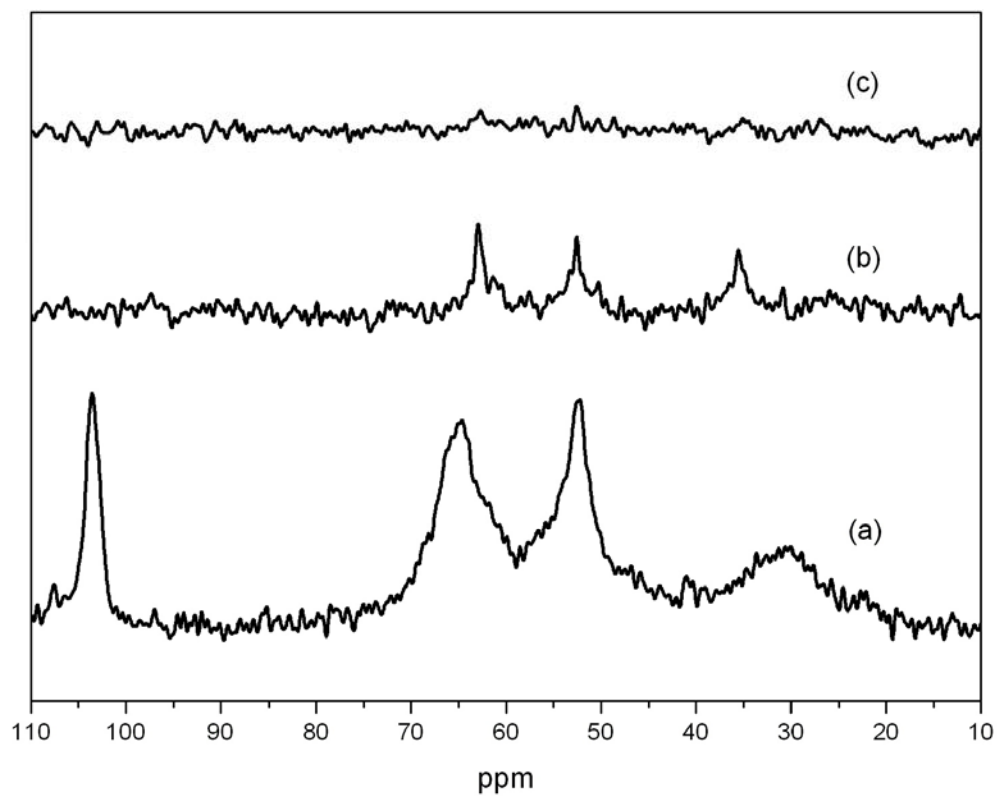


Figure 4-9.  $^{13}\text{C}$  CP MAS NMR spectra for: (a) as-made mordenite (SDA : **VIII**), and (b) after an acidic treatment with 1N HCl at 135°C (c) after further ion-exchange with NaCl/NaOH at 100°C.

Table 4-1. Zeolite syntheses using ketal-containing SDAs

SDA <sup>a</sup>	Composition per mol of SiO <sub>2</sub>	Temp (°C)	Time (days)	Rpm <sup>d</sup>	Phase
<b>II</b>	0.04 <b>II</b> : 0.24KOH : 0.06Al(OH) <sub>3</sub> : 40H <sub>2</sub> O	170	7	60	ZSM-5
<b>VII</b>	0.04 <b>VII</b> : 0.24KOH : 0.06Al(OH) <sub>3</sub> : 40H <sub>2</sub> O	170	7	60	ZSM-5
<b>VIII</b>	0.04 <b>VIII</b> : 0.24KOH : 0.06Al(OH) <sub>3</sub> : 40H <sub>2</sub> O	170	7	60	ZSM-5
<b>IV</b>	0.15 <b>IV</b> : 0.15NaOH : 0.055Al <sup>b</sup> : 27H <sub>2</sub> O	160	14	60	ZSM-12
<b>VIII</b>	0.15 <b>VIII</b> : 0.15NaOH : 0.055Al <sup>b</sup> : 27H <sub>2</sub> O	160	14	60	ZSM-12
<b>II</b>	0.2 <b>II</b> : 0.1NaOH : 0.01Na <sub>2</sub> B <sub>4</sub> O <sub>7</sub> : 44H <sub>2</sub> O	160	14	60	ZSM-12
<b>IV</b>	0.2 <b>IV</b> : 0.1NaOH : 0.01Na <sub>2</sub> B <sub>4</sub> O <sub>7</sub> : 44H <sub>2</sub> O	160	14	60	ZSM-12
<b>VIII</b>	0.2 <b>VIII</b> : 0.1NaOH : 0.01Na <sub>2</sub> B <sub>4</sub> O <sub>7</sub> : 44H <sub>2</sub> O	160	14	60	ZSM-12
<b>III</b>	0.3 <b>III</b> : 1.33KF : 0.067Al(OH) <sub>3</sub> : 45H <sub>2</sub> O	150	14	0	MOR
<b>IV</b>	0.14 <b>IV</b> : 0.06Al <sup>b</sup> : 0.53Na <sup>c</sup> : 32H <sub>2</sub> O	150	14	0	MOR
<b>VIII</b>	0.14 <b>VIII</b> : 0.06Al <sup>b</sup> : 0.53Na <sup>c</sup> : 32H <sub>2</sub> O	150	14	0	MOR
<b>II</b>	0.3 <b>II</b> : 0.05LiOH : 0.03Zn(CH <sub>3</sub> COO) <sub>2</sub> : 30H <sub>2</sub> O	150	6	0	VPI-8
<b>V</b>	0.3 <b>V</b> : 0.05LiOH : 0.03Zn(CH <sub>3</sub> COO) <sub>2</sub> : 30H <sub>2</sub> O	150	6	0	VPI-8
<b>VII</b>	0.3 <b>VII</b> : 0.05LiOH : 0.03Zn(CH <sub>3</sub> COO) <sub>2</sub> : 30H <sub>2</sub> O	150	6	0	VPI-8
<b>VIII</b>	0.3 <b>VIII</b> : 0.05LiOH : 0.03Zn(CH <sub>3</sub> COO) <sub>2</sub> : 30H <sub>2</sub> O	150	6	0	VPI-8

<sup>a</sup> SDA short names as defined in Figure 1

<sup>b</sup> Aluminum from NaY (Silica to Alumina ratio = 6)

<sup>c</sup> Sodium from sodium silicate solution (27% SiO<sub>2</sub>, 14% NaOH)

<sup>d</sup> Rotation speed: revolutions per minute

Table 4-2. Properties of ZSM-5s with different organic contents and Si/Al ratios

	ROH/SiO <sub>2</sub> (gel)	Si/Al (gel)	Organic Content (Solid) <sup>a</sup>	Si/Al (Solid) <sup>b</sup>
Case 1	0.04	16.7	6.4%	13.8
Case 2	0.10	16.7	7.8%	14.0
Case 3	0.15	50	7.7%	40.8

<sup>a</sup> measured by TGA (200~600°C)

<sup>b</sup> measured by elemental analysis

## **Chapter Five**

Concluding Remarks

## 5.1. Potential Applications of the New Methodology

The methodology proposed in this work can reduce the synthesis cost of zeolitic materials by recycling organic SDAs, although re-use of the recovered SDA is not demonstrated here. The evaluation of economical efficacy for the proposed methodology will be beneficial for its actual application in industry. The yield of recovered SDAs and the recovering cost including purification steps should be carefully estimated. This methodology will be especially useful for synthesis of pure-silica molecular sieves with extra-large pores. As shown in Table 1 of Chapter 1, the bulky SDAs have been successfully used to find pure silica molecular sieves with extra-large pore 14MR, such as UTD-1 and CIT-5. The attempts to synthesize zeolitic materials with extra-large pore using even bulkier molecules such as sugar derivatives are continued. Because the synthesis cost of this bulky SDA is probably very high, SDA recycling will be particularly important in the applications. In addition, the removal of the fragmented SDA pieces will be easier in pure silicate system due to weak interactions of the organic molecules and the framework. The pieces can be removed by simple solvent extraction rather than ion-exchange, and this will facilitate easier purification of the recollected pieces. Therefore, the proposed methodology can contribute to the economical application of new zeolitic materials (especially pure silicate material) that will probably be discovered using bulkier SDAs.

The avoidance of high temperature procedures can provide tremendous opportunities to zeolitic materials as well. The proposed methodology suggests an unprecedented way to make inorganic crystalline materials porous at mild conditions. As novel applications of zeolitic materials have received much attention as explained in Chapter 1 and new classes of inorganic crystalline materials have appeared such as

metal-organic frameworks (MOF), the need for methods to handle the materials at varied conditions has increased. Potential applications to which the proposed methodology can contribute to expanding the use of zeolitic materials are suggested as below.

- *Preservation of organic functional groups anchored on inorganic frameworks*

Organic groups have been anchored on inorganic crystalline frameworks[1-3] or hybrid materials with organic frameworks have been synthesized[4, 5]. Various organic functional groups such as phenyl, cyanoethyl, iodopropyl, allyl, bromopropyl, aminopropyl, mercaptopropyl groups were anchored on BEA frameworks and employed as catalytic sites[3]. Organic-inorganic hybrid zeolites with Si-CH<sub>2</sub>-Si were synthesized and the materials showed shape-selective lipophilicity indicating that it is not a physical mixture of conventional zeolite and amorphous organic-containing material but contains a genuine organic-inorganic hybrid zeolite[4]. Open metal-organic frameworks consisting of inorganic clusters and organic linkers have been discovered, mainly by Yaghi group. Often zinc clusters with various connectivities have been used with rigid organic linkers such as 1,4-benzenedicarboxylate in order to construct MOFs[5]. Many of these hybrid materials also use organic templates to fill the space in the porous structure. Organically functionalized molecular sieves (OFMS) use various SDAs such as TEA and TPA, and MOF materials also use organic guest molecules as space-filler especially when flexible organic linkers were used[6, 7]. When these organic guests were used, the removal of only organic guests, not organic functionality is a key for their applications. In the case of OFMS, there has been only one case that the SDA can be removed from zeolite pore by extraction – TEA from zeolite β. The biggest obstacle for further applications of OFMS has been

difficulty to remove only guests. If calcination is used for removal, the high temperature would also destroy the organic functionality as well as the organic guest molecules. If the proposed methodology is used to remove SDAs, however, the organic functionality can be preserved inside the pore while the SDA can be removed by fragmentation as shown Fig. 1. The porous materials with organic functionality in the pores can be used as catalysts with enhanced catalytic activity or fuel cell composite materials with improved proton conductivity. On the other hand, when organic groups serve as constituents of the framework, calcination would destroy the whole framework by burning the organic framework and porosity would be lost. The proposed methodology can remove the organic guests while preserving the organic framework. There are many cases that porous crystalline materials cannot be prepared since the framework is destroyed upon the removal of guest molecules. Some cases are due to instability of the framework itself, but the other cases are on account of harsh condition that the framework cannot endure during the removal. The new 'porous' MOF materials that has been unable to be prepared using existing methods can be made by adapting the method shown in this work.

- *Preventing aggregation of zeolite nanoparticles*

Recently, zeolite nanoparticles have been actively studied as building blocks for various hierarchical structures such as patterned films, self-standing films, zeolite fibers, ordered macroporous monoliths, etc[8-10]. Since the hierarchical materials are expected to be used for separation, catalysis, and microelectronics, organic SDAs inside the zeolite nanoparticles must be removed first from the zeolite nanoparticles. Later removal of the SDAs after construction would deform the hierarchical structures. However, calcination is unsuitable for SDA removal because it leads to significant

irreversible aggregation of colloidal nanoparticles. Wang et al. reported the preparation of SDA-removed zeolite nanocrystals by using an organic polymer network as a temporary barrier during calcination to prevent zeolite nanocrystal aggregation[11]. Also, monolayers of zeolite microcrystals have been synthesized by using various covalent linkages such as chemical linkers as amine or halide[12], ionic linkers using polyelectrolytes[13], and hydrogen bonding linkers using adenine-thymine[14]. However, the zeolite crystals usually have large size of a few  $\mu\text{m}$  in these studies. They removed organic SDAs from zeolite microcrystals prior to monolayer formation by calcination at  $550^\circ\text{C}$ . When the patterning technique using various covalent bonds is to be applied for zeolite nanoparticles with smaller size, calcination would produce aggregates with broader size distribution and it will be hard to obtain a uniform zeolite microarray using those aggregates. The proposed methodology can provide a new way for SDA-removal while preventing aggregation and keeping narrow size distribution of zeolite nanoparticles.

- *Construction of pore-patterned film*

Zeolite micropatterns have been produced using zeolite nanoparticles or pre-patterned substrates as shown in Fig. 2[10, 12]. The pattern in Fig. 2(a) was produced by applying a patterned polydimethylsilane (PDMS) stamp facedown with a compression pressure onto a drop of nanoparticles suspension. In Fig. 2(b), organic moieties were attached onto glass or silicon wafer in a patterned manner, then zeolite particles with functional groups on the exterior surface were immobilized by chemical reaction with pre-patterned organic moieties. All of these works used separate zeolite crystals as building units to construct the micropatterns. On the other hand, a micropattern where the zeolite is porous only at selected areas within a single

crystalline film may be formed. The proposed methodology can be used to construct such a pore-patterned film by selectively removing SDAs from a zeolite film. When the SDA is fragmented at only a selected area of the film, the film will have non-porous and porous areas in a patterned way after removing the fragments. Photolytic organic compounds can be used as a SDA for such a selective fragmentation.

## 5.2. Conclusions

A new methodology has been proposed for synthesizing zeolite and zeolite-like materials. The existing method of preparing porous zeolitic materials has mostly used a high-temperature step – calcination – to remove organic compounds trapped inside the pore cavity during zeolite synthesis. The high temperature step, however, causes several undesired aspects, which include waste of valuable organic compounds, destruction of catalytic sites or, more severely, crystalline framework, additional synthesis cost due to the need for treatment of effluent gas generated by the combustion, etc. The new method, which removes trapped organic molecules without the high temperature step, provides an alternative that avoids such problems. A key component of the new methodology proposed in this work is *a priori* rational design of organic compounds that are usually used for zeolite synthesis. Organic molecules that can be easily cleaved to smaller fragments and recombined to their original shape are used to structure-direct zeolites. The trapped organic molecules are fragmented after synthesizing zeolites and the fragments are removed more easily than the whole molecules mainly due to their smaller size. The fragments can be recombined and the recovered organic molecules can be used for more zeolite synthesis. Porous zeolite-

like materials can be prepared by following these steps without using high temperature.

The new methodology was realized by using an organic molecule containing a cyclic ketal group. 8,8-dimethyl-1,4-dioxo-8-azaspiro[4,5]decane successfully structure-directed the formation of ZSM-5. The organic molecule was cleaved using hydrolysis into its corresponding ketone molecule and ethylene glycol upon the acidic treatment and it was confirmed that the cleavage occurred inside the pore cavity. The fragments were removed from the pore by ion-exchange. The smaller size caused by fragmentation was considered a key for the successful removal. The ZSM-5 after the removal of the fragments showed equivalent microporosity to calcined ZSM-5. The porous ZSM-5 prepared by the proposed new methodology had the same catalytic activity and shape selectivity as conventional ZSM-5.

There have been cases, however, where ketal molecules remained intact inside pore cavity in spite of chemical treatments. Additional molecules such as  $H^+$  and  $H_2O$  are necessary for the hydrolysis of ketal molecules. Tight packing of ketal molecules seemed to hinder movement of the additional molecules due to lack of space inside the pores. The necessary space was prepared by using two different kinds of organic molecules during zeolite synthesis. A ketal molecule with an ammonium group was used as the structure-directing agent and a small amine molecule with no electrostatic charge was used as a pore-filling agent. The amine had no influence on the structure of produced zeolite. The synthesized zeolite contained both of the ketal and amine molecules in the pore cavity. The amine was easily extracted, unlike the ketal, because of its smaller size and weaker interaction with zeolite framework. While the ketal had no chemical change upon acidic treatment before extraction of the amine, the same molecule was successfully hydrolyzed after removing the amine by

extraction. As previously discussed, the original methodology was expanded by using different kinds of organic molecules for zeolite synthesis.

Various ketal molecules (many different ketal groups were attached onto 1,1-dimethylpiperidinium) were synthesized and used as structure-directing agents. ZSM-5, ZSM-12, VPI-8, and MOR were synthesized using these organic molecules. The change of ketal group has less impact on the synthesized structure compared with the reactant gel composition. The effect of hydrophilicity and pore connectivity on the cleavage reaction of organic molecules in the pore cavity was evaluated with the synthesized zeolites. ZSM-5s with different Si/Al ratios were synthesized to investigate the effect of hydrophilicity. ZSM-5 with a lower Si/Al ratio has more hydrophilic character than ZSM-5 with a high Si/Al ratio and ketal molecules in the ZSM-5 pore cavity were more easily cleaved due to better mass transport of H<sub>2</sub>O molecule through the pore space. Comparing ZSM-5 with a 3-dimensionally (3-D) connected pore structure, MOR with 2-D, and ZSM-12 with 1-D, ketal molecules were degraded more easily in the zeolite with higher pore connectivity because of facilitated transport of H<sup>+</sup> and H<sub>2</sub>O. The ketal molecule in MOR was degraded under a harsher condition.

The method developed in this work will be beneficial for future applications of zeolitic materials due to its ability to preserve organic functionality selectively and to minimize the deformation of inorganic crystalline phase. The new methodology is a powerful tool for controlling inorganic crystalline materials such as zeolites and molecular sieves rationally in a molecular level.

**References**

1. C.W. Jones, K. Tsuji, and M.E. Davis, Organic-functionalized molecular sieves as shape-selective catalysts, *Nature* 393 (1998)
2. C.W. Jones, K. Tsuji, and M.E. Davis, Organic-functionalized molecular sieves (OFMSs) : II. Synthesis, characterization and the transformation of OFMSs containing non-polar functional groups into solid acids, *Microporous and Mesoporous Mater.* 33 (1999) 223.
3. K. Tsuji, C.W. Jones, and M.E. Davis, Organic-functionalized molecular sieves (OFMSs) I. Synthesis and characterization of OFMSs with polar functional groups, *Microporous and Mesoporous Mater.* 29 (1999) 339.
4. K. Yamamoto, Y. Sakata, Y. Nohara, Y. Takahashi, and T. Tatsumi, Organic-inorganic hybrid zeolites containing organic frameworks, *Science* 300 (2003) 470.
5. H. Li, M. Eddaoudi, M. O'Keeffe, and O.M. Yaghi, Design and synthesis of an exceptionally stable and highly porous metal-organic framework, *Nature* 402 (1999) 276.
6. D.T.d. Lill, N.S. Gunning, and C.L. Cahill, Toward templated metal-organic frameworks: Synthesis, structures, thermal properties, and luminescence of three novel lanthanide-adipate frameworks, *Inorg. Chem.* 44 (2005) 258.
7. Z. Shi, G. Li, L. Wang, L. Gao, X. Chen, J. Hua, and S. Feng, Two three-dimensional metal-organic frameworks from secondary building units of  $Zn_8(OH)_4(O_2C^-)_{12}$  and  $Zn_2((OH)(O_2C^-)_3$ :  $[Zn_2(OH)(btc)]_2(4,4'$ -bipy) and  $Zn_2(OH)(btc)(pipe)$ , *Crystal Growth & Design* 4 (2004) 25.

8. H. Wang, Z. Wang, L. Huang, A. Mitra, and Y. Yan, Surface patterned porous films by convection-assisted dynamic self-assembly of zeolite nanoparticles, *Langmuir* 17 (2001) 2572.
9. K.H. Rhodes, S.A. Davis, F. Caruso, B. Zhang, and S. Mann, Hierarchical assembly of zeolite nanoparticles into ordered macroporous monoliths using core-shell building blocks, *Chem. Mater.* 12 (2000) 2832.
10. L. Huang, Z. Wang, J. Sun, L. Miao, Q. Li, Y. Yan, and D. Zhao, Fabrication of ordered porous structures by self-assembly of zeolite nanocrystals, *J. Am. Chem. Soc.* 122 (2000) 3530.
11. H. Wang, Z. Wang, and Y. Yan, Colloidal suspensions of template-removed zeolite nanocrystals, *Chem. Commun.* (2000) 2333.
12. K. Ha, Y.-J. Lee, D.-Y. Jung, J.H. Lee, and K.B. Yoon, Micropatterning of oriented zeolite monolayers on glass by covalent linkage, *Adv. Mater.* 12 (2000) 1614.
13. G.S. Lee, Y.-J. Lee, and K.B. Yoon, Layer-by-layer assembly of zeolite crystals on glass with polyelectrolytes as ionic clusters, *J. Am. Chem. Soc.* 123 (2001) 9769.
14. J.S. Park, G.S. Lee, Y.-J. Lee, Y.S. Park, and K.B. Yoon, Organization of microcrystals on glass by adenine-thymine hydrogen bonding, *J. Am. Chem. Soc.* 124 (2002) 13366.

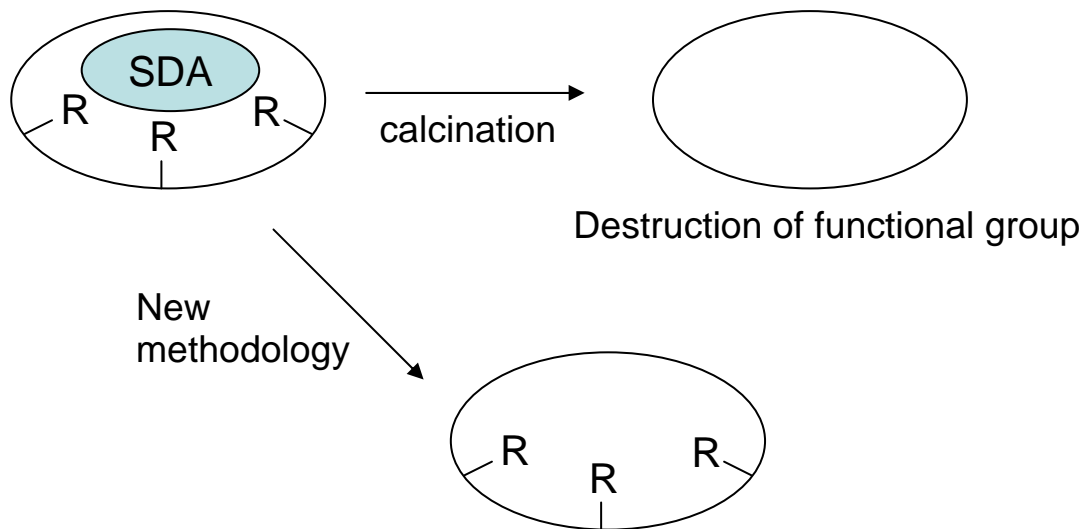
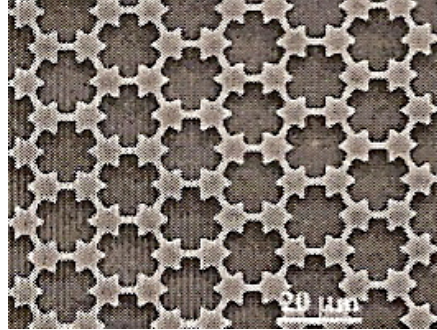


Figure 5-1. Removal of organic SDAs from organically functionalized zeolites.



(a)



(b)

Figure 5-2. Micropatterns prepared (a) by using zeolite nanoparticles [10], (b) by using pre-patterned substrates and functionalized zeolite microcrystals [12].